TOPSAFE

Dubrovnik, Croatia, 30.09 - 3.10.2008

TopSafe 2008

Transactions

Dubrovnik, Croatia
30.9. - 3.10.2008

HND

AEN NEA

IAEA International Atomic Energy Agency
Atoms For Peace

European Nuclear Society
Rue Belliard 65
1040 Brussels, Belgium
Phone + 32 2 505 30 54
Fax +32 2 502 39 02
E-mail ens@euronuclear.org
Internet www.euronuclear.org

ISBN 978-92-95064-06-5

These transactions contain all contributions submitted by 30 September 2008.

TOPSAFE

Dubrovnik, Croatia, 30.09 - 3.10.2008

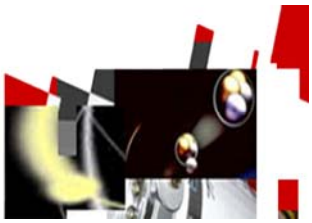

Safety of Future Reactor Designs

TOPSAFE
Dubrovnik, Croatia, 30.09 - 3.10.2008

A Critical Overview of Heat Transfer Phenomena through Different Solutions of In-Pool Condensers for Passive Safety Systems

Davide Papini*, Antonio Cammi
Politecnico di Milano – Department of Energy
Nuclear Division-CeSNEF
Via La Masa, 34 – 20156 Milano, Italy
davide.papini@mail.polimi.it, antonio.cammi@polimi.it

ABSTRACT

Safety systems for advanced LWRs often rely on natural phenomena like the natural circulation, in order to increase simplicity and improve their safety.
Emergency heat removal is a fundamental safety function which in some designs of advanced light water reactors is guaranteed by means of a passive circuit. A typical passive safety system for that purpose is the two-phase flow, natural circulation, closed loop system, where the heat is removed by means of a steam generator or heat exchanger, a condenser and a pool.
Various solutions of condenser tubes arrangement have been implemented for applications to the next generation NPPs. In this paper two possibilities, which represent the simplest and most used configurations, are analyzed. Horizontal U-tubes have been chosen e.g. in the emergency condenser of the SWR1000, whereas a vertical pipes solution has been adopted in the GE-SBWR1000 Isolation Condenser (IC), as well as in the IRIS Emergency Heat Removal System (EHRS).
The horizontal solution with a U-tubes disposition offers the advantage to inherently allow the thermal expansions, while a straight single pass vertical tube could create dangerous thermal stresses due to prevented dilatations. Nevertheless, the better thermalhydraulic performance, mostly with the meaning of higher heat transfer coefficients, provided by vertical tubes is noticeable. In a horizontal tube, the HTC is strongly influenced by the flow pattern, which can be very different (ranging from annular to stratified) without avoiding intermittent regimes; in a stratified regime the HTC is negatively affected by the sump accumulation on the bottom of the pipe. The two-phase flow path is instead well defined in a vertical tube. An annular film of condensate forms on the wall and is driven by gravity reaching higher velocities: resulting higher HTCs for the vertical solution.
This paper deals with a critical comparison between condensation in horizontal and vertical tubes, focusing on the thermalhydraulic aspects and describing the best-estimate correlations, with the aim to point out the global advantages of the vertical tubes arrangement. At the end, an experimental validation of the correlations proposed for the vertical tube, is provided relying on PERSEO facility (SIET labs, Piacenza), showing a good accordance with the model discussed.

* Corresponding author.
Tel.: +39 02 2399 6333; *Fax:* +39 02 2399 6309
E-Mail address: davide.papini@mail.polimi.it

Acronyms

ECT	Emergency Cooldown Tank
EHRS	Emergency Heat Removal System
ESBWR	European Simplified Boiling Water Reactor
GDCS	Gravity Driven Cooling System
HTC	Heat Transfer Coefficient
HX	Heat eXchanger
IC	Isolation Condenser
IRIS	International Reactor Innovative and Secure
KNGR	Korea Next Generation Reactor
LWR	Light Water Reactor
PCCS	Passive Containment Cooling System
PERSEO	in-Pool Energy Removal System for Emergency Operation
PRHRS	Passive Residual Heat Removal System
RPV	Reactor Pressure Vessel
SBWR	Simplified Boiling Water Reactor
SIET	Società Informazioni Esperienze Termoidrauliche
SMART	System integrated Modular Advanced ReacTor
SWR1000	Siede Wasser Reaktor – 1000 MW_e
VISTA	experimental Verification by Integral Simulation of Transient and Accidents

Nomenclature

D	tube diameter [m]
f_i	interfacial roughness factor [-]
G	mass flux [kg/(m^2s)]
g	acceleration of gravity [m/s^2]
h	condensation heat transfer coefficient [W/(m^2K)]
h_c	convective condensation heat transfer coefficient [W/(m^2K)]
h_f	film condensation heat transfer coefficient [W/(m^2K)]
j^*_D	dimensionless vapour velocity [-]
k_l	liquid thermal conductivity [W/(mK)]
L	tube length [m]
p_r	reduced pressure (p/p_{cr}) [-]
Pr_l	condensate Prantdl number [-]
Re_l	local condensate Reynolds number [-]
Re_L	condensate Reynolds number evaluated at the end of the considered regime [-]
T	temperature [°C]
U	overall heat transfer coefficient [W/(m^2K)]
x	equilibrium thermodynamic quality [-]

Greek Symbols

α	void fraction [-]
Δh_{lg}	latent heat of vaporization [J/kg]
δ	film thickness of annular ring [m]
Φ_i	heat flux related to internal diameter [W/m^2]
Γ	mass flowrate [kg/s]
Γ_l	condensate mass flowrate [kg/s]
μ_l	liquid dynamic viscosity [Pa s]
ν_l	liquid cinematic viscosity [m^2/s]
θ	falling film stratification angle [-]
ρ_g	steam density [kg/m^3]
ρ_l	liquid density [kg/m^3]

Subscripts

cond	condensation
e	external
i	internal
lam	laminar regime
lam_wavy	laminar wavy regime
pool	pool boiling
sat	saturation
tube	tube metal
turb	turbulent regime
w	wall

1 INTRODUCTION

The nuclear advanced water reactors design is primarily focused on the achieving of innovative safety characteristics. The main goal of a safety design is to establish and maintain core cooling and ensure containment integrity, for any transient situation, so to minimize the core damage and the fission product release probabilities. This is permitted in practice by means of an integral layout, where the vessel contains all the principal components of the primary circuit (reactor core, cooling pumps, steam generators, pressurizer etc.).

Another important strategy in an advanced safety concept is the large utilization of passive systems. They need no operator action, nor AC power sources, being based only on natural forces, such as gravity and natural circulation, for their continued operation.

A typical passive safety system is a natural circulation loop able to transfer core decay heat and sensible heat from the reactor coolant to the environment during transients, accidents or whenever the normal heat removal paths are lost. Usually, such a system consists of a steam generator (behaving as hot well), a hot leg (circuit riser), a heat sink composed by a heat exchanger bundle submerged in a pool, and a cold leg (circuit downcomer). Its operation is based on the high heat transfer capability offered by the steam generator, which is able to remove decay heat producing steam which rises up in the loop and then condenses rejecting this heat into the pool; the downcomer closes the circuit by bringing back the cold condensed water to the steam generator.

This paper is based on a critical analysis of a component of the circuit discussed above, which is the condenser submerged in the pool. The aim is to compare and asses two different approaches for realizing the condensation, i.e. using a horizontal tubes arrangement or instead a vertical tubes arrangement. The comparison is mainly focused on the thermalhydraulic aspects, reproducing by means of simple Matlab/Excel codes the most updated and reliable modelling of condensation found in literature.

2 LITERATURE REVIEW OF PASSIVE SAFETY SYSTEMS FOR DECAY HEAT REMOVAL

A first concept of in-pool immersed heat exchangers deals with a parallel arrangement of horizontal U-tubes between two common headers. This configuration has been provided in the emergency condenser of a SWR1000, as *Fig.1* shows. The top header is connected via piping to the reactor pressure vessel steam plenum, while the lower header is connected to the reactor vessel below the water level. The heat exchangers are located in a lateral pool filled with cold water, forming a system of communicating pipes with the vessel. At normal reactor water level, the emergency condensers are flooded with cold water; if a reactor trip occurs, the level can drop so that the heat exchanging surfaces inside the tubes are gradually uncovered. The incoming steam condenses on the cold surfaces, and the condensate is simply returned to the reactor vessel, avoiding any core uncovering [1].

Other advanced water reactors chose a vertical tubes arrangement. This has been followed, for example, in the Isolation Condenser (IC) of a SBWR and in the Passive Containment Cooling System (PCCS) of a KNGR. In both cases, decay heat is removed passively from the containment by the condenser submerged in a suitable pool. In a SBWR the system ICs are designed to passively limit the reactor pressure under accident conditions, whereas the containment ICs have to remove the decay heat after a LOCA. The physical locations of the ICs are above the RPV, Suppression Pools and Gravity Driven Cooling System (GDCS), in order to utilize the gravity induced return flow of the condensate from the ICs to the respective ports. The reactor layout is reported in *Fig.2* [2].

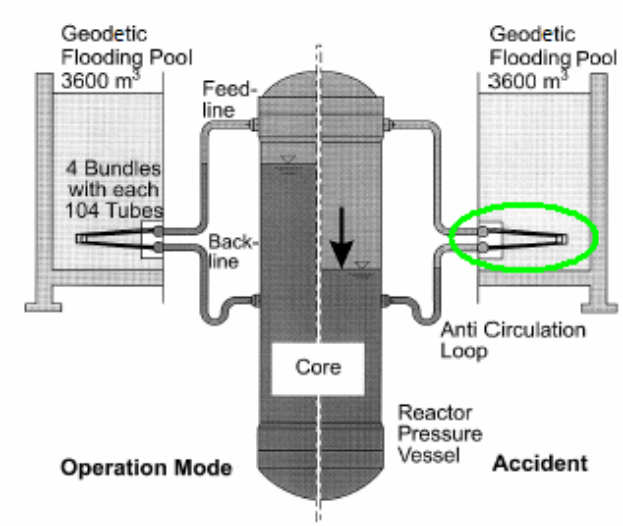

Fig.1- *Emergency condenser of the SWR1000.*

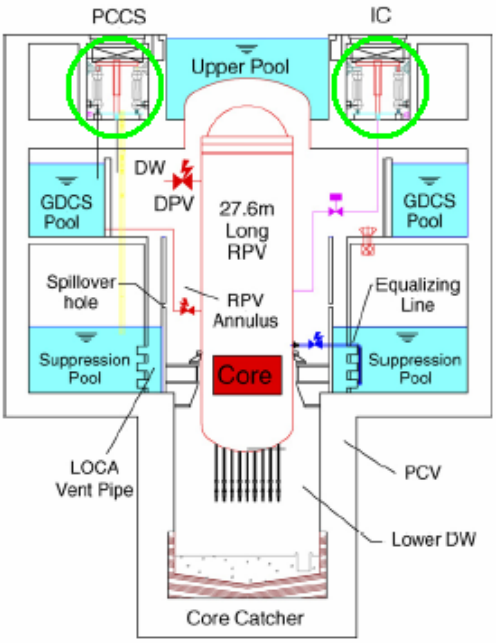

Fig.2- *Isolation condenser (IC) of the SBWR.*

The PCCS of a KNGR (shown in *Fig.3*) is perfectly similar to the passive containment cooling system in the Simplified Boiling Water Reactor. It is provided with two heat exchangers, relevant lines and water tanks, and guarantees a way of external containment cooling through a natural circulation circuit. Heat transferred from the containment atmosphere to the coolant through the primary heat exchanger tube is, in the same way described above, removed by the condenser tubes to the water tank, which is outside the containment [3].

Also the innovative IRIS reactor has its passive safety system for removing the decay heat, which is the Emergency Heat Removal System (EHRS), reproduced in *Fig.4*. Firstly a horizontal U-tubes heat exchanger should have been provided; then the choice fell on a vertical tubes arrangement, adopting the same condenser used for the IC of the SBWR [4]. The Korean SMART reactor is conceived according to the same philosophy of modularity and integral layout; the decay heat removal function is accomplished by the natural circulation in the PRHRS, based again on steam generators for heat extraction and on submerged condensers, precisely located in the Emergency Cooldown Tank (ECT), for heat discharging. A vertical tubes arrangement has been proposed [5].

The different solutions developed in the Generation III+ reactors pointed out a dominance of vertical condensers, whose better performance can be demonstrated with a careful study of the different phenomena involving the condensation process.

3 THERMALHYDRAULIC PHENOMENA IN HORIZONTAL AND VERTICAL TUBES CONDENSERS

The main advantages offered by the vertical tubes solution concern the thermalhydraulic features. The power that should be rejected in a passive system condenser is roughly 20 - 30 MW, which brings to the establishing of low mass fluxes (surely $G < 100$ kg/sm^2) in the loop.

The condensation in horizontal tubes is strongly influenced by the flow pattern, which can be very different (ranging from annular to stratified) without avoiding intermittent regimes. In a defined interval of mass flux and qualities, in fact, the possibility of pulsation is concrete.

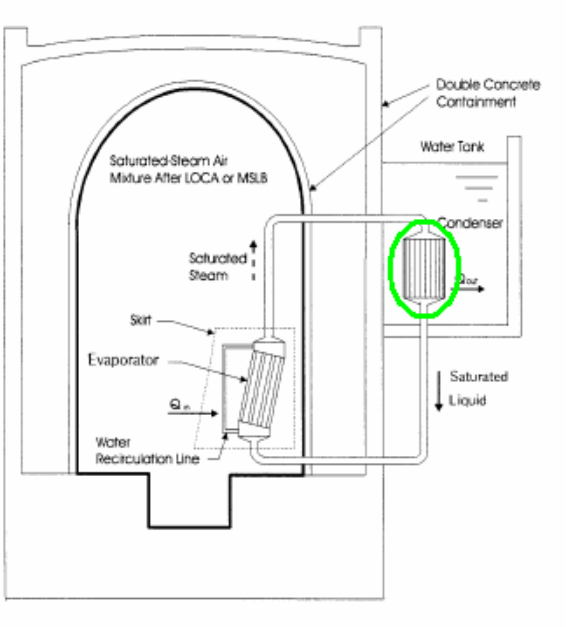

Fig.3- *PCCS condenser of the KNGR.*

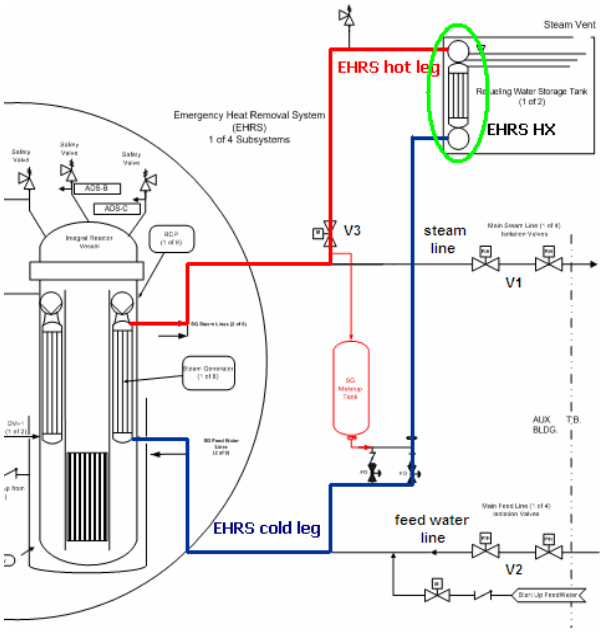

Fig.4- *EHRS condenser of the IRIS.*

At low flowrates and at the medium-high pressures characterizing a natural circulation loop for decay heat removal (typically 60 - 100 bar), a fully stratified/stratified wavy regime occurs. A thin condensate film drains down from the upper part of the tube under the influence of gravity force, whereas a water sump accumulates and flows on the bottom. The HTC is of course negatively affected by this sump, especially when it reaches subcooling conditions towards the end. The effect of interface waves, increasing with the flowrate, does not overcome this disadvantage. Average heat transfer coefficients around 4000 - 6000 W/m^2K result (evaluated considering G equal to 60 kg/sm^2). Condensation in a horizontal tube deals thus with complex phenomena, which deserve a careful analysis.

The two-phase flow path is instead well defined in a vertical tube. An annular film of condensate forms on the wall, and falls down driven by gravity, filling up the cross section only at the end of the tube and assuring thus a better condensation process. Usually, the condensate flows at higher velocity, and this reduces fouling and corrosion effects, besides assuring higher HTCs. At fixed quality, the bigger velocities (pulled by gravity) lead to a thinner film, with a smaller thermal resistance, a smaller laminar boundary layer and thus higher turbulence. Average heat transfer coefficients are strongly enhanced with respect to the horizontal solution, leading to values around 8000 - 11000 W/m^2K. In literature, a lack of high pressure steam condensation data for large diameter condenser vertical

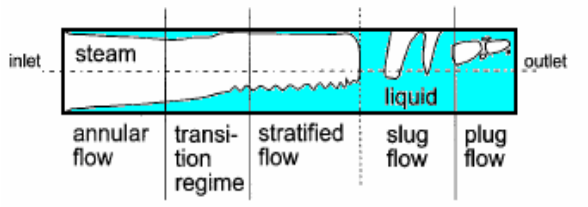

Fig.5- *Different flow patterns during condensation in a horizontal tube.*

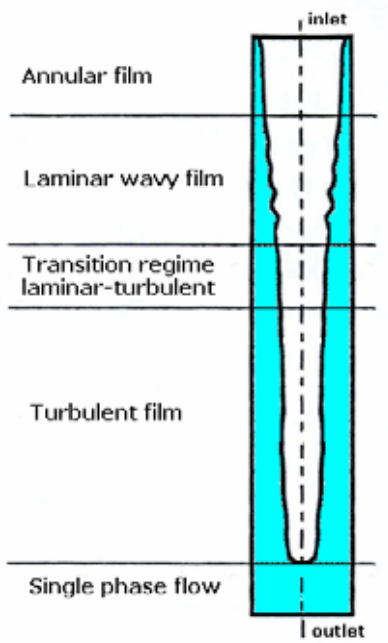

Fig.6- *Different flow patterns during condensation in a vertical tube.*

tubes, which is the case of the passive heat removal systems in KNGR and SBWR, has been noticed. A comprehensive investigation of how condensation is provided in a vertical tube appears thus useful. The different physical phenomena interesting horizontal and vertical pipes can be easier understood considering the drafts in *Fig.5* and *Fig.6*.

The better thermalhydraulic performance of a vertical tube (assuring HTCs even doubled in comparison with a horizontal pipe) is anyway modulated by the strong influence that the tube metal thermal conductance has on the heat transfer. The material revealing as the most suitable for in-pool condensers is INCONEL 600, thanks to its better mechanical properties at high temperature ($\approx$300 °C) and its higher resistance to corrosion phenomena.

4 CONDENSATION MODELS

4.1 Modelling of condensation in a horizontal tube

In early models, the flow patterns were classified just under two categories, i.e. stratified or annular. The first, dominated by gravity forces, considers a thick condensate layer flowing along the bottom of the tube, while a thin liquid film forms on the wall in the upper portion. The latter, dominated by shear effects, leads to an annular ring of condensate flowing uniformly along the tube. Actually, different flow regimes can be induced. When the stratified condensate layer in the tube sump reaches medium-high velocities, often ripples or waves are generated at the phase surface (stratified wavy). If these waves become so large to wash the top of the tube, an intermittent flow pattern (slug – plug) can establish, which has a very complex flow structure. At very high velocities, instead, a mist (spray) regime can occur, characterized by impinging droplets on the thin unsteady liquid film.

Two models are proposed as the most updated and reliable concerning the condensation in a horizontal tube, each one based on a proper flow pattern map for the identification of the flow regime (reported in *Fig.7* and *Fig.8*).

In Thome's model the intermittent (both slug and plug) and mist flows are considered and evaluated as annular flow. For annular flow, a uniform film thickness is assumed and the actual larger thickness of the film at the bottom than the top due to gravity is ignored. Stratified and stratified wavy are instead characterized by the so called stratification angle, which subtends the cross sectional area occupied by the liquid, assumed as truncated annular ring of uniform thickness. *Fig.9* is useful to understand the simplifications provided.

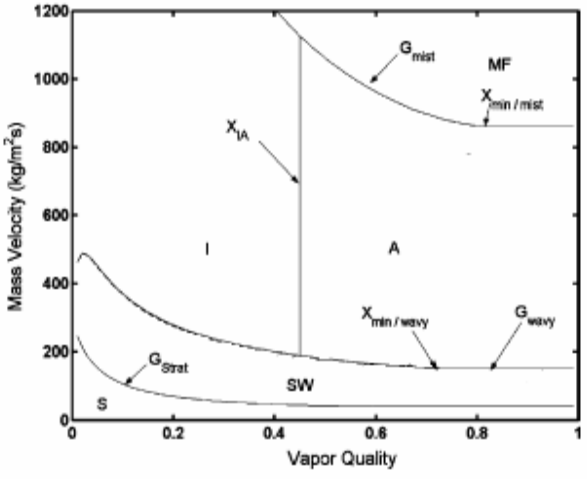

Fig.7- *Thome's flow pattern map for condensation in a horizontal tube.*
S→stratified SW→stratified wavy A→annular
I→intermittent MF→mist flow

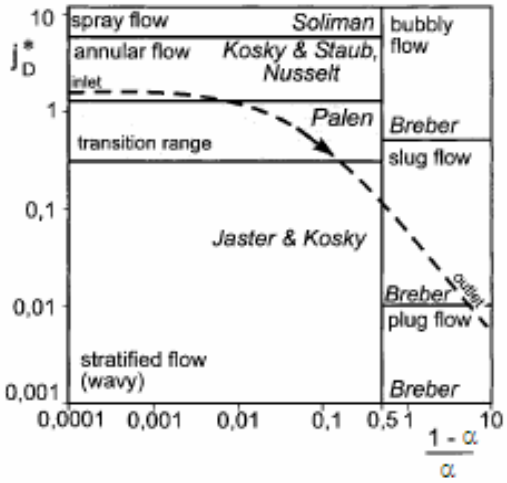

Fig.8- *Tandon's flow pattern map for condensation in a horizontal tube.*

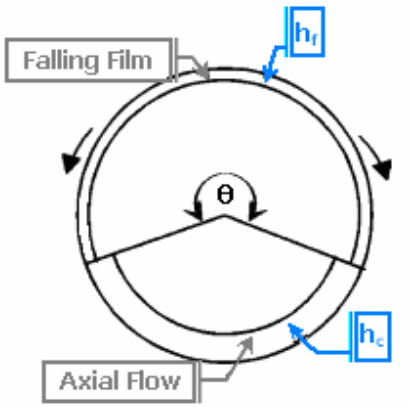

Fig.9- *Heat transfer model showing convective and falling film.*

Two different heat transfer mechanisms are considered within the tube: convective condensation and film condensation. The first refers to the axial flow of the condensate along the channel due to the imposed pressure gradient; the second refers to the flow of condensate from the top of the tube towards the bottom due to gravity. The convective condensation heat transfer coefficient h_c is applied to the perimeter wetted by the axial flow of liquid film, which is the entire perimeter in annular flow, but only part of the perimeter in stratified wavy and stratified one. The film condensation heat transfer coefficient h_f, characterizing only stratified – stratified wavy regime, is obtained by applying the Nusselt's falling film theory to the inside of the horizontal tube, assuming the falling film laminar [6]. Thus, the condensation HTC is given combining these two coefficients according to:

$$h = \frac{h_f \theta D_i/2 + h_c (2\pi - \theta) D_i/2}{\pi D_i} \tag{1}$$

The convective condensation heat transfer coefficient h_c can be obtained from the following film equation, assuming the axial flow as turbulent:

$$h_c = 0.003 \,\mathrm{Re}_l^{0.74} \,\mathrm{Pr}_l^{0.5} \frac{k_l}{\delta} f_i \tag{2}$$

where δ is the film thickness, considered uniform in all the cross section. This is an only liquid correlation type, i.e. just the liquid part of the two-phase flowrate has to be considered. Resulting:

$$\mathrm{Re}_l = \frac{4G(1-x)\delta}{(1-\alpha)\mu_l} \tag{3}$$

The interfacial roughness correction factor f_i takes into account the shear effects that dominate an annular flow regime, leading to a remarkable increasing of the heat transfer.

The film condensation heat transfer coefficient h_f, instead, is given from a modification of the Nusselt's theory for laminar flow of a falling film outside a horizontal tube (around the perimeter, from top to bottom), applied to the condensation on the inside. Any effect of axial shear on the falling film is ignored. Since heat exchanger design codes are typically implemented assuming the heat flux in each incremental zone along the exchanger, the heat flux version of the Nusselt's equation is preferable to be considered:

$$h_f = 0.655 \left[\frac{\rho_l (\rho_l - \rho_g) g \Delta h_{\mathrm{lg}} k_l^3}{\mu_l D_i \Phi_i} \right]^{1/3} \tag{4}$$

The heat transfer coefficient given by equation (4) has to be intended as average HTC if referred to the tube average heat flux, whereas represents a local value if the tube length is divided into different cells and the local heat flux for each cell is taken into account. In the same way, equation (2) gives a local HTC if the mean quality at half cell is considered. All the computational details to calculate h_c and h_f can be anyway found in literature [7] [8].

Schaffrath's model was developed for the investigation of the operation mode of the SWR1000 emergency condenser (NOKO test facility) [1] [9]. It uses the flow regime map of Tandon for the determination of the actual flow regime and switches to flow regime semi-

empirical correlation for the calculation of HTC: Soliman for spray flow [10], Nusselt for laminar annular flow, Kosky and Staub for turbulent annular flow, Rufer and Kezios for stratified flow, Breber for slug-plug flow. The parameters chosen to identify the flow pattern are the dimensionless vapour velocity j^*_D and the volume ratio of liquid and gas in a cross-sectional area $(1-\alpha)/\alpha$.

4.2 Modelling of condensation in a vertical tube

In a vertical pipe condensation takes place with a condensate film growing up in contact with the wall, while vapour phase flows along the bulk of the channel; according to Nusselt's approximation, the condensation occurs just at the interface (and only conductive processes are considered within the film) [6]. Many methods have been proposed for predicting the film condensation heat transfer coefficient; these range from empirical or semiempirical correlations to highly sophisticated analytical treatments of the transport phenomena.

In this paper the distinction of film condensation into three different regimes has been provided, according to the different physical phenomena which can occur: laminar, laminar wavy and turbulent. The main parameter which governs the process is the condensate velocity, expressed by its Reynolds number Re_l. Resulting:

$$\mathrm{Re}_l = \frac{4\Gamma_l}{\pi D_i \mu_l} \tag{5}$$

where Γ_l is the liquid flowrate, to be expressed according to an only liquid approach:

$$\Gamma_l = \Gamma(1-x) \tag{6}$$

- *Laminar* $\mathrm{Re}_l < 30$:

In the laminar region, condensation HTCs decrease with increasing film thickness due to the increased thermal resistance. Nevertheless, the laminar condensation occupies a very short portion of the tube and can be so neglected in the calculations. Nusselt correlation (i in *Tab.1*), which can be derived analytically by solving the momentum and the energy equations inside the condensate layer, is valid in case of laminar film.

- *Laminar wavy* $30 < \mathrm{Re}_l < \mathrm{Re}_{tr} = 4658\,\mathrm{Pr}_l^{-1.05}$:

When the film becomes wavy, HTCs (again a decreasing function of film thickness) grow up because the waves promote turbulence in the film and increase heat exchange surface [11]. Re_{tr} represents the transition value between laminar (wavy) and turbulent film condensation. Kutateladze correlation (ii in *Tab.1*) is recommended.

- *Turbulent* $\mathrm{Re}_l > \mathrm{Re}_{tr} = 4658\,\mathrm{Pr}_l^{-1.05}$:

Once the film has become turbulent, the highest HTCs are provided; the trend is now different from previous case (i.e. an increasing function of film thickness) due to the fact that mixing effects exceed the greater thermal resistance. Two different semiempirical correlations due respectively to Labuntsov (iii in *Tab.1*) and Chen (iv in *Tab.1*) can be applied [12] [13].

All these correlations, listed in the first column of *Tab.1*, give a local HTC value. Sometimes, especially in design applications, a general expression giving an average heat transfer coefficient is more useful. The easiest way to evaluate the average heat transfer coefficients is to integrate the equations for local coefficients along the tube length, resulting:

$$\bar{h}_L = \frac{1}{L}\int_0^L h(s)ds \tag{7}$$

	Local heat transfer coefficient		Average heat transfer coefficient	
Nusselt	$h_{lam} = k_l \left(\frac{\nu_l^2}{g} \right)^{-1/3} 1.1 \mathrm{Re}_l^{-1/3}$	(i)	$\bar{h}_{lam} = k_l \left(\frac{\nu_l^2}{g} \right)^{-1/3} 1.47 \mathrm{Re}_L^{-1/3}$	(vi)
Kutateladze	$h_{lam\_wavy} = k_l \left(\frac{\nu_l^2}{g} \right)^{-1/3} 0.756 \mathrm{Re}_l^{-0.22}$	(ii)	$\bar{h}_{lam\_wavy} = k_l \left(\frac{\nu_l^2}{g} \right)^{-1/3} \frac{\mathrm{Re}_L}{1.08 \mathrm{Re}_L^{1.22} - 5.2}$	(vii)
Labuntsov	$h_{turb} = k_l \left(\frac{\nu_l^2}{g} \right)^{-1/3} 0.023 \mathrm{Re}_l^{0.25} \mathrm{Pr}_l^{0.5}$	(iii)	$\bar{h}_{turb} = k_l \left(\frac{\nu_l^2}{g} \right)^{-1/3} \frac{\mathrm{Re}_L}{8750 + 58 \mathrm{Pr}_l^{-0.5} \left(\mathrm{Re}_L^{0.75} - 253 \right)}$	(viii)
Chen	$h_{turb} = k_l \left(\frac{\nu_l^2}{g} \right)^{-1/3} 0.00402 \mathrm{Re}_l^{0.4} \mathrm{Pr}_l^{0.65}$	(iv)	$\bar{h}_{turb} = k_l \left(\frac{\nu_l^2}{g} \right)^{-1/3} \left(\mathrm{Re}_L^{-0.44} + 5.82 \cdot 10^{-6} \mathrm{Re}_L^{0.8} \mathrm{Pr}_l^{1/3} \right)^{1/2}$	(ix)
Shah	$h_{turb} = h_l \left[(1-x)^{0.8} + \frac{3.8 x^{0.76} (1-x)^{0.04}}{p_r^{0.38}} \right]$	(v)	$\bar{h}_{turb} = h_l \left(0.55 + 2.09 p_r^{-0.38} \right)$	(x)

Tab.1- *List of the correlations presented for the evaluation of local and average HTCs during condensation inside a vertical tube.*

The correlations proposed for the evaluation of a mean HTC, according to the different flow regimes, are listed in the second column of *Tab.1*. Also the local and the average versions of Shah correlation are reported. This is an empirical correlation based on a wide range of experimental data, and mostly considered as the best correlation for the turbulent film condensation heat transfer both in horizontal, vertical and inclined pipes. It is based on a liquid only approach, referring the two-phase HTC to the single-phase coefficient computed with Dittus-Boelter correlation assuming all the flowrate being liquid [14]. Nevertheless, the validity of Shah correlation is questionable for high pressure and large diameter tube applications with water, as has been recently experimentally confirmed by Kim [15]. Furthermore, this correlation predicts a decreasing HTC with decreasing quality, exactly the opposite trend of film condensation theory. It is also questionable how the same correlation could be suitable for all the flow orientations, since it has been widely seen how the physical phenomena involved are different.

5 CALCULATION RESULTS

In order to test the proposed models of condensation, the data of SBWR Isolation Condenser (IC) mean tube design have been taken as reference. The aim is to show with simple calculations (without the utilization of a code) how a vertical pipe can guarantee the highest HTCs during condensation, as well as the best trend (i.e. increasing along the tube abscissa).

The considered mean tube (with an inner diameter of 46.2 mm and an outer diameter of 50.8 mm) is submerged in a pool of boiling water at 100°C; it is made up of INCONEL 600 (17.4 W/mK of thermal conductivity), and its inlet conditions are represented by saturated steam at 72.4 bar. The utilization of this HX in the EHRS of IRIS has been taken into account. Thus, following design prescriptions, two units of the condenser (with 120 tubes each one) have to exchange altogether a thermal power of 35 MW; fouling effects for both internal and external side (with an additional thermal resistance of $5 \cdot 10^{-5}$ m^2K/W), plus a possible plugging of the 5% of the tubes, are also considered. Resulting a flowrate per tube of 0.103 kg/s, giving a mass flux G equal to 61.47 kg/sm^2.

Working out from the real contest to which these data are reported and evaluating just a flow in a horizontal tube, such value of mass flux leads to a stratified pattern. Heat transfer coefficient trend along the pipe has been reconstructed, applying first Thome's analysis and then Schaffrath's model, switching to the proper correlation (Rufer and Kezios formula). Also an indication of the tube length needed to achieve saturated liquid at outlet has been given. A total tube length of about 2.50 m results. As it is shown in *Fig.10*, a very good agreement can be observed between the two different models: an average heat transfer coefficient of around 5500 W/m^{2}K occurs along almost the entire length, except for the end, where the sump effects become dominant and oppose the heat transfer. Besides, in the final part of the pipe (corresponding to low qualities), the Schaffrath's analysis suggests the possibility of a slug-plug flow (when x<0.1), which could induce instabilities. Thus, the condensation in a horizontal tube is not a so confident phenomenon, since these instabilities could create some problems during the condenser working.

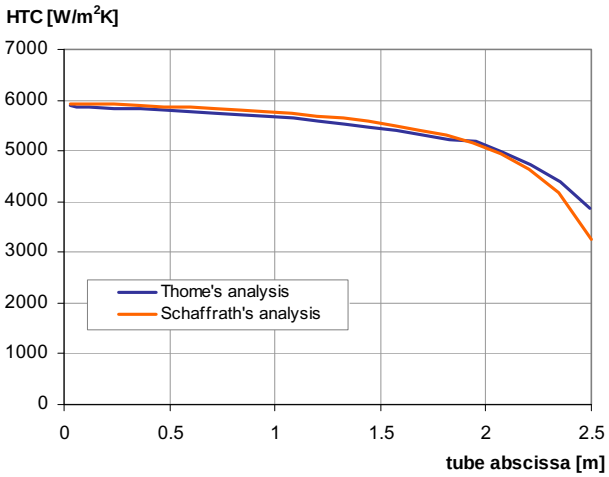

Fig.10- *Comparison between Thome's analysis and Schaffrath's analysis in stratified flow* [G=61.5 kg/sm^2].

The other condensation regimes, which can occur in a horizontal tube according to the different values of flowrate, have been investigated with Fortran simple codes. Two different values for inlet flowrate have been considered: 0.7 kg/s (giving a dominant annular flow) and 1.5 kg/s (inducing a mist flow at the beginning of the pipe). The outputs of the implementations are reported in *Fig.11* and *Fig.12*. The calculations have been provided considering all the water properties at 72.4 bar.

The condensation models proposed for the vertical tube have been then tested. Resulting a pipe length of 2.17 m as regards the film condensation, and of 3.04 m for the Shah correlation. Since the first model is surely more trustworthy, being based on physical principles, it appears evident how for the IC conditions of pressure, flowrate and tube diameter (globally representative of the typical conditions for the working of an in-pool immersed HX in a natural circulation loop), the Shah's model broadly under-predicts the

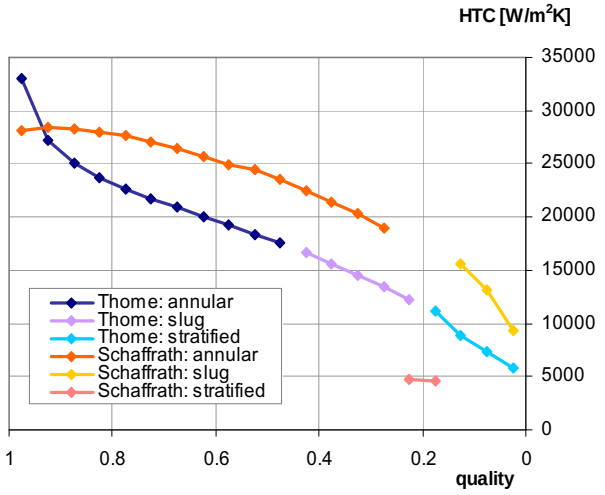

Fig.11- *Comparison between Thome's analysis and Schaffrath's analysis with dominant annular flow* [G=417.6 kg/sm^2].

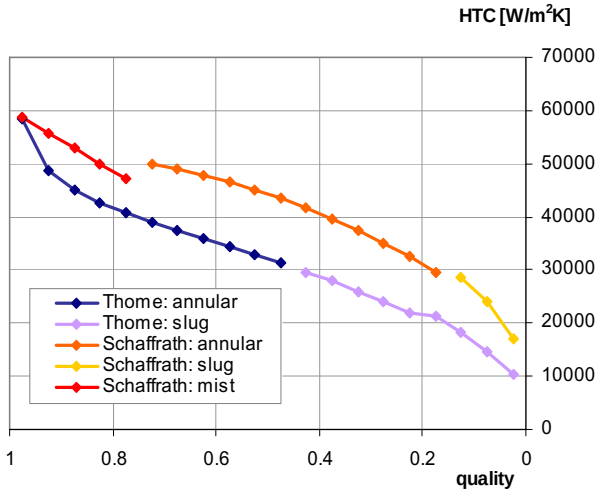

Fig.12- *Comparison between Thome's analysis and Schaffrath's analysis at very high flowrates* [G=984.8 kg/sm^2].

condensation HTC. Furthermore, an opposite trend of turbulent heat transfer coefficient with quality decrease has been confirmed between the two models (increasing for film condensation, but decreasing for Shah's model). The comparison is given by the graphs reported in *Fig.13* and *Fig.14*. In film condensation, laminar zone is absolutely negligible, and laminar wavy portion (with its decreasing trend of HTC with tube abscissa) lasts up to a quality value of 0.95. As regards turbulent zone, both Labuntsov and Chen correlations have been considered; the latter leads to lower HTCs appearing more conservative (and thus it has been used in the sizing calculations). Chen correlation proposed for the mean HTC along the tube (ix in *Tab.1*), gives a value of about 8000 W/m^{2}K. It is clear how the vertical tube is in position to assure better performance; a direct consequence of this is the greater length required by horizontal tubes for a complete condensation of the steam (i.e. 2.50 m against the 2.17 m of the vertical model).

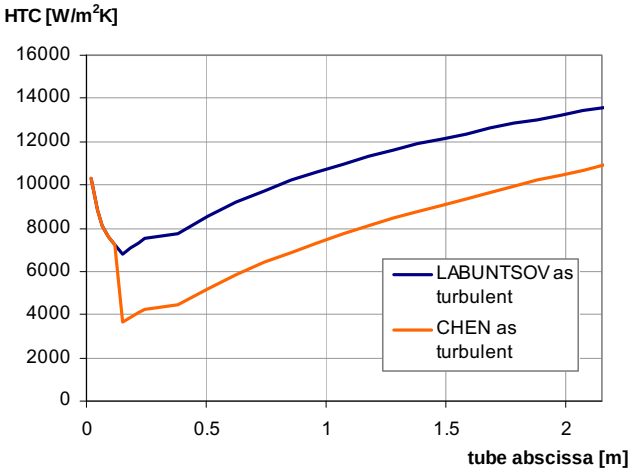

Fig.13- *Condensation HTC along the tube abscissa, according to condensation film theory* [G=61.5 kg/sm^2].

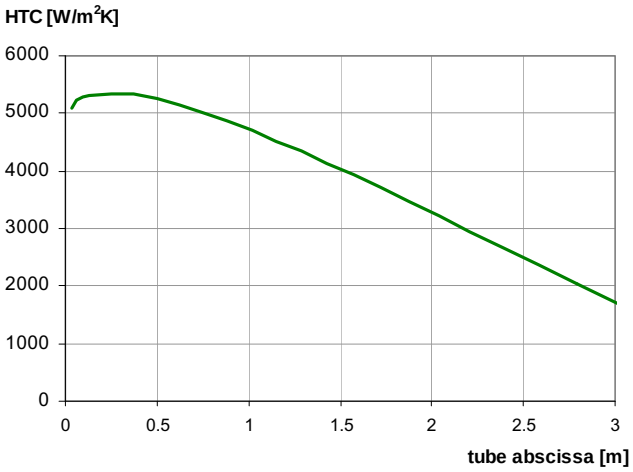

Fig.14- *Condensation HTC along the tube abscissa, according to Shah correlation* [G=61.5 kg/sm^2].

6 SHORT REVIEW ON EXPERIMENTAL FACILITIES

A critical discussion on the best solution for a decay heat removal HX cannot go without a short description of the experimental work found on this matter in literature.

For the experimental investigation of the SWR1000 emergency condenser effectiveness, the NOKO test facility has been constructed at the Forschungszentrum Jülich. The condenser operation conditions were determined as a function of the primary and pool pressure, characterizing the tube surface available for condensation by studying the geodetic pressure drops variation as a consequence of vessel water level decrease. A single tube test, besides, was provided to clarify the condensation flow regimes inside a horizontal tube and to validate Tandon's flow map condensation model (reproduced in *Fig.8*). This work led to the improvement of ATHLET thermalhydraulic code, implementing the correlations discussed at the end of paragraph 4.1 [9].

The large scale PANDA facility was constructed at the Paul Scherrer Institute (PSI) for the investigation of both overall dynamic response and the key phenomena of passive containment systems. The major aspect of the tests dealt with the evaluation of the ESBWR PCCS performance in case of main steam line break. As regard the condensation issues, PANDA facility was very useful for studying the degradation of HTC in presence of non-condensable gasses, both lighter than steam (hydrogen, simulated by helium), and heavier (nitrogen or air). The provided tests permitted furthermore to extend the data base available for containment analysis code qualification [16] [17].

The VISTA facility was instead developed by the KAERI to simulate the primary and secondary systems as well as the PRHRS of the SMART reactor. An attractive objective was to confirm the capability of MARS code to predict the overall thermalhydraulic behavior of the PRHRS. An important outcome was that the code under-predicted the heat transfer at the heat exchanger [5]. The condensation model used in the code, exactly the same of that implemented in RELAP5 code, considers the maximum value between the Nusselt correlation (7) for the laminar flow and the Shah correlation (v in *Tab.1*) for the turbulent flow. The most suitable heat transfer correlations proposed in the paper are thus required to be implemented in these codes.

The reliability of the active valves involved in the passive systems actuation is fundamental. A new concept of valve liquid side, instead of steam side in the primary system, located on a line connecting two pools at the bottom, has been proposed in the PERSEO facility, developed in SIET labs (Piacenza) for testing a full scaled module for the GE-SBWR in-pool heat exchanger. The valve (named triggering valve) is closed during normal operation and the pool containing the heat exchanger (HX pool) is empty; the other pool (Overall pool) is full of cold water. In emergency conditions the valve is opened and the heat exchanger is flooded, with consequent heat transfer from the primary side to the pool. The effectiveness of the actuation valve movement from the high pressure primary side of the reactor to the low pressure pool side, has been tested during the experimental campaign, both in steady and in unsteady conditions [18].

6.1 Experimental results from PERSEO facility

The strong collaboration between POLIMI and SIET made possible the analysis of the experimental data collected during the PERSEO campaign. In particular, the greater interest focused on the condenser performance. Some tubes were monitored with wall thermocouples (K-type, nominal accuracy of ±1.5°C), mounted on the outer surface at three different axial positions: at the top, at the middle and at the end of the pipe. The circuit pressure (equal to 7 MPa) was measured with a pressure transmitter installed inside the HX upper header, whereas primary flowrate (on average 0.1 kg/s per tube) was measured by an orifice differential pressure transmitter (with an uncertainty of ±0.25% of the instrument full scale). Due to the lack of accuracy of fluid thermocouples, saturated steam has been considered at condenser inlet and saturated liquid at outlet. This assumption permitted to calculate the exchanged thermal power, and then to obtain the local heat flux needed for the computation of the heat transfer coefficients. The saturation temperature at the circuit pressure has been adopted as fluid bulk temperature, while the inner wall temperature has been calculated by the external tube value (measured) considering the thermal jump in the metal. Resulting:

$$T_{w,\mathrm{int}} = T_{w,ext} + \frac{D_i \ln\left(D_e / D_i\right)}{2k_{tube}} \Phi_i \tag{8}$$

The local heat flux value Φ and the local HTC h_{cond} have been obtained by solving the following equation system, where $T_{w,int}$ must be calculated according to equation (8):

$$\begin{cases} U_i = \dfrac{\Phi}{T_{sat,\mathrm{int}} - T_{sat,ext}} = \left(\dfrac{1}{h_{cond}} + \dfrac{D_i \ln\left(D_e / D_i\right)}{2k_{tube}} + \dfrac{1}{h_{pool}} \dfrac{D_e}{D_i} \right)^{-1} \\ \dfrac{\Phi}{T_{sat,\mathrm{int}} - T_{w,\mathrm{int}}} = h_{cond} \end{cases} \tag{9}$$

The reference is the situation depicted in *Fig.15*. The results are presented in *Fig.16*, where the HTC trend according to film condensation theory (in particular, Kutateladze correlation for the laminar wavy zone and Chen correlation for the turbulent zone) and to a semi-empirical model proposed by Kim et al. [15] are also reported. It is pointed out that the experimental work of Kim was the only one found in literature dealing with a large diameter vertical tube used for condensing high pressure steam; in particular, the test section consisted in a tube with the same geometrical features of the SBWR IC tested in the PERSEO facility (i.e. outer diameter of 50.8 mm, thickness of 2.3 mm and length of 1.8 m). A turbulent film condensation model based on the similarity between the single-phase turbulent convective heat transfer and the annular film condensation heat transfer has been developed. For any computational detail, refer to [15].

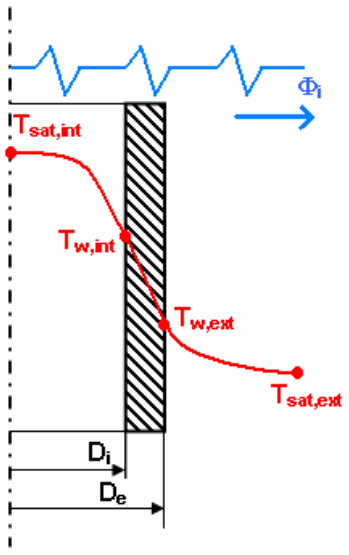

Fig.15- *Sketch of the heat transfer and of temperatures distribution in a single tube.*

The graph in *Fig.16* reveals that only at the end of the tube a remarkable shifting between theory and experimental data is present; this is maybe due to the fact that when the void fraction falls down (exactly at the bottom of the pipe), the liquid film at the wall cannot be considered thin anymore, and thus the conditions for the applicability of the presented theory fail. *Fig.17* shows the comparison of the PERSEO data with the ones found in literature; the model proposed by Kim and the Shah correlation (v in *Tab.1*) are considered in order to predict the experimental values. The new data are slightly bigger than Kim ones; this should be due to the higher condensate Reynolds numbers reached in PERSEO facility. The order of magnitude is however well captured. Anymore, both the data bases confirm that the Shah model is not accurate to deal with the condensation phenomena at high pressure, whereas the turbulent annular model proposed gives more reasonable results.

At the end, the film condensation model based on Kutateladze correlation (ii) and Chen correlation (iii) is considered to predict PERSEO data. The results are reported in *Fig.18*. The set of correlations proposed in this paper gives the best agreement with PERSEO data, while the turbulent annular condensation model proposed by Kim fails at low qualities. Except for the tube inlet (high qualities), the Shah model broadly under-predicts the condensation HTC.

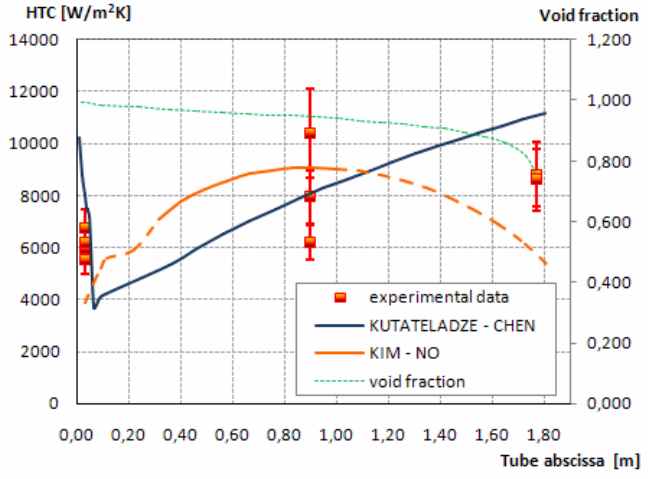

Fig.16- *Comparison of PERSEO facility condensation data with film condensation theory and Kim model [15].*

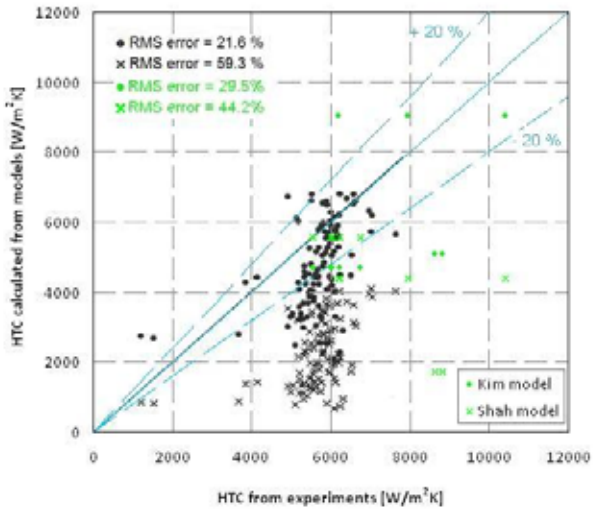

Fig.17- *Comparison between PERSEO facility data (green) and Kim data (black) [15].*

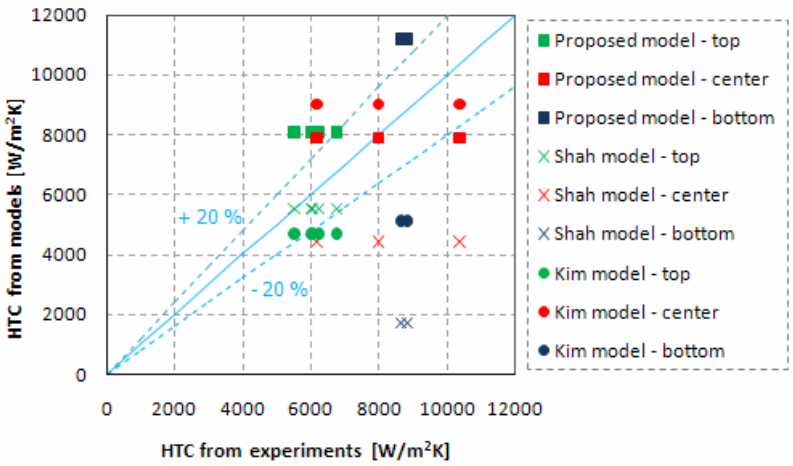

Fig.18 - *Comparison of condensation models with the PERSEO data.*

7 CONCLUSIONS

A review on the concept of in-pool condenser for passive safety systems has been carried out in the first part of the paper. A preponderance of vertical tubes arrangement solutions has been pointed out; the main advantages offered by a vertical configuration are:

- higher heat transfer coefficients (even doubled with respect to the horizontal solution);
- better and more predictable in-tube flow distribution.

In order to prove the better thermalhydraulic performance of condensation in a vertical pipe, the most updated and reliable models for condensation in horizontal and vertical tubes have been found in literature and tested. As regards the horizontal pipe, two methods of analysis have been focused. The first is due to Thome and, distinguishing between annular, stratified and stratified wavy regimes, considers two heat transfer mechanisms: convective condensation and film condensation. The second method has been proposed by Schaffrath, and it is based on Tandon's map. Condensation in a vertical pipe is instead dealt according to a physical principle analysis based on the film condensation theory. In this paper the distinction of film condensation into three different regimes has been provided: laminar, laminar wavy and turbulent. Suitable correlations for each regime have been proposed.

A comparison between all the models has been provided by means of simple Excel/Matlab codes, referring to the SBWR IC mean tube data, considering the utilization of this condenser for the IRIS EHRS. A stratified flow is induced in case of horizontal tube; resulting a quite constant value of HTC (around 5500 W/m^{2}K), except for the end, when the sump effects become dominant. Film condensation theory have been then applied for a vertical pipe. The establishing of turbulence is responsible for the dominant increasing trend. Chen correlation indicates a mean HTC clearly bigger (around 8000 W/m^{2}K). A direct consequence of this fact is the minor length required for completely condensing the entering steam (resulting 2.17 m against the 2.50 m of a horizontal tube).

A strong corroboration of the model proposed in this paper for the condensation inside a vertical tube came from the analysis of PERSEO experimental campaign results. The trend of HTC along the tube abscissa has been reconstructed for the condenser tubes provided with wall thermocouples. The results, in good accordance with a previous experimental work due to Kim et al., indicate an increasing trend going down along the tube, definitely confuting Shah model predictions. The correlations selected in the paper as regards the vertical tubes configuration, appear finally the most reliable, proposing themselves for a possible future implementation in the best-estimate thermalhydraulic codes, as RELAP.

REFERENCES

[1] A. Schaffrath, A.-K. Krüssemberg, A. Fjodorow, U. Gocht, W. Lischke – *Modelling of condensation in horizontal tubes* – Nucl. Eng. Des., 204 (2001) 251-265.

[2] H.J. Kahn, U.S. Rohatgi – *Performance characterization of Isolation Condenser of SBWR* – Brookhaven National Laboratory Upton, NY 11973, 1992.

[3] S.J. Cho, B.S. Kim, M.G. Kang, H.G. Kim – *The development of passive design features for the Korean Next Generation Reactor* – Nucl. Eng. Des., 201 (2000) 259-271.

[4] M.D. Carelli, L.E. Conway, L. Oriani, B. Petrovic, C.V. Lombardi, M.E. Ricotti, A.C.O. Barroso – *The design and safety features of the IRIS reactor* – Nucl. Eng. Des., 230 (2004) 151-167.

[5] Y.-J. Chung, H.-C. Kim, B.-D. Chung, M.-K. Chung, S.-Q. Zee – *Two phase natural circulation and the heat transfer in the passive residual heat removal system of an integral type reactor* – Annals of Nuclear Energy, 33 (2006) 262-270.

[6] F.P. Incropera, D.P. Dewitt, T.L. Bergman, A.S. Lavine – *Fundamentals of heat and mass transfer* – Sixth Edition, John Wiley & Sons, 2007.

[7] J. El Hajal, J.R. Thome, A. Cavallini – *Condensation in horizontal tubes, part 1: two-phase flow pattern map* – Int. J. Heat Mass Transfer, 46 (2003) 3349-3363.

[8] J.R. Thome, J. El Hajal, A. Cavallini – *Condensation in horizontal tubes, part 2: new heat transfer model based on flow regimes* – Int. J. Heat Mass Transfer, 46 (2003) 3365-3387.

[9] A. Schaffrath, E.F. Hicken, H. Jaegers, H.-M. Prasser – *Operation conditions of the emergency condenser of the SWR1000* – Nucl. Eng. Des., 188 (1999) 303-318.

[10] H.M. Soliman – *The mist-annular transition during condensation and its influence on the heat transfer mechanism* – Int. J. Multi-Phase Flow, 12 (1986) 277-288.

[11] S.S. Kutateladze – *Fundamentals of heat transfer* – Academic Press, New York, 1963.

[12] D.A. Labuntsov – *Heat transfer in film condensation of pure steam on vertical surfaces and horizontal tubes* – Teploenergetika, 4, 72, 1957.

[13] S.L. Chen, F.M. Gerner, C.L. Tien – *General film condensation correlations* – Exp. Heat Transfer, Vol.1 1987, pp. 93-107.

[14] M.M. Shah – *A general correlation for heat transfer during film condensation inside pipes* – Int. J. Heat Mass Transfer, 22 (1979) 547-556.

[15] S.J. Kim, H.C. No – *Turbulent film condensation of high pressure steam in a vertical tube* – Int. J. Heat Mass Transfer, 43 (2000) 4031-4042.

[16] N. Aksan – *Overview on PANDA test facility and ISP-42 PANDA tests data base* in *Natural circulation in water cooled power plants* – IAEA November 2005, IAEA-TECDOC-1474.

[17] T. Bandurski, M. Huggenberger, J. Dreier, C. Aubert, F. Putz, R.E. Gamble, G. Yadigaroglu – *Influence of the distribution of noncondensibles on passive containment condenser performance in PANDA* – Nucl. Eng. Des., 204 (2001) 285-298.

[18] R. Ferri, A. Achilli, G. Cattadori, F. Bianchi, P. Meloni – *Design, experiments and RELAP5 code calculations for the PERSEO facility* – Nucl. Eng. Des., 235 (2005) 1201-1214.

Ansaldo Research Activities on Critical and Sub-critical Lead Reactors

Monica Frogheri, Alessandro Alemberti, Luigi Mansani
Ansaldo Nucleare
Corso Perrone, 25 16152 Genova, Italy
monica.frogheri@ann.ansaldo.it, alessandro.alemberti@ann.ansaldo.it,
luigi.mansani@ann.ansaldo.it,

ABSTRACT

The Generation IV International Forum (GIF) member countries, identified the six most promising advanced reactor systems and related fuel cycle as well as the R&D necessary to develop these concepts for potential deployment. Among the promising reactor technologies for fast reactors (Sodium and Lead Fast Reactors) being considered by the GIF, the LFR has been identified as a technology with great potential to meet the needs for both remote sites and central power stations.
Ansaldo Nucleare, with its past experience on fast reactors, is promoting research and development of a pure Lead cooled fast reactor as the coordinator of the ELSY project (European Lead SYstem) funded by the European Commission in the frame of the sixth framework program.
Activities are being carried out by Ansaldo Nucleare also on waste transmutation as part of another sixth framework program funded project: IP-EUROTRANS. The project aims to the conceptual design of an European Facility for Industrial Transmutation (EFIT), and the detailed design of a prototype of a smaller eXperimental Transmutation in an Accelerator Driven System (XT-ADS), an irradiation facility to be constructed in the short term for demonstration of key features of the larger EFIT.
The paper presents a summary of the two projects, with the description of the main components of ELSY reactor and EFIT and XT-ADS facilities, with a particular reference to the parts of projects developed by Ansaldo Nucleare.

1 INTRODUCTION

Concerns over energy resource availability, climate change, air quality, and energy security suggest an important role for nuclear power in future energy supplies. While the current Generation II and III nuclear power plant designs provide an economically and publicly acceptable electricity supply in many markets, further advances in nuclear energy system design can broaden the opportunities for the use of nuclear energy (Figure 1). To explore these opportunities, the U.S. Department of Energy's Office (DOE) of Nuclear Energy has engaged governments, industry, and the research community worldwide in a wide-ranging discussion on the development of next-generation nuclear energy systems known as "Generation IV."

In January 2000, the Generation IV International Forum (GIF) was established to investigate innovative nuclear energy system concepts for meeting future energy challenges. GIF members included Argentina, Brazil, Canada, Euratom, France, Japan, South Africa,

South Korea, Switzerland, United Kingdom, and United States, with the OECD-Nuclear Energy Agency and the International Atomic Energy Agency as permanent observers. China and Russia signed the GIF Charter on 15 November 2006, bringing GIF membership to thirteen. The forum serves to coordinate international research and development on promising new nuclear energy systems for meeting future energy challenges.

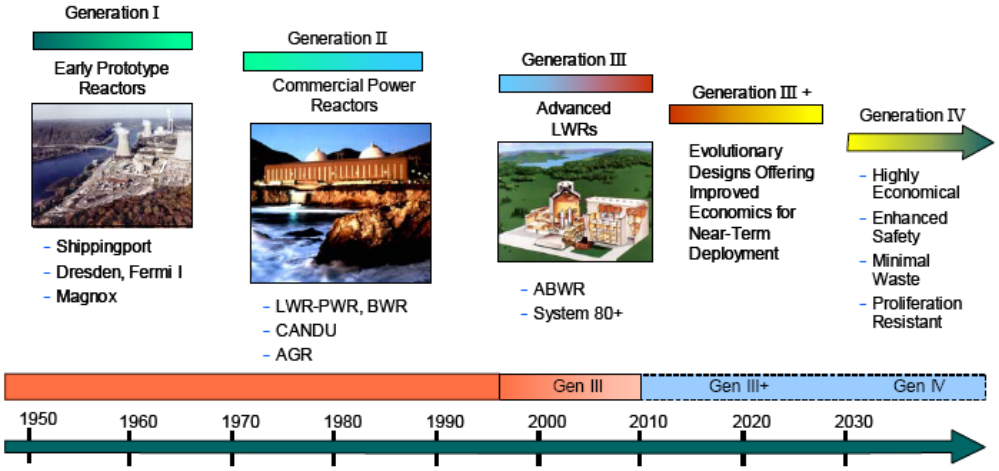

Figure 1: Evolution of nuclear energy systems

In 2001, the GIF agreed to proceed with the development of a Technology Roadmap [1] for Generation IV nuclear energy systems. The purpose of the roadmap was to identify the most promising nuclear energy systems (consisting of both a reactor and fuel cycle) for meeting the challenges of safety, economics, waste, and proliferation resistance.

The Generation IV roadmap process culminated in the selection of six most promising Generation IV systems: Gas-Cooled Fast Reactor System (GFR), Lead-Cooled Fast Reactor System (LFR), Molten Salt Reactor System (MSR), Sodium-Cooled Fast Reactor System (SFR), Supercritical-Water-Cooled Reactor System (SCWR), Very-High-Temperature Reactor System (VHTR).

Among the above promising reactor technologies, the Lead Fast Reactor (LFR) has been identified as a technology with great potential to meet needs for both remote sites and central power stations. The LFR system features a fast-neutron spectrum and a closed fuel cycle for efficient conversion of fertile uranium and management of actinides. A full actinide recycle fuel cycle with central or regional fuel cycle facilities is envisioned. The LFR can also be used as a burner of actinides from spent fuel by using inert matrix fuel. A burner/breeder could use thorium matrices. The system considered by GIF would use either lead or Lead/Bismuth Eutectic (LBE) as the liquid-metal coolant for the reactor.

A major step in favour of the LFR, occurred when EURATOM decided to fund ELSY [2] (the acronym for the European Lead cooled System) - a Specific Targeted Research Project of the 6th European Framework Program (FP6) – proposed to investigate the economical feasibility of a lead-cooled, critical reactor of 600 MWe power for nuclear waste transmutation. The ELSY project, scheduled to last three years, aims at demonstrating the possibility to design a competitive and safe Lead-cooled fast power reactor using simple engineered features. The use of compact, in-vessel steam generators and a simple primary circuit with all internals possibly being removable are among the reactor features needed for competitive electric energy generation and long-term protection of investment.

Ansaldo Nucleare has gained considerable expertise on heavy liquid metal coolants (initially on LBE and, currently, also on Lead) in the frame of R&D activities on

transmutation of Long Lived radioactive waste (Minor Actinides - MA - as well as some Long Lived Fission Products -LLFP).

Following a preliminary design developed in 1998, which was based on the Energy Amplifier concept proposed by CERN [3], a first configuration of a Lead-Bismuth Eutectic cooled Experimental ADS (LBE-XADS) [4] was worked out in the period 1999-2001 by a group of Italian organizations led by Ansaldo Nucleare, with the aim of assessing the feasibility of a small-sized (80 MWth) ADS.

The activity continued within the 5th Framework Program of the European Commission, in the context of the research on Fission Reactors Safety, that funded a project named PDS-XADS (Preliminary Design Studies of an Experimental Accelerator Driven System) [5] with a three-year contract (2002-2004) involving the participation of 25 European partners (industries, research organizations and Universities). The PDS-XADS Project was the first major step of a joint European effort that, as a key-milestone, did allow the detailed design of an XADS for demonstration of the transmutation technology by means of a subcritical reactor.

In the frame of the project IP EUROTRANS [6] of the 6th FP of the EU, 51 European Organizations have the strategic R&D objective to pursue forward an ETD in a step-wise manner. The aim of the 4-year (from April 2005 to March 2009) IP-EUROTRANS project is twofold: develop the conceptual design of an European Facility for Industrial Transmutation (EFIT) [7] with a pure lead-cooled reactor; carry out the detailed design of the smaller eXperimental Transmutation in an ADS (XT-ADS) [8] as irradiation facility and for demonstration of key features of EFIT

In the following sections, more details on ELSY and EUROTRANS Projects are reported and the description of reference configuration of ELSY reactor and of EFIT and XT-ADS facilities is provided. Particular relevance is given to the parts of projects developed by Ansaldo Nucleare.

2 THE ELSY PROJECT

The goal of the Specific Targeted Research Project " European Lead-cooled System (ELSY)" performed in the frame of the 6th Framework Programme (FP) is to investigate the potential of the lead-cooled fast critical reactor to transmute nuclear waste, assessing its advantages and disadvantages, and assess the critical scientific issues and the technical feasibility of the lead-cooled fourth generation reactor system and the fuel cycle.

The project is structured to confirm the compliance with the main GEN IV requirements. Beside the goals of sustainability, safety and Proliferation Resistance and Physical Protection, emphasis is given to economics in order to always keep the capital cost under control.

Ansaldo Nucleare is the project coordinator, it has in charge the design of the main components/systems (such as the Reactor Vessel, the Steam Generators, the Primary Pumps, the Secondary System and the Decay Heat Removal System). Moreover, Ansaldo Nucleare contributes to the Design objectives, to the cost estimates, to the future R&D needs and to the compliance with the waste transmutation in a critical reactor and with the more general goals of Generation IV, to the system integration (Reactor Assembly configuration, Plant Layout, and the Application of Digital Engineering Technology) and to the Safety and to the transient analysis.

2.1 ELSY preliminary configuration

The configuration of the primary system is pool-type, similar to the design adopted for most sodium-cooled reactors and of the XADS design. The pool design has important

beneficial features, verified by the experience of design and operation of sodium-cooled fast reactors. These include a simple low temperature boundary containing all primary coolant, the large thermal capacity of the coolant in the primary vessel, a minimum of components and structures operating at the core outlet temperature.

The primary coolant is pure lead, characterized by good nuclear properties and no fast chemical reaction with water and air, instead of Lead-Bismuth Eutectics (LBE). Since lead is much more abundant (and less expensive) than bismuth, in case of deployment of a large number of reactors, pure lead as coolant offers enhanced sustainability. Furthermore, the use of lead strongly reduces the production of the highly radioactive, and hence decay-heat generating polonium in the coolant with respect to LBE.

The ELSY power plant is sized at 600 MWe because only plants of the order of several hundreds MWe are expected to be economically affordable on the existing, well-interconnected grids of Europe.

The choice of a large reactor power suggests the use of forced circulation to shorten the reactor vessel, thereby avoiding excessive coolant mass and alleviating mechanical loads on the reactor vessel. Thanks to the favorable neutronic characteristics of lead, the fuel pins of a lead-cooled reactor, similarly to LWRs, can be spaced apart, resulting in a lower pressure drop across the core. As a consequence, in spite of the higher density of lead, the pump head can be kept low (on the order of one to two bars) with a reduced requirement for pumping power.

A possible primary-side thermal cycle of 400°C/480°C in lead, without an Intermediate Cooling System, offers reduced risk of steel creep and milder thermal transients, while providing the thermal efficiency above 40% with a supercritical Rankine steam cycle at 240 bar, 450°C. The reactor vessel is designed to operate at the cold temperature of 400°C, which would be a safe condition even if oxygen control in the melt is temporarily lost. All reactor internals will have to operate at higher temperatures, at which it is necessary to rely on oxygen control, whereas fuel cladding could be surface-treated (aluminization seems to be a promising) for a greater safety margin. An improved primary-side thermal cycle at higher core outlet temperature could be adopted in the longer term, as new materials become available.

According to the predicted low primary system pressure loss and the favorable thermodynamic characteristics of lead, decay heat can be removed with lead in natural circulation in the primary system. A simple system for decay heat removal is the Reactor Vessel Air Cooling System (RVACS), which consists basically of an annular pipe bundle of U-pipes arranged in the reactor pit with atmospheric air flowing pipe-side in natural circulation. RVACS is a passive system, but its use without other systems can only be considered for small-size reactors since the vessel outer surface is relatively large in comparison with the reactor power. In the case of ELSY, the RVACS performance is sufficient only in the long term (after about one month after shut down) and two additional systems (under conception) are needed and will be implemented according to the stringent safety requirements of redundancy and diversification. A Reactor Pit Cooling System (RPCS) is additionally included for use during in-service inspection of the reactor vessel.

Figure 2 shows the cylindrical inner vessel concept, a scheme evaluated as a starting point for the primary system design of ELSY. The steam generator (SG) and primary pump (PP) assembly, consisting of two SG Units (SGUs) and one PP arranged between the SGUs and casing, is an integral part of the primary loop, i.e. from PP suction to SGU exit. Hot lead is pumped into the pool above the PP and SGU and driven shell-side downwards through the SGU tube bundle into the cold pool. The free level of the hot pool inside the casing is higher than the free level of the cold pool outside that is higher, in turn, than the free level of the hot pool above the core enclosed by the inner vessel.

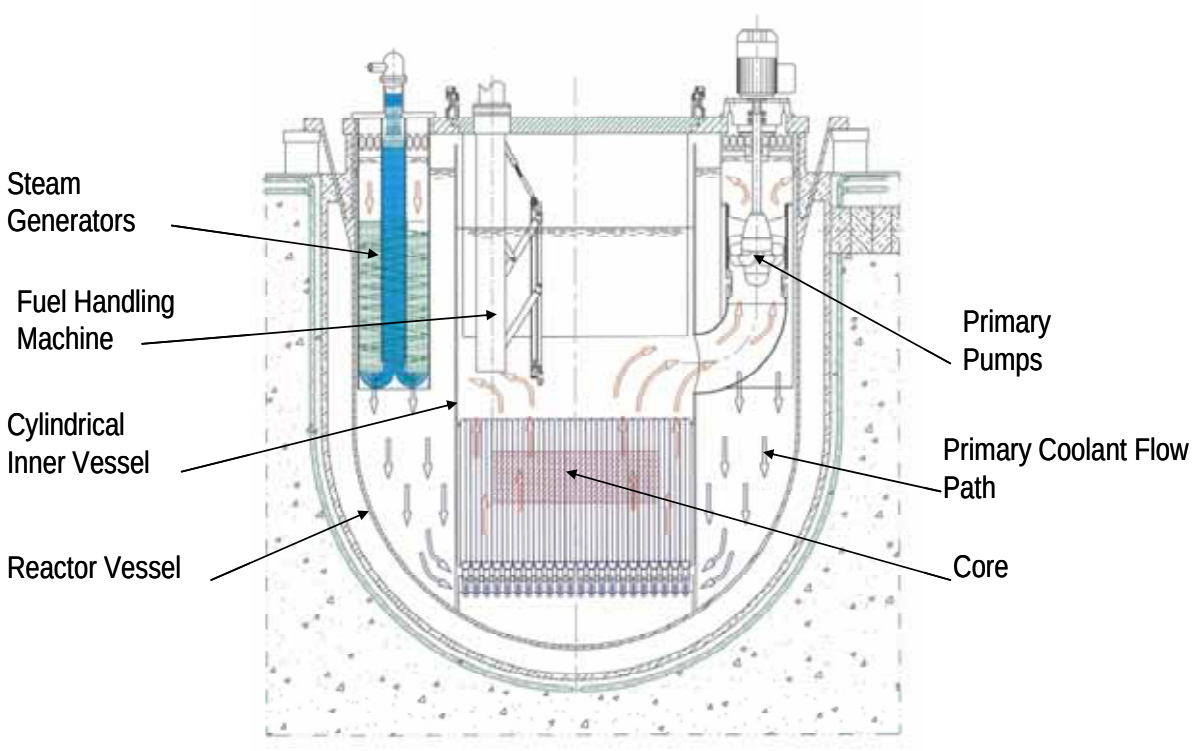

Figure 2: ELSY conceptual sketch

A free level difference of cold and hot collectors at normal operating condition of only 1-2 m is sufficient to feed the core, eliminating the complicated, pressurized core feed system typical of the pool-type, sodium-cooled reactors. Simplification of the internals will offer the possibility of removable in-vessel components, a provision for investment protection. Compactness of the reactor building is the result of reduced footprint and height. The reduced footprint is allowed by the elimination of the Intermediate Cooling System, the reduced elevation is the result of the forced circulation and of the design approach of reduced-height components.

2.2 Ansaldo contribution to ELSY Project

The following activities have been carried out by Ansaldo Nucleare in the frame of the preliminary design of ELSY reactor:

- Proposed Decay Heat Removal System:
  A high reliability Decay Heat Removal function is requested, since the complete function failure has to be practically eliminated. The PRA method (in future) will be used to confirm the overall architecture, today a more simple Line Of Defence (LOD) method is used: 2 strong and one medium LOD are requested to consider the event in the Residual Risk. On this basis, two Decay Heat Removal Systems are proposed, diverse, independent and characterized by high reliability
  - DHR N° 1: 4 Water Loops-Dip Coolers in the Cold Collector of the Primary System (improvement of the concept proposed by the Elsy partner Del Fungo). The total Heat Removal capacity is equal to 24 MW, so that 3 loops are sufficient to fulfill the Decay Heat removal function.
  - DHR N° 2: 4 Isolation Condenser connected to the Steam and Feed-water Lines of the Secondary System (same concept of EFIT, see Section 3.2.3)

- A preliminary functional sizing of primary pumps has been performed on the basis of an analytical approach and the resulting configuration has been verified with a CFD calculation using the CFX code (Figure 3)
- The thermo-mechanical verification of the vessel has been performed

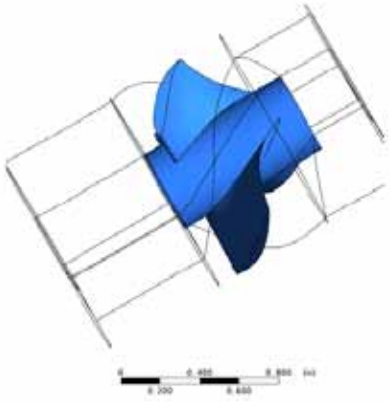

Impeller characteristics		Notes
Outside impeller diameter	1.1 m	To limit Reactor Vessel diameter
Hub diameter	0.43 m	
Impeller speed	140 rpm	Optimised for stable flow rate
Number of vanes	3	
Vane profile	NACA 23012	
Velocity in suction pipe	1.6 m/s	Less than the limit (2 m/s)
Velocity relative to the vane at vanes tip	8.7 m/s	Less than the limit (10 m/s)
Meridian velocity (at impeller entrance and exit)	3.1 m/s	Higher than the limit (2m/s), it implies pump hub and case of the same blades material

Figure 3: ELSY primary pump model and input characteristics

3 THE EUROTRANS PROJECT

Among the prior research and development topics of EURATOM 6th Framework Programme is the management of high-level nuclear wastes. A reference approach to reduce the burden on a geological repository is to remove the long-term radiotoxic isotopes occurring in the nuclear waste (Partitioning) and to burn them in dedicated systems (Transmutation). A promising system for the transmutation of the long-lived radioactive isotopes, as Pu and Minor Actinides (i.e. Am, Np), is a sub-critical system driven by an accelerator (ADS).

The implementation of partitioning and transmutation of a large part of the high level nuclear wastes in Europe needs the demonstration of the feasibility of several installations at an "engineering" level. This is the general objective of the integrated project EUROTRANS (European Research Programme for the Transmutation of High Level Nuclear Waste in an Accelerator Driven System).

To demonstrate the technical feasibility of an ADS, a two step approach has been developed. This approach foresees the definition of an advanced design of an eXperimental facility, which has the aim to demonstrate the technical feasibility of Transmutation in an Accelerator Driven System (XT-ADS). In parallel a conceptual design of a modular European Facility for Industrial Transmutation (EFIT) realisation in the long-term. Both designs bear the same fundamental system characteristics in order to allow

Ansaldo Nucleare is the coordinator of the Work Package related to the development and assessment of XT-ADS and EFIT Design, it has in charge the design of the main components/systems (such as the Reactor Vessel, the Steam Generators, the Primary Pumps, the Decay Heat Removal System for both XT-ADS and EFIT, the Secondary System and the Target of EFIT) and to the system integration (Reactor Assembly configuration, Plant Layout of EFIT). Moreover, Ansaldo Nucleare contributes to the design objectives, to the cost estimates, to the future R&D needs, and to the safety and transient analysis.

3.1 EFIT Primary System

The configuration of the primary system is pool-type, similar to the design solution adopted for most sodium-cooled reactors and of the previous XADS design. The pool concept allows to contain all the primary coolant within the Reactor Vessel, thus eliminating all problems related to out-of-vessel transport of the primary coolant. The pool design has important beneficial features, including a simple low temperature boundary containing all primary coolant, the large thermal capacity of the coolant in the primary vessel, a minimum of components and structures operating at the core outlet temperature.The primary coolant is molten lead, which is characterized by higher melting point than LBE or sodium.

The operating temperatures are: 400°C at core inlet (to have sufficient margin from the risk of lead freezing) and 480°C at core outlet. The core outlet temperature is chosen taking into account, on the one hand, the corrosion risk of structures in molten lead environment that increases with temperature (the current limit for candidate structural materials protected from corrosion by oxygen dissolved in the melt is about 500°C) and, on the other hand, considering that the outlet temperature cannot be too low because the associated increase of coolant flow rate would bring about unacceptable erosion of the structures. The proposed operating temperatures are, hence, a compromise between corrosion/erosion protection and performance.

The primary circuit is designed for effective natural circulation, i.e. relatively low pressure losses and driving force brought about by the core mid plane elevation arranged wide below the mid plane of the steam generators or, in case of emergency decay heat removal, the mid plane of the DHR dip coolers.

The speed of the primary coolant is kept low by design (less than 2 m/s), in order to limit the erosion. Wherever this cannot be complied with, e.g. at the tip of the propellers blades, the relative speed is kept lower than 10 m/s and appropriate construction materials are selected for qualification (among them, the machinable Ti_3SiC_2).

Protection of structural steel against corrosion is ensured, in general, by controlled activity of oxygen dissolved in the melt and additional coating for the hotter structures. Wherever stagnation of the primary coolant is predicted, e.g. within dummies, provisions ensure a minimum coolant flow.

The EFIT primary system (Figure 4) is described in the following sections, mainly referring to the systems designed by Ansaldo.

3.1.1 Reactor Vessel and Internal Structure

The Reactor Vessel is a welded structure without nozzles, made of a cylindrical shell with hemispherical bottom head and top Y-piece, both branches of which terminate with a flange. The conical, outer branch is flanged to, and hangs from, the Annular Structure anchored to the civil structure of the Reactor Cavity, whereas the inner branch supports the reactor roof. A cylindrical structure, welded inside on the vessel bottom head, is a radial restraint for inner vessel and core. All welds can be accessed for in-service inspection by means of remotely-operated vehicles.

The Internal Structure is located inside the Reactor Vessel and hangs from the Fixed Plate of the Reactor Roof. The functional parts welded together are the following

- Bottom Support: The Internal Structure ends at the bottom with a short cylindrical support, which engages with the support welded to the Reactor Vessel Bottom during installation and maintenance operations. In normal operation no connection between Internal Structure and Reactor Vessel exists.

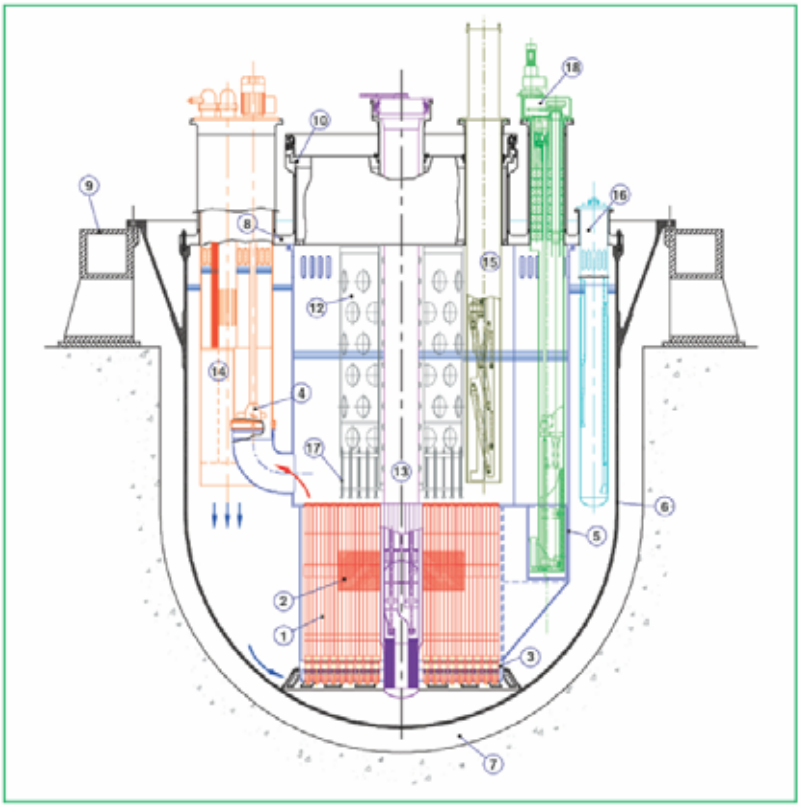

Figure 4: EFIT Primary System

- Diagrid: It is a very thick perforated plate with a large hole on its axis to centre the bottom of the target unit. The holes allow positioning all the fuel assemblies, and they are shaped to receive the subassembly spike with a little clearance. The diagrid holes have a conical shape to facilitate the assembly spike insertion, and to accommodate the assembly transition cone.
- Inner Vessel with upper core restraint plate: it has the following main functions: separates the Core Region and the above Core Volume from the Downcomer, houses the Core, the Above Core Structure and the In Vessel Fuel Handling System, limits the Core Assemblies oscillations due to seismic accelerations. The Inner Vessel is welded to the upper side of the diagrid. It ends with a flange by which it is connected to the fixed plate of the Reactor Roof. The Inner Vessel delimitates two distinct plena: a lower plenum between diagrid and core restraint plate (and assembly heads), where the main primary coolant flow path takes place and an upper plenum of almost stagnant primary coolant, formed by an upstanding of larger cross section than the lower part of the Inner Vessel, welded to the core restraint plate and connected to the Reactor Roof by means of a flange.
- Elbow connections: they are welded on the upper part of the cylindrical inner vessel and allow the connection with the suction pipe of the primary pumps that are engaged in the piston seal.

3.1.2 Steam Generator and Primary Pump Sub-Assembly

The SG-PP_SA (Steam Generator and Primary Pump Sub-Assembly), is an integral part of the primary loop, i.e. from pump suction to steam generator outlet. It is made of two Steam Generator Units (SGU) and one Primary Pumps (PP) arranged between the SGU, all included in a casing supported by, and hung from, the reactor vessel roof. It is designed to carry out both functions of hot coolant circulation and power heat transfer.

The casing cross section is arranged in the annular space between cylindrical inner vessel and reactor vessel. It is immersed in the cold pool. The only connection with the reactor internals is by the suction pipe of the PP that is engaged in the piston seal at the upper end of the elbow welded to the inner vessel. Thus, the whole sub-assembly can be easily put in and out of the reactor vessel with relatively short handling time.

The lead coolant flow path is illustrated by arrows in Figure 4. The hot lead is pumped into the enclosed pool above the PP and SGUs and driven shell-side downwards across the SGU helical-tube bundles into the cold pool.

The Steam Generator Unit is a contra-flow heat exchanger, whose size is 52 MW, giving eight units per station to achieve the nominal Thermal Power of EFIT (=416 MW).

The SGU is a vertical unit with an inner and an outer shell. The primary coolant flows downwards shell-side through the inner shell and the annulus between inner and outer shell. The tube bundle is made of U-tubes, the inlet legs of which are straight inside the inner shell. After the U-turn, the outlet tube legs are helical inside the annulus and become straight again at the exit of the annulus.

The total length of tubes is less than the current maximum length of commercially available tubes (=28 m). Therefore the tube bundle can be fabricated without welds in the tubes. The tube ID of 14.2 mm allows the visual inspection of the inner surface.

The Primary Pump is to operate at 480°C and to supply the coolant at a rate of 8625 kg/s. Its most important part is the impeller, the circumferential speed of which reaches 9 m/s. The speed of flowing lead relative to the rotating propeller blades shall be limited by design to about 10 m/s as order of magnitude. Such operating conditions can give rise to problems associated with erosion-corrosion and cavitation wear as well as with the high stresses in the working parts of the pump. These problems are to a certain extent obviated by an engineering solution found in the development of the pump design. It reduces the stresses involved and ensures cavitation-free operation of the pump, which allows drawing on the operational experience of facilities with lead under erosion conditions in selection of materials.

3.1.3 The Target Unit

The coupling of the accelerator to the sub-critical core takes place via the Target Unit. This has been designed as a removable component, because its service life is anticipated to be shorter than the reactor lifetime, owing to the intense irradiation and local high thermal stresses.

The Target Unit is a slim component of cylindrical form, positioned co-axially with the Reactor Vessel and hung from the Reactor Roof. Because it serves also as inner radial restraint of the core, the outline of its outer shell fits the inner outline of the core. Its main component parts are the Proton Beam Pipe, the Heat Exchanger and the two axial-flow pumps arranged in series in the vertical legs of the loop upstream and downstream the horizontal target region.

3.1.4 In-vessel Fuel Handling System

The In Vessel Fuel Handling System provides the means to transfer the absorber assemblies from their storage positions in the outer rows of the Diagrid (Reactor in operating

conditions) to the inner rows location (Reactor in shutdown conditions), and to transfer the core assemblies to and from all in-vessel positions.

Functionally, this system consist of:

- the Rotating Plug
- the extendable Above Core Structure
- the Transfer Machine (pantograph type)
- the Rotor Lift Machine

Access to any core position is achieved by rotation of both Rotating Plug and Transfer Machine.

3.2 EFIT Decay Heat Removal System

Three systems contribute to the DHR function in EFIT: the non safety-grade water/steam system, the safety–related DHR N1 (Direct Reactor Cooling - DRC) system and the DHR N2 system (Isolation Condenser). Following reactor shutdown, the non safety-grade water/steam system is used for the normal decay heat removal. In case of unavailability of the water/steam system, the DRC system is called upon.

The DRC System is composed of four identical loops (3 loops out of 4 are sufficient to perform the DHR intended functions), one of which is shown schematically in Figure 5. The main components of the loop are: a molten lead-diathermic oil heat exchanger (dip cooler, DHX); an air-diathermic oil vapor condenser (AVC) with stack chimney.

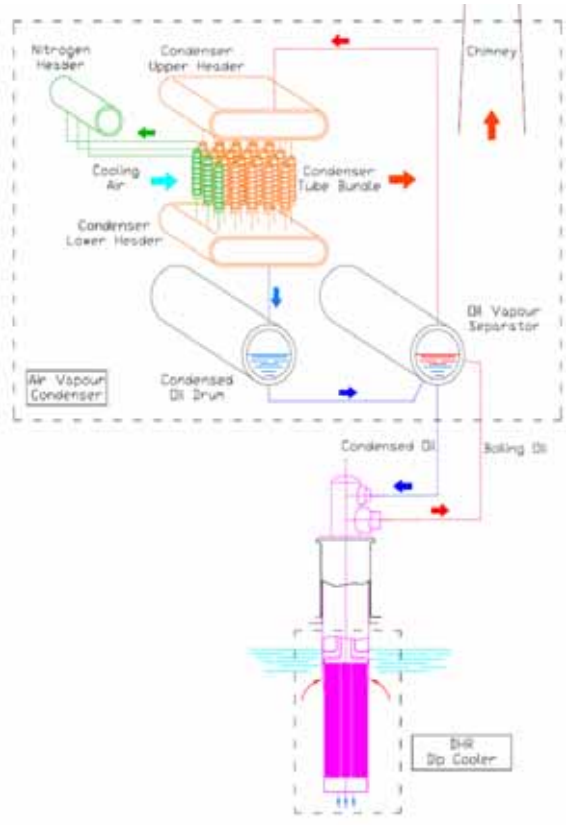

Figure 5: EFIT Direct Reactor Cooling System

The dip coolers DHX are placed in the reactor vessel in the upper part of the cold collector, where the primary coolant presents a mild thermal gradient, owing to convection streams brought about by the heat losses from the hotter Internals. Both oil vapors separator

and condensed oil drum in the lower part of the AVC are half filled of oil and half of a mixture of oil vapors and nitrogen, while tube bundle, upper header and nitrogen header are filled with nitrogen at the temperature of the atmospheric air. Since the oil in the DHX is prevented from vaporizing at temperatures lower than 400°C by the superimposed pressure and the temperature difference between oil and lead in the DHX is a few K, oil is kept circulating at the flow rate brought about by the small density difference between hot and cold leg. Vaporization take place because of increasing lead temperature due to the heat losses from the hot internals. Condensation of oil vapor takes place in a short portion of the tube bundle entrance of the AVC because the heat losses are a few hundred kW. As a consequence, the DRC loops are almost idle during normal operating conditions.

In case of unavailability of the water/steam system, the DRC system is called upon to passively enhance its performance and remove decay heat to specification. At start of the emergency condition, lead enters the DHX at higher temperature and flow rate, driven by the larger density difference between the cold shell-side leg and the hot outside leg, and oil starts to vaporize massively, speeded to circulate at higher flow rate by the large hydrostatic head between vaporizing and return legs of the loop. A recirculation ratio of more than four times the once-through vapor rate is achieved, having installed the oil vapor separator and condensate drum at the appropriate level above the DHX. The recirculation ratio is defined as the flow rate of liquid leaving the DHX compared with the vapor rate alone.

The vapor requires, to be condensed at the nominal rate, the whole AVC surface. In fact, owing to the increasing pressure, vapor floods the finned tubes while displacing the nitrogen gas. Vapor condensation takes place on the tube inner walls, and condensate runs down by gravity into the lower header and condensate drum, and mixes up in the separator with the oil rising from the DHX dip cooler. The sub-cooled oil returns the DHX via the cold leg, closing thereby the natural recirculation loop of the oil. The displaced nitrogen gas enters the extra tubes placed in front of the tube bundle, and hence cooled by fresh air, rises up, being lighter than the oil vapor, and eventually, at steady state, is confined in the nitrogen header connected to the upper ends of the tubes. Any vapor entrained by nitrogen or evaporating from the oil free surface below, would condense and fall before reaching the header. The system pressure has increased, at steady state, because of the added mass of vapor, but the pressure increase has been kept limited by the large-volume header, and, hence, also the oil boiling point has remained almost unchanged. Thermal expansion of nitrogen, that would further increase system pressure and the oil boiling point, an occurrence that would affect the thermal stability of the oil and is therefore undesirable, does not occur, because the nitrogen header is kept at the temperature of the ambient air being hydraulically connected, but thermally isolated from the loop.

3.2.1 Isolation condenser

In 1992 Ansaldo Nucleare designed the so called “Isolation Condenser” as part of the cooperation for the development of the SBWR design. Recently, GE used the component developed by Ansaldo for the ESBWR design. Ansaldo Nucleare successfully proposed the same type of arrangement for the IRIS Westinghouse reactor. The same arrangement can be proposed for EFIT, taking advantage of the fact that the condenser has been already tested in Italy by SIET (Enea) at full scale SBWR conditions.

The inlet piping of the system is attached to the main steam line. Steam is then routed to a vertical condenser immersed in a pool and the outlet of the condenser is connected to the Vessel. In normal operation the isolation valve below the condenser is closed, the condenser is full of water and no heat exchange takes place. To put in operation the component, the feed

water line and steam line must be isolated and the condenser isolation valve opens injecting water in the vessel and starting the steam condensation process.

For EFIT, respect to the original configuration, the condenser has been down-sized. The sizing is such that with three units in operation the DHR is able to remove the decay power.

A scheme of the EFIT Isolation Condenser is reported in Figure 6. From the MSL a 12" piping is routed to the upper collector of the condenser. Inclination of the inlet line provides the filling of the condenser during normal operation when the lower isolation valve is closed. A Hot Storage Tank is located below the isolation valve (the piping connection to the top of FW line is such to promote natural convection of the FW fluid to the tank). The storage tank is used to provide additional water mass in case of isolation valves leakage and to limit the thermal shock to SGs at DHR start-up. Safery Relief Valves located on MSL are used to limit to 150 bars the system pressure rise due to system isolation (MSV and FWV closure) and water injection into the SGs. Condenser pools have to be sized to provide the required design grace period (3 days)

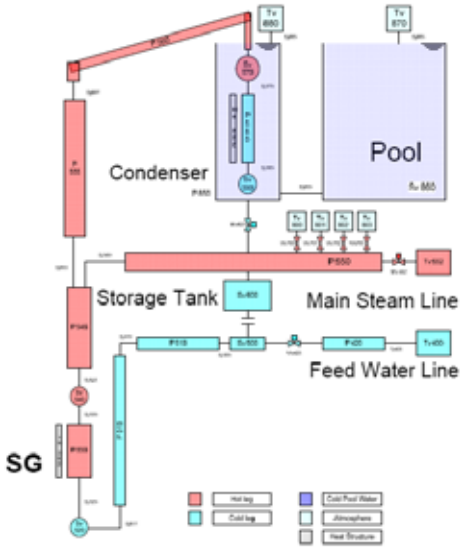

Figure 6: Isolation condenser scheme

Preliminary simulations (performed with Relap5 code) indicate that the system can be successfully operated: with 4 DHRs operation and pump on the margin to lead solidification is of one hour (at this point it is possible to rely on operator action to isolate one of the DHRs); with 3 DHRs in operation and pumps off, the maximum lead temperature reached at the SG inlet is below the design Lead Temperature at the SG inlet.

3.3 XT-ADS design

Already at the beginning of the EUROTRANS project, SCK•CEN offered to use the MYRRHA Draft II design file as a starting basis for the XT-ADS design. This allowed optimizing an existing design towards the needs of XT-ADS and within the limits of the safety requirements. Although XT-ADS has maintained the design scope of the former MYRRHA Draft II project, namely a multipurpose ADS for R&D activity and medical radioisotopes production, it has also the function of demonstration facility of important design elements of the larger EFIT ADS. XT-ADS differs from MYRRHA Draft II, therefore, on several topics for each field of the design and for the general configuration of the primary system.

Ansaldo Nucleare participated to the development of the present XT-ADS design, illustrated by Figure 7.

The configuration of the primary system is pool-type. The primary coolant is the lead-bismuth eutectic (LBE). Using the eutectic instead of pure lead allows the thermal cycle in the range of relatively low Tin = 300°C inlet and Tout = 400°C outlet temperatures, with the associated benefit of using known structural steels that can be employed without risk of large corrosion. The maximum velocity of the LBE coolant is also limited to 2 m/s in order to keep erosion under control.

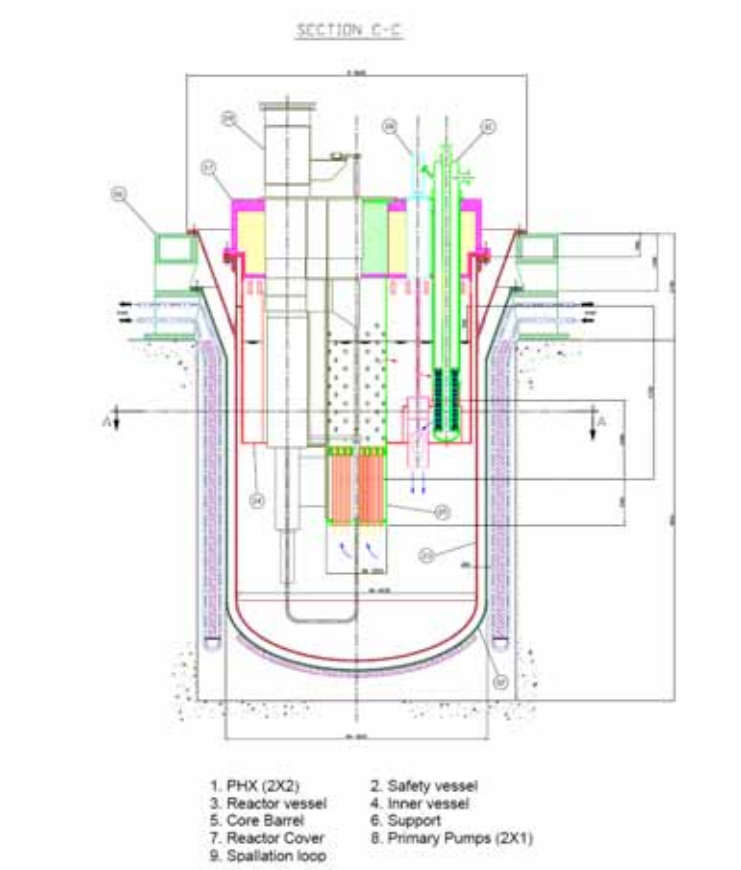

Figure 7: XT-ADS reactor assembly – Vertical section

The XT-ADS heat transfer system, that ultimately dissipates the heat to the atmosphere, is made of the Primary Circuit and of two Secondary Circuits. Within the main vessel, the hot and cold pools are separated by a diaphragm, which is basically an inner tank, spanning the reactor vessel. Two mechanical axial-flow pumps and four conventional PHX (an evaporator shaped similar to the classical straight-tube IHX of the sodium-cooled reactors) penetrate the diaphragm wall.

Controlled dissolved oxygen activity in the LBE melt is the technique employed to prevent corrosion/erosion. The activity has to be controlled at the level that promotes the formation and self-healing of a stable, compact oxide layer on the surface of the structural steels in order to prevent the excessive corrosion and the penetration of lead into the fuel cladding and other structures materials.

In the primary loop the pumps draw the LBE from the PHXs bottom window and pass it to the mass of the cold plenum and provide the head required for the LBE to flow through the core, where it is heated up again. The pump flow does not pass entirely through the core, so that a significant core by-pass flow is present.

When leaving the core, the LBE mixes with the mass of the hot plenum and with the colder by pass flow (the temperature drop from the core exit to the PHX's at steady state, due to thermal exchange between the hot and cold plenum, has temporarily not been taken into account, because predictably of a few degrees). The LBE flows shell-side through the four PHX's and exits into the cold plenum.

Each of the two secondary circuits is made of two PHXs serving as the evaporators, a steam separator of the water/steam mixture rising from the PHXs, a steam condenser, interconnecting piping, and a stack chimney.

In each circuit, saturated water enters tube-side the two PHXs, operating in parallel, and leaves as a steam-water mixture. Ferruling is provided at tube inlet in order to stabilize the flow. Steam rising from the Separator is condensed into the AC condenser, from which the condensate falls into the separator where it adds to the water plenum and feeds the PHXs, thereby closing the water circuit.

The water flows in natural circulation in the loop owing to the hydrostatic head provided by the density difference between saturated water in the inlet pipe and the steam/water mixture in the outlet pipe.

The driving force for the natural circulation is provided by the hydrostatic head difference between the hot leg and the cold leg of the circuit, achieved by arranging the separator at a sufficient elevation with respect to the PHXs.

The Reactor Vessel is a welded structure without nozzles, made of a cylindrical shell with elliptical bottom head. It is closed by the reactor roof. The top end is an Y-piece, both branches of which terminate with a flange. The conical, outer branch is flanged to, and hangs from, the Annular Support anchored to the civil structure of the Reactor Cavity, whereas the inner branch supports the reactor roof.

The outer Safety Vessel has the same general shape as the reactor vessel. It is hung from the top to the support structure. The connection between the safety vessel and the supporting structure is obtained by a bolted flange. This vessel is the inner wall of an annular inter-space, surrounding the reactor. The purpose of the inter-space is to collect the reactor primary coolant in case of reactor vessel rupture.

The Inner Vessel separates the cold lower plenum from the hot upper plenum of the primary coolant. It has a flat bottom since this will simplify fabrication, while offer more efficient penetrations (PHX, PP, spallation loop, fuel manipulator, in-vessel inspection manipulators, core barrel, and LBE conditioning system) reducing the diaphragm by-pass flows. The diaphragm is supported by the reactor vessel. It serves as the support structure for the two in-vessel suspended fuel storage racks and the in-vessel recovery manipulators.

The four Primary Heat Exchangers (PHX) are grouped in two subsystems of reactor block that include two PHX and one PP each. The PHX is a one-tube-pass, vertical natural-circulation evaporator connected with a disengaging drum elevated above the evaporator. The main features are shell-side LBE flow, straight-tube bundle, and the upper tube plate immersed in the hot pool.

The pumps, installed vertically with fluid fed from the top, draw the LBE from the hot plenum at about the level of the PHX's outlet window and pass it to the mass of the cold LBE providing the static head required to feed the core. Their most important part is the impeller, the circumferential speed of which is limited to 10 m/s. The speed of flowing lead relative to the rotating propeller blades shall be limited by design. The pump is specified to operate at the temperature of the cold plenum and to provide the total static head, that makes up most of the driving force of the natural circulation of the primary loop, at steady-state and during transients, when the temperature of the hot plenum changes with the core power. After looking at a pump coverage chart available in handbooks, based on normal ranges of operation of commercially available pumps, the type that meets the head-capacity operating

point of Table B.1 is the axial flow pump, the same type of the EFIT primary pump. This pump is a high-capacity, low-head pump, normally designed for flows in excess of 450 m3/h against heads of 15 m or less. The pump sizing performed by Ansaldo resulted in an 3-vaned 480 mm O.D. axial impeller. The vane profile being chosen by engineering judgement as the 5-digits N.A.C.A 23012 profile, adjustments of hub ratio, the vane inlet and discharge angles have been combined and simulated iteratively by means of CFD runs in order to make the design point the best efficiency point.

ACKNOWLEDGMENTS

The authors thank the Partners of the ELSY and IP-EUROTRANS projects for their fruitful contribution to the projects. Special thanks to the European Commission for the financial support through the FP5 and FP6 programs.

REFERENCES

[1] US DOE Nuclear Committee and Generation IV International Forum, “Energy Advisory A Technology Roadmap for Generation IV Nuclear Energy System”, GIF-002-0, (2002)

[2] Aït Abderrahim H., Benamati G., Cinotti L., Locatelli G., Monti S., Orden A., Struwe D., Wider H. “ The ELSY Project”, European Nuclear Conference (ENC 2007), Brussels, Belgium, 16-20 September 2007.

[3] C.Rubbia et al., “Conceptual Design of a Fast Operated High Power Energy Amplifier”,CERN/AT/95-44(ET), September 1995.

[4] “XADS Pb-Bi Cooled Experimental Accelerator Driven System – Reference Configuration –Summary Report”, ANSALDO ADS1SIFX0500, Rev.0, June 2001.

[5] B. Carluec, L. Cinotti, D. Coors, M.T. Dominguez, S. Ehster, L. Mansani, G. Rimpault, R. Sehgal, “Status of the Studies Performed by the European Industry on the LBE Cooled Xads”, International Workshop on P&T and ADS Development, SCK-CEN Club House, Belgium October 6-8 2003.

[6] H. Aït Abderrahim, L. Cinotti, F. Delage, C. Fazio, M. Giot, B. Giraud, E. Gonzalez, G. Granget, J. Knebel, L. Mansani, S. Monti, A. Mueller, “EUROTRANS: European Research Programme for the Transmutation of High-level Nuclear Waste in an Accelerator-driven System” Ninth Information Exchange Meeting, Nimes, France, 25-29 September 2006.

[7] Artioli C., Barbensi A., Corsini G., Glinatsis G., Mansani L, “EFIT: The European Facility for Industrial Transmutation of Minor Actinides”, Eight International Topical Meeting on Nuclear Applications and Utilization of Accelerators (ACCAPP’07), Pocatello, Idhao, July 29-August 2, 2007.

[8] D. De Bruyn, B. Giraud, D. Maes, L. Mansani, “From MYRRHA to XT-ADS: the design evolution of an experimental ADS system”, Eight International Topical Meeting on Nuclear Applications and Utilization of Accelerators (ACCAPP’07), Pocatello, Idhao, July 29-August 2, 2007.

SLOW REACTIVITY INSERTION IN SUBCRITICAL REACTORS. APPLICATION TO ADS

C.Montalvo, A.García-Berrocal, M.Balbás
School of Mines of Madrid, Technical University of Madrid(UPM)
Ríos Rosas, 21 28003 Madrid, Spain
cristina.montalvo@upm.es, agustin.garciaberrocal@upm.es, miguel.balbas@upm.es

J.Blázquez
Nuclear Fission Division, CIEMAT
Avenida Complutense, 2 28040 Madrid, Spain
juan.blazquez@ciemat.es

ABSTRACT

As there is a need to deal with the problem of radioactive waste of nuclear plants, prototypes of subcritical reactors are being developed at the moment. They are known as ADS and they have as their main goal, the actinides transmutation. The neutron source, which keeps the reactions in a subcritical reactor, is very intense, that is why a high energy proton accelerator is required. For many applications, it is important to design methods to measure the intensity of the source. ADS are expected to work in a subcritical range between $0.92< k_{eff} <0.97$ and because of that, control rods have a limited use and many designers are considering not to include them. They can be substituted by reflector or combustible elements displacements. In order to calibrate in reactivity these displacements, one can either take advantage of the pulsing structure of the neutron source in microseconds time scale, or can design methods for the minute time scale wherein the source is constant, that is the objective we want to achieve here. If the reactivity control is made with the reflector, in between the extreme states of open reflector and closed reflector, both k_{eff} are calculated and a reactivity ramp is estimated appropriate to the reflector movement velocity. This calibration should be made empirically by measuring the response to the ramp with neutron detectors. In the response to the ramp, the specific parameters are: the source intensity, the initial k_{eff} and the ramp slope, which defines the objective to be reached in the calibration process. Measurements are available from experimental subcritical reactors in the operation range of the ADS, which allow getting ready this calibration method based on the reactivity ramps. However, in order to fit the measurements to a theoretical model, the point kinetics equations need to be solved for this case. With the Prompt-Jump approximation and the consideration of slow ramp compared to the time constants of delayed neutrons, the integration of these equations and the non-linear fit of the measurements to the resulting method are detailed. The static approximation is enough when the reactor is in a typical subcritical state. However, when close to a critical state, the reactivity is no longer a ramp but a parabola which lead us to estimate the neutron source by means of a non-linear fit of the experimental values and assuming a known reactivity initial value.

1 INTRODUCTION

For the sake of actinide transmutation, Accelerator Driven Systems (ADS) are actually under design [1],[2]. ADS are subcritical reactors operating in the approximate range $0.90 < k_{eff}<0.97$, so they require an intense neutron source for maintaining the neutron chain. Such a neutron source is driven by a high energy proton accelerator [3]. In the microsecond time

scale, the source is pulsed; but in the minute time scale, it can be considered as a constant intensity source [4].

Taking advantage of both time scales, a method for reactivity calibration is developed. It is based on a quasi-static change of reactivity. Firstly, a theoretical model is built by using the prompt jump approximation of the one group point kinetic equations; later, the model is tested in a subcritical experimental reactor by changing continuously the reactivity in the range that ADS are expected to operate.

2 THEORETICAL DEVELOPMENT

The operation range of a transmutator is between -14 $ and -4 $, (referred to ^{235}U); it is a very subcritical state wherein the prompt jump approximation is valid for solving the kinetics equations. The spallation neutron source comes from an accelerator pulsed at a high frequency (above 1 Kz), so that for times below 1 ms, the source is not constant, but when the characteristic unit time is the minute, the source can be considered to be constant, in the sense that a neutron source would always indicate the same counts per second if reactivity does not change.

A typical calibration process would consist in going from the initial state (for instance, open reflector) to the final state, closed reflector, at a very slow and constant velocity. If the initial and final subcritical k_{eff} are estimated through a calculation code, the velocity can be fitted to an average ramp of 1 $/min. These ramps are slightly slower than the delayed neutrons whose characteristic time (inverse of the disintegration constant λ) is 12 seconds. From now on, we will name them as slow ramps.

If $k_{eff}(0)$ is calculated in the most subcritical state and the neutron population,N_0 is measured, then [5]:

$$\frac{N_0}{l} = \frac{S}{1-k_{eff}(0)} \Rightarrow \frac{N_0}{\Lambda} = \frac{S}{-\rho} \quad (1)$$

where l is the average neutron lifetime, Λ is the average neutron generation time; ρ the reactivity (negative) and S the intensity of the neutron source. The source can be obtained from the right hand side of the equation (in counts per second). The reactivity is obtained at any subcritical configuration from the source and the measurement of the neutron population. If the calculation of $k_{eff}(0)$ is not accurate enough, then the reactivity can be measured through a pulse of the source in the microseconds time scale as it can be seen in Fig.1.

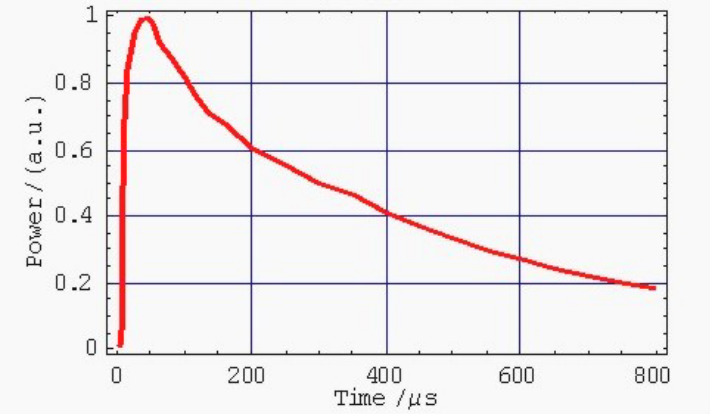

Figure 1: Response to the pulse for the initial reactivity measurement

It may be observed that the response to the pulse is only required for the initial reactivity and the calculation of the source, the rest of the calibration can be achieved with the instrumentation of the Plant.

For the case of a continuous reactivity insertion, expressed in dollars, the kinetic equation is:

$$\frac{dN}{dt} = \frac{\lambda\rho(t) + \rho'}{1-\rho(t)} N + \frac{\lambda S\Lambda/\beta}{1-\rho(t)} \quad (2)$$

where β is the delayed neutrons fraction and λ the time constant of one precursor group of delayed neutrons, and ρ' the reactivity time derivative. In the case of a ramp, this equation has an analytical solution; if the ramp is slow as well, $\lambda\rho >> \rho'$, which simplifies the calculation considerably.

Writing the kinetics equation as:

$$\frac{1}{\lambda}\frac{dN}{dt} = \frac{\rho N}{1-\rho} + \frac{S\Lambda/\beta}{1-\rho} \quad (3)$$

due to the slow ramp condition, the derivative term turns out negligible; therefore, it can be derived that, as a first approximation, the solution is the static equation:

$$N_e(t) = \frac{S\Lambda/\beta}{-\rho(t)} \quad (4)$$

Considering that the derivative term is a perturbation, $N(t)$ can be substituted for $N_e(t)$ and N is obtained, leading to:

$$N(t) = N_e(t)\left[1 + \frac{1-\rho}{(-\rho)}\left(\frac{\rho'}{\lambda}\right)\right] \quad (5)$$

It may be observed that if the ramp is slow, the static approximation is correct until close to a critical state, that is, out of the operation range of transmutators.

3 EXPERIMENTAL VALIDATION

As the transmutators are still under design, the measurements were taken from the literature. In the CORAL-I reactor, with β=0.0068, the evolution of the neutron population is measured from an initial state with reactivity -13.5 $ to a final state with reactivity -0.5 $. The movement lasted 15 minutes, so that the average ramp was around 0.86 $/min, what can be considered as “slow ramp”. The term $S/\beta = (8.6 \pm 0.2) \times 10^3$ (c/s)$^{-1}$ was measured as well. The evolution of the neutron population $N(t)$ is represented in Fig.2.

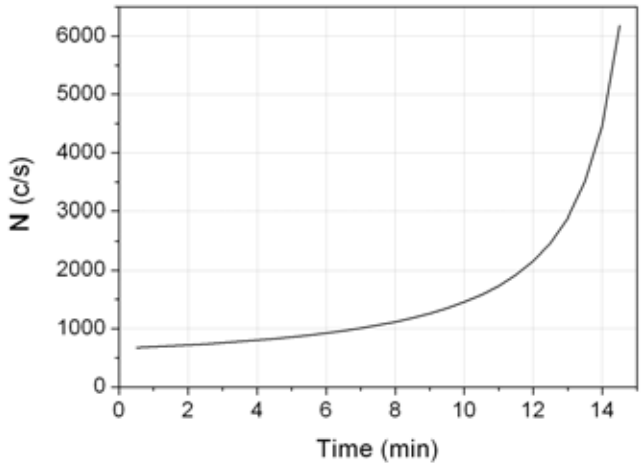

Figure2: Example of response to the ramp of a subcritical reactor

At first, it can not be stated that the inserted reactivity is exactly a ramp, to verify this is enough representing the inverse of the static approximation respect to time; if a negative slope straight line is obtained, the hypothesis of the ramp is correct. In Fig.3, $1/N$ versus time is represented:

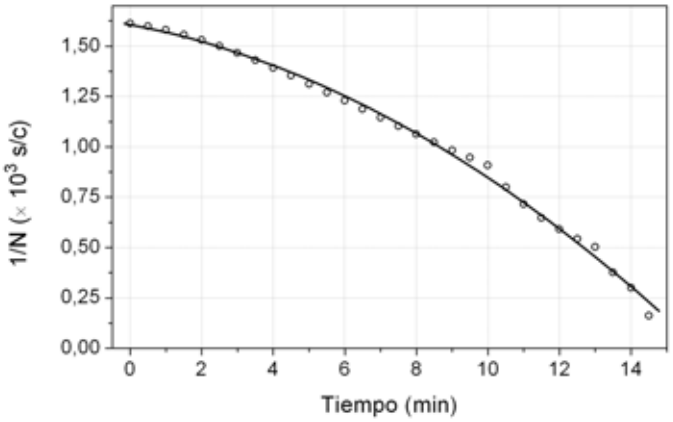

Figure 3: The dotted line is the experimental data, the continuous one, the fit to the static approximation.

In figure 3, it can be observed that at instant *t=10* min the ramp approximation is correct, but from 10 min up to 14.5 min there is a clear change of slope. That is why a parabolic reactivity insertion is supposed, and the static approximation has been used to fit the data. The obtained fitting parabola is:

$$\rho(t) = -13,8 + 0,288t + 0,0365t^2 \quad (6)$$

Then, Fig.4 is obtained:

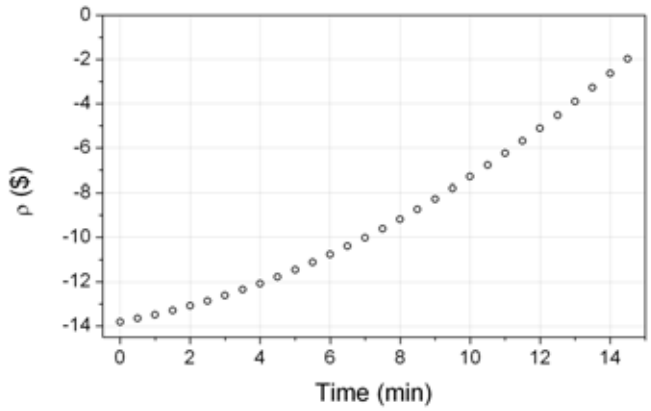

Figure 4: Inserted reactivity. Ramp between -13.4 $ and -8 $

It is convenient to take into account that the static approximation needs the value of the source to obtain the reactivity, or the initial reactivity value to obtain the source and the rest of the parameters. Besides, above subcritical values of -2 $ (t=14 min) the static approximation must be corrected.

It is necessary to go through a non-linear fit to obtain the source from the corrected solution of the kinetics equation. Such a fit must be done assuming that the reactivity follows a parabolic equation like the following:

$$\rho(t) = a_0 + a_1 t + a_2 t^2 \quad (7)$$

Where initial reactivity(-13.8 $) is supposed to be a_0. In this way, the solution $N(t)$ can be written as a non linear function (rational type) with three undetermined coefficients: the source value, a_1 and a_2. By fitting the neutron population experimental data used in Figure 3, we have obtained Figure 5.

The value obtained for the neutron source is $(8.6 \pm 2.5) \times 10^3 \, (c/s)\$^{-1}$. This value is exact within an error margin of 30 %. (the exact determination of the source was made with an error of 3 %).

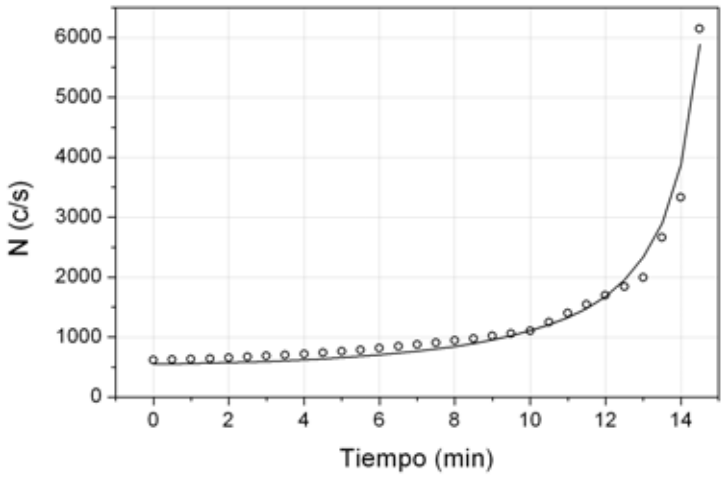

Figure 5: Neutron population data fitted to a non linear function

4 CONCLUSIONS

Data coming from a continuous reactivity insertion have been analysed in an experimental reactor at the typical subcritical conditions of the transmutators. In this range of reactivity and with a constant source, we have deduced and proved that the static approximation is enough to calibrate the movement in reactivity.

We have also derived the correction when the static approximation is not enough, as it happens in the subcritical states close to critical ones(> -2 $). The reactivity is no longer a ramp and it is necessary to approximate it to a parabola.

A known initial reactivity value, which can be obtained from the response to a pulse of the spallation source, is required. The rest of the cases need to go through a non-linear fit.

ACKNOLEDGEMENTS

The authors would like to thank Dr P. Vilarroig for careful review of the manuscript

REFERENCES

[1] Physics and Safety of Transmutation Systems. A Status Report, OECD/NEA No. 6090, ISBN 92-64-01082-3 (2006).

[2] C. RUBBIA et al, “Conceptual Design of a Fast Neutron Operated High Power Energy Amplifier”, CERN/AT/95-44, Geneva (September 1995).

[3] W. GUDOWSKI, “Impact of accelerator based technologies on nuclear fission safety”, IABAT project, EURATOM, EUR 19608 EN, ISBN 92-828-9653-6 (2000).

[4] R. SOULE and E. GONZÁLEZ-ROMERO,"The MUSE experiments for subcritical neutronics validation and proposal for a computer benchmark on simulation of MASURCA critical and subcritical experiments", OECD, Sixth Information and Exchange Meeting on Actinide and Fission Product Partitioning and Transmutation, Madrid, Spain, 11-13 dec (2000).

[5] Z. AKCASU et al., Mathematical methods in nuclear reactor dynamics, Chap. 3-4, Academic Press, New York (1971).

TOPSAFE
Dubrovnik, Croatia, 30.09 - 3.10.2008

CONCEPT OF A FUTURE HIGH PRESSURE-BOILING WATER REACTOR, HP-BWR

Frigyes Reisch
Nuclear Power Safety, KTH, Royal Institute of Technology
Alba Nova University Centre, Roslagstullsbacken 21, S-10691 Stockholm, Sweden
frigyes@kth.se

ABSTRACT

Some four hundred Boiling Water Reactors (BWR) and Pressurized Water Reactors (PWR) have been in operation for several decades. The presented concept, the High Pressure Boiling Water Reactor (HP-BWR) makes use of the operating experiences. HP-BWR combines the advantages and leaves out the disadvantages of the traditional BWRs and PWRs by taking in consideration the experiences gained during their operation. The best parts of the two traditional reactor types are used and the troublesome components are left out. HP-BWR major benefits;

1. Safety is improved; -Gravity operated control rods -Large space for the cross formed control rods between fuel boxes -Bottom of the reactor vessel without numerous control rod penetrations -All the pipe connections to the reactor vessel are well above the top of the reactor core -Core spray is not needed -Internal circulation pumps

2. Environment friendly; -Improved thermal efficiency, feeding the turbine with ~340 ^{0}C (15 MPa) steam instead of ~285 ^{0}C (7MPa) -Less warm water release to the recipient and less uranium consumption per produced kWh

3. Cost effective, simple; -Direct cycle, no need for complicated steam generators - Moisture separators and steam dryers outside the reactor vessel, inside the containment - Simple dry containment

.

1 INTRODUCTION

Now the time has come to move a step further and develop an improved type of power reactors. Common sense, public confidence and economic considerations demand that this new design should not be a big leap from the presently functioning devices; however it should be a significant improvement. Therefore it is important to avoid those parts of the older designs which have caused trouble in the past e.g. PWR steam generators, BWR perforated reactor vessel bottoms and instead rely only on a stable construction with proven components which served well in the past. The High Pressure – Boiling Water Reactor, HP-BWR (Figure 1) attains these goals, by partly using the PWR concept, i. e. the pressure vessel, the electro-magnetic control rod operator, and partly the BWR concept, i. e. core internals, internal circulation pumps and steam and moisture separators. All the figures here are made by the combination of the CAD codes of existing BWRs and PWRs. The subject was introduced by the ENS as is given in the References

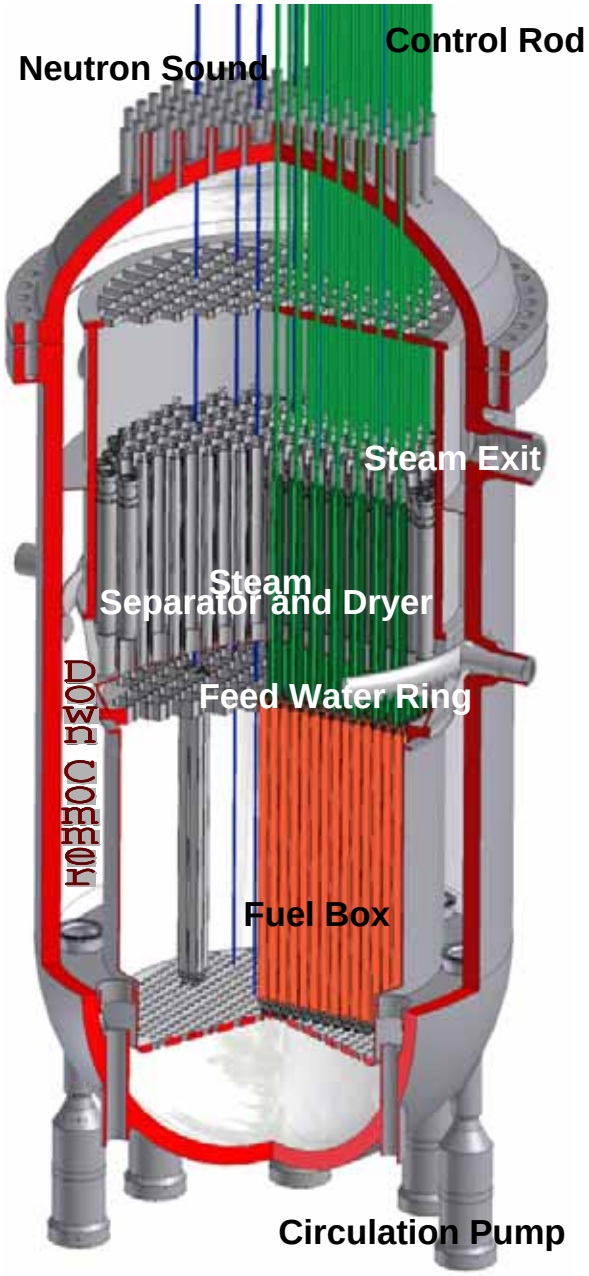

Figure 1: The High Pressure Boiling Water Reactor

2 SAFETY IS IMPROVED

The control rods are gravity operated instead of be operated by an intricate hydraulic system. The gravity operated control rod system has served well in PWRs. The stems are introduced into the reactor vessel via the vessel head (Figure 2). The control rods themselves are in the form of a cross, as it is in the BWRs. This assures large space for the cross formed

rods between the BWR type fuel boxes. Also the neutron measurement sounds are introduced via the reactor pressure vessel head the way it is used in BWRs.

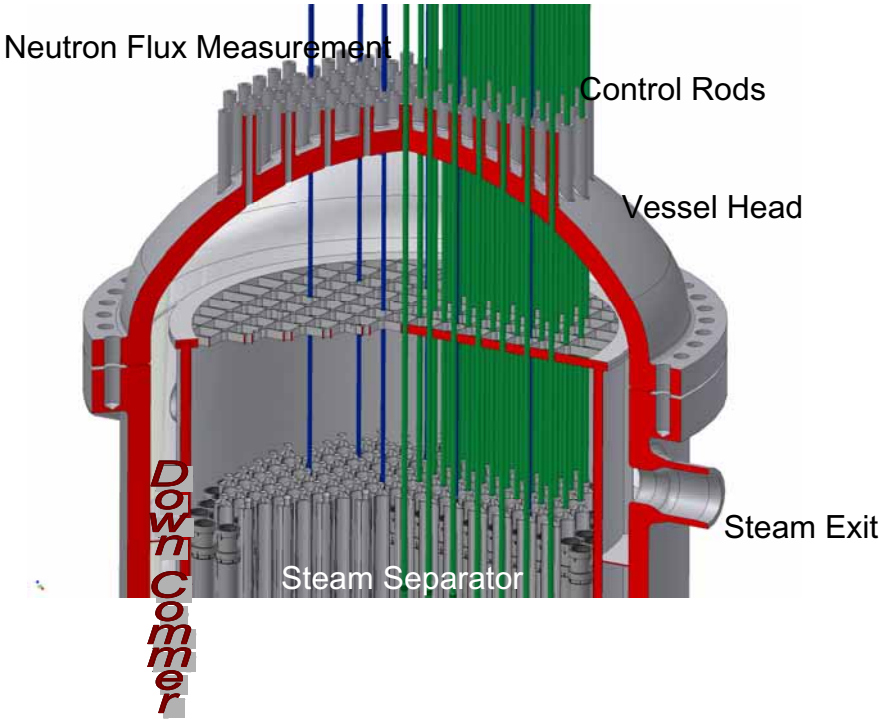

Figure 2: Reactor vessel head and reactor internals

The bottom of the reactor vessel (Figure 3) now is without numerous control rod penetrations, a great advantage compared with the previous design.

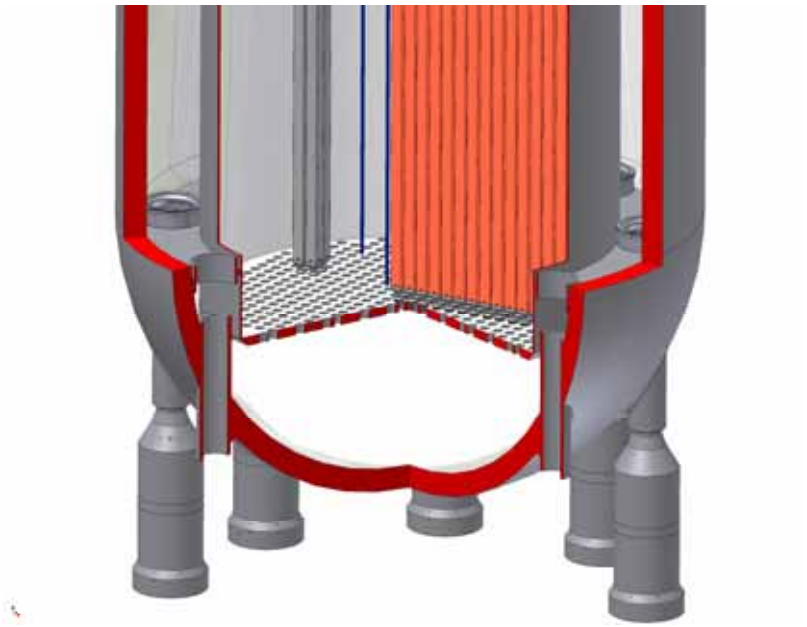

Figure 3: The bottom of the reactor vessel and internal circulation pumps

All the pipe connections to the reactor vessel are well above the top of the reactor core. This means that a major pipe break will not empty the reactor vessel. Therefore core spray is not needed. In Sweden for example the core spray in all BWRs with internal pumps are disconnected after the approval of the safety authority. Detailed studied of this subject is available at the Swedish Radiation Safety Authority

Internal circulation pumps are used to assure hydrodynamic stability. In this way the orifices at the fuel channel inlets are chosen so that the one phase pressure drop will dominate over the two phase pressure drop to avoid hydrodynamic oscillations. By utilizing natural circulation one could omit the circulation pumps. However the margin to avoid hydrodynamic oscillations may be reduced. This is an experience gained at several Boiling Water Reactors and a phenomenon studied at thermal hydraulic loops at research institutes universities and manufacturers. There is a wealth of literature on this subject which can easily be fined e.g. on the Web.

Compared to the traditional BWR the HP-BWR has further advantages, namely improved thermal efficiency due to the higher temperature and further improved inherent stability due to the increased negative power reactivity coefficient (see Figure 4). Table 1 below shows a comparison calculated - with the RELAP code - between a BWR and a HP-BWR. Using presently available PWR pressure vessel and presently available BWR fuel boxes the approximate power output would be some 1200 MWe

Comparison

	BWR	HP-BWR
Feedwater temperature	486.6 K	486.6 K
Outlet void temperature	559 K	617.8 K
Pressure in the steam dome	7 MPa	15.5 MPa
Inlet temperature to the core	550.29 K	582.3 K
Inlet core quality	-3.909E-02	-0.254
Outlet quality from the core	0.128	0.323
Total Mass Flow Rate from the core	13634 [kg/s]	5955 [kg/s]
Total Mass Flow Rate in the steam lines	1795 [kg/s]	2026 [kg/s]
Total Mass Flow Rate through the pumps	13634 [kg/s]	5955 [kg/s]
Total Power Coefficient	-1.64e-4 [Δk/%]	-4.4e-4 [Δk/%]

Table 1: Comparison between BWR and HP-BWR
calculated with the RELAP code

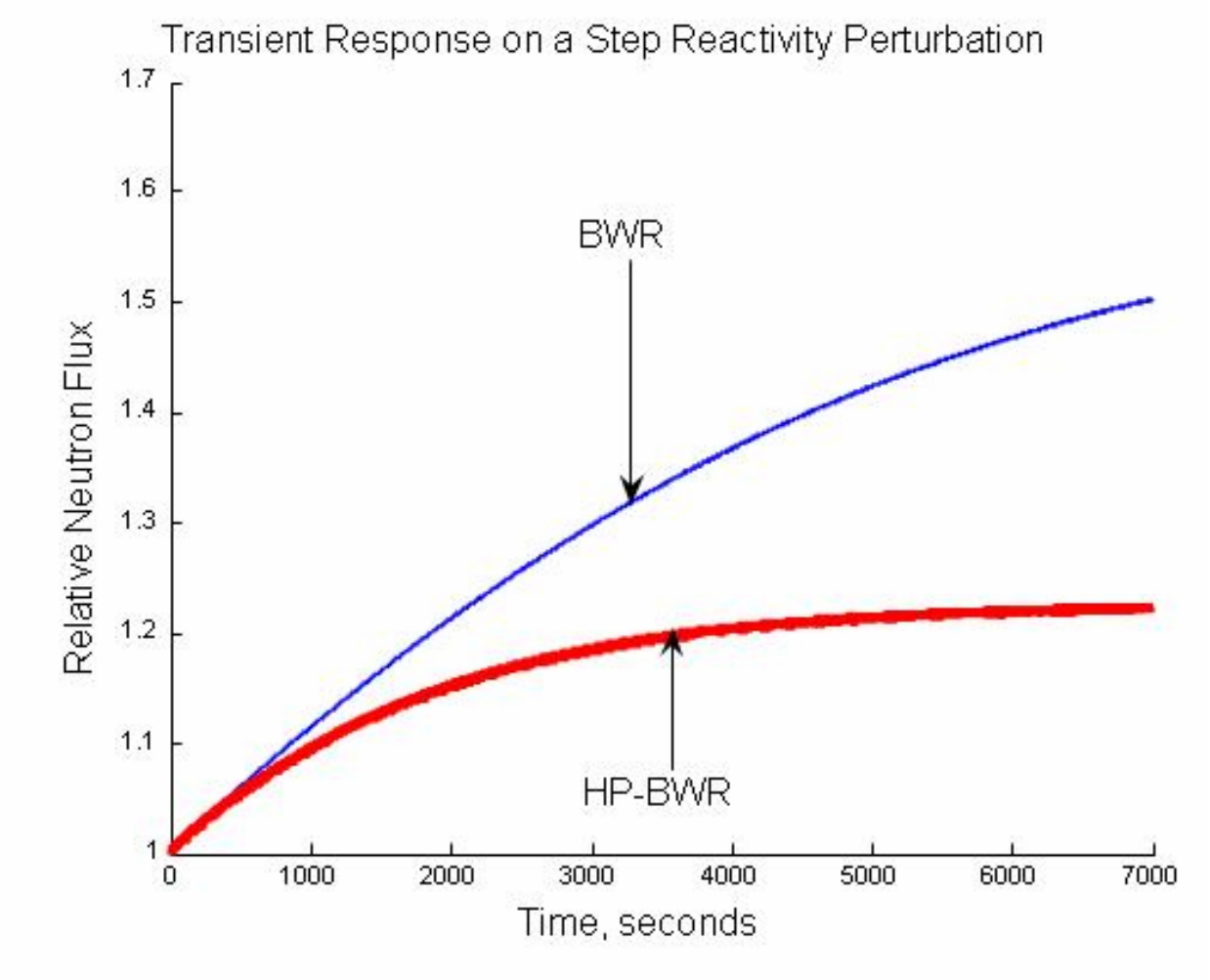

Figure 4: Long term stability without the use of any control system
calculated with the MATLAB code
Inherently stable reactor

3 ENVIRONMENT FRIENDLY

Improved thermal efficiency is attained by feeding the turbine with ~340^{0}C (15.5MPa) steam instead of ~286 ^{0}C (7MPa). The Carnot cycle theoretical efficiency $(T_{Hot} - T_{Cold})/ T_{Hot}$ is for BWR ~46% and for HP-BWR ~51% at $T_{Cold} = 300\ ^0$K, i.e. an increase by a factor of 1.109. Assuming the same improvement ratio, today's efficiency of ~33% would increase to ~37%. This demonstrates the advantage of the HP-BWR which utilizes the fuel more efficiently and releases less warm cooling water to the environment per produced kWh. There are several conventional thermal power plants with 15.5 MPa turbines. Though to use dry saturated water might need some development work.

4 COST EFFECTIVE, SIMPLE

The HP-BWR operates in direct cycle mode, with no need for complicated and expensive PWR steam generators and also instead the rather complicated BWR reactor pressure vessel bottom a simplified one is used. The main steam separators are inside the pressure vessel and secondary separators and dryers can be installed outside the reactor vessel, inside or outside the containment. The containment (Figure 5) is a simple dry containment which allows easy entrance and inspections and also minor repairs during operation.

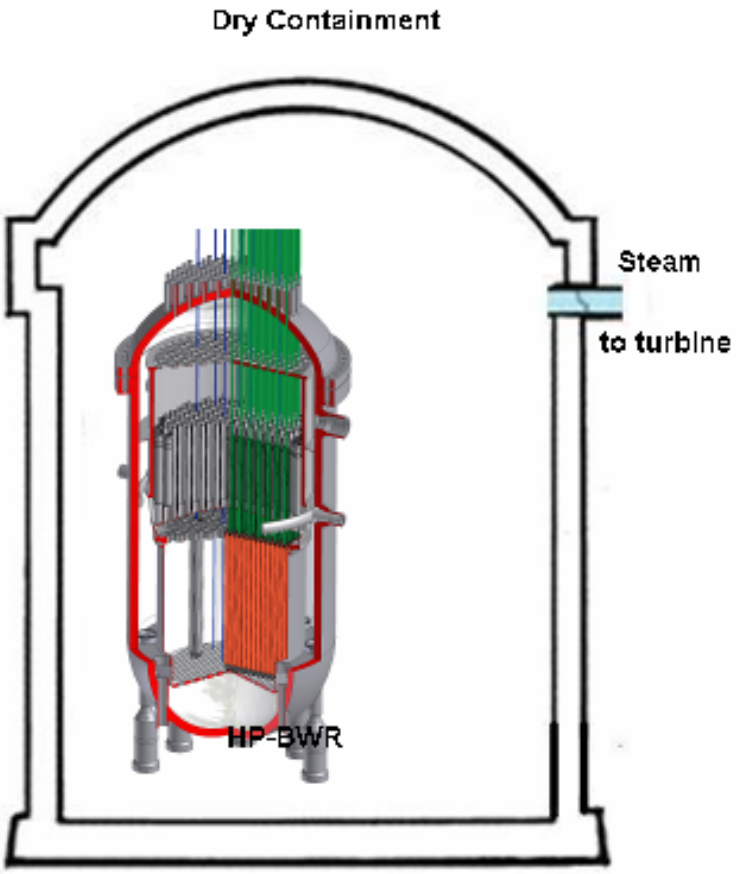

Figure 5: HP-BWR in a dry containment

The flow scheme of the reactor is clear and simple. The strait forward flow scheme is shown in Figure 6

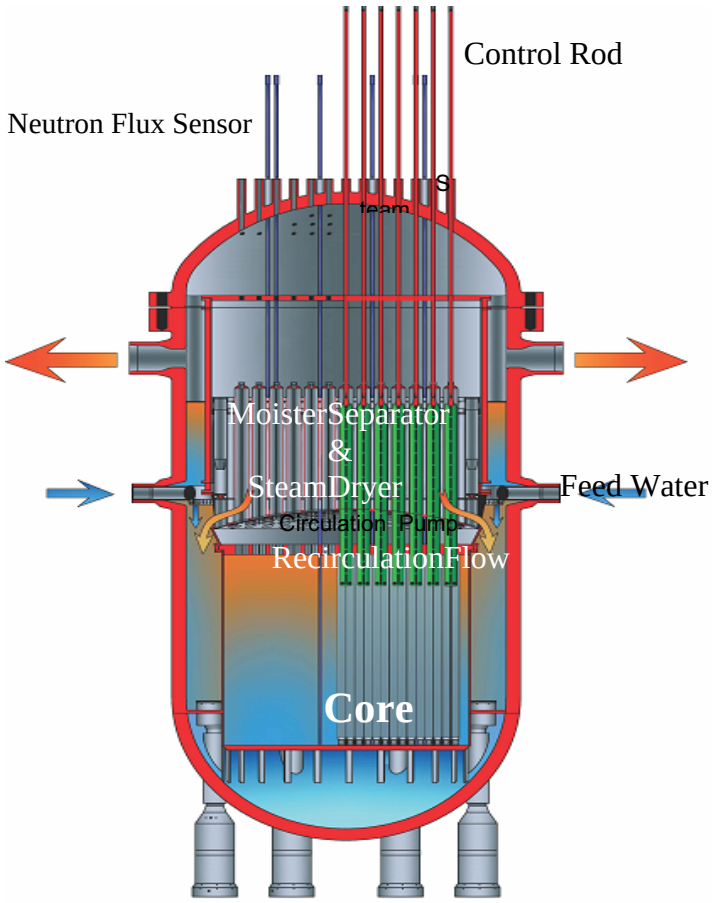

Figure 6: Flow scheme

5 CONCLUSIONS

As a reactor inspector on leave from Sweden I participated in IAEA's OSART and ASSET missions. Also due to my engagement at the International Electrotechnical Commission (ICE) I visited nuclear installations in Europe, Asia and America. This way I gained insight of the operational experiences of most reactor types. As a result now I can contribute to the advancement of nuclear energy independently. As I have no obligation to any vendor or reactor type I can suggest an optimal reactor construction which hopefully will lead to further detailed studies at some vendors, power companies, research institutes and universities, especially after this conference. In Sweden already some universities expressed interest to make further studies of this concept.

ACKNOWLEDGMENTS

Thanks to Hernan Tinoco and Karl–Axel Bartholf of the Forsmark NPP for the CAD designs and Joanna Peltonen of KTH for the RELAP calculations.

REFERENCES

ENS News, October 2007 http://www.euronuclear.org/e-news/e-news-18/HP-BWR.htm
Transactions of the European Nuclear Conference (ENC) 2007, Brussels

ENS, 18 March 2008, HP-BWR http://www.euronuclear.org/reflections/HP-BWR.htm

TOPSAFE
Dubrovnik, Croatia, 30.09 - 3.10.2008

Superior Safety Response of the Very High Temperature PB Reactor[1]

David Saphier
Soreq Nuclear Research Center, Yavne 81800, Israel
Saphier1@013.net.il
Present address: 21 Netiv Halamedhe, Rehovot 76223, Israel
Tel: +972 8 9451743; Fax: +972 8 9491233

ABSTRACT

In the present study it is shown that choosing the Pebble Bed (PB) concept for the VHTR is not only a very effective way to supply all the world energy needs, it is also one of the safest nuclear reactor concept. Depending on the fuel cycle chosen, it is possible to reduce significantly the transuranic radioactive waste (TRU) normally produced in light water reactors and thus further reduce the environmental concerns of long living FP. Due to the very high coolant temperature, in the vicinity of 1000°C, this reactor can provide energy to produce hydrogen for motor transportation, electricity at efficiencies close to 50%, and process heat for desalination and other industrial applications.

A conceptual 600MWt High Temperature Pebble Bed reactor is proposed, and its safety characteristics are analyzed by simulating various hypothetical accidents, using the DSNP (Dynamic Simulator for Nuclear Power-plants) simulation system. Analyzing various LOFA (Loss of Flow Accidents), LOCA (Loss of Coolant Accident), and load rejection accidents, it is shown that the maximum temperatures reached in the fuel will not result in significant release of radioactive fission products. In addition, the transients are extremely slow due to the core large heat capacity, and will proceed for hours and days rather than seconds and minutes as in LWRs. It is concluded from the present study that the VHTR can provide sustainable, safe and emission free energy for the next generations, thus complying with the proposed Generation IV reactor requirements.

1 INTRODUCTION

For the energy hungry world there is a single power plant solution which has the potential to supply most of the present and future energy needs, with almost zero pollution at high thermal efficiency. The Very High Temperature Reactor (VHTR) can produce Hydrogen for automotive needs to replace the polluting gas and oil; it can produce electricity at very high efficiency with almost no pollution, and provide clean process heat for the industry and the energy needed for desalination plants to provide fresh water.

In the present study it is shown that choosing the Pebble Bed concept for the VHTR is not only a very effective way to supply all the energy needs, it is also one of the safest nuclear reactor concepts[1]. Depending on the fuel cycle chosen, it is possible to reduce significantly the TRU waste[2] normally produced in light water reactors and thus further reducing the environmental concerns of long living FP. Appropriate design and fuel cycle optimization can enhance the burning of minor actinides. Past studies have shown that the fuel kernels used in HTGRs can be subjected to much higher BU[3] and consequently produce much lower waste.

[1] Pap-264-Rev1, Topsafe-2008; Dubrovnik Croatia

An extensive experimental program is underway in the Osiris reactor (the SIROCCO program) [4], to test FP retention capability of newly developed HTR fuel under normal and accidental conditions. A conceptual 600MWt High Temperature Pebble Bed[5] reactor is proposed, and its safety characteristics are analyzed by simulating various hypothetical accidents, using the DSNP[11] simulation system.

2 VHTR GEN-IV REACTORS

Various Generation IV reactor concepts are being studied world-wide with the objective to develop inherently safe, pollution free, superior economics, sustainable and proliferation resistance energy supply for the 21st century and beyond. The countries participating in the VHTR development project include: US, UK, Japan, Russia, China, France, South-Africa, Germany and Switzerland. Presently two major HTGR construction projects are underway. The GT-MHR[12], developed in Russia for burning military Pu, with the support of an international consortium (General Atomics and DOE (USA), Minatom (Russia), Framatome ANP (France) and Fuji Electric (Japan); and the PBMR[13], developed by ESKOM in South Africa, with the involvement of several European organisations (BNFL, FZJ, HTR-GmbH, NRG, AEA Technology etc.) and a utility (Exelon). China is also planning to extend its HTR-10 technology to build a ~200MW version funded partly by China's largest electricity generator, Huaneng[14], and to start construction in 2009 in Rongcheng City.

Superior economics can be obtained by using very high temperatures; hence the various VHTR concepts are planned to have coolant exit temperatures from 900 to 1000°C. The various designs include the Fast Breeder Reactor (FBR)[6] either liquid metal or gas cooled[7], the Lead or Lead-Bismuth-cooled[8] Fast Reactor, the Molten Salt Reactor (MSR), and the gas cooled graphite moderated reactor using either prismatic fuel, or spherical fuel elements – the pebble bed reactor. The reactors using Helium as coolant can reach very high temperatures, particularly in combination with graphite. Lead and Molten salt reactors have boiling points above 1400°C which enables them also work with coolant temperatures above 1000°C if corrosion and other technical problems can be resolved. The safety merits of PB-VHTR concept is the subject of the present study. One of the major advantages of the PB-VHTR is that its construction can be based on proven technology. Several countries have[9] or are operating pebble-bed reactors with exit temperatures of up to 950°C.

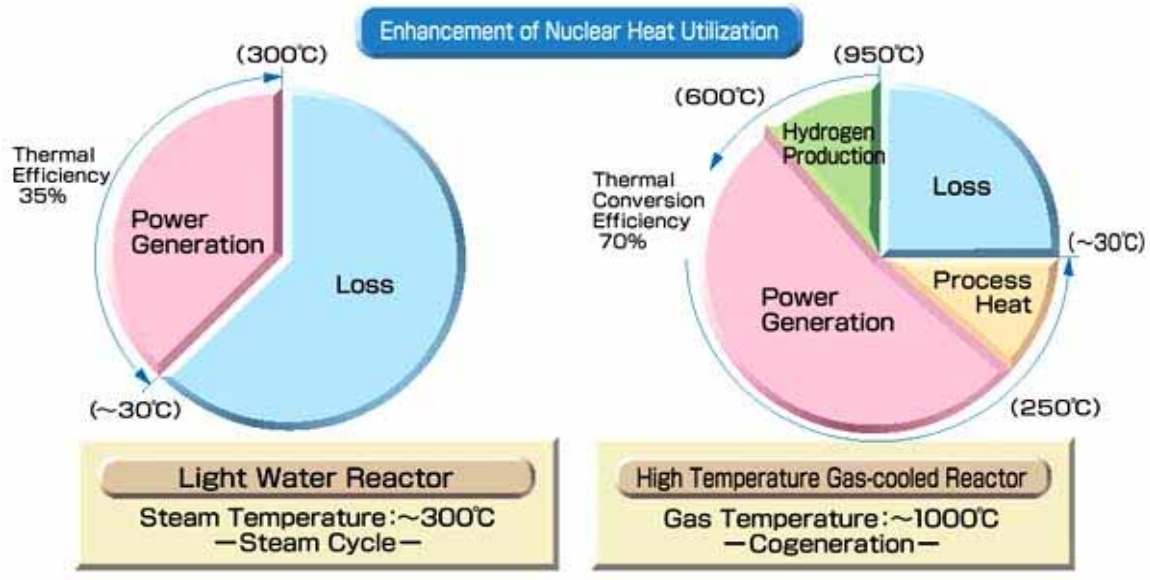

Fig 1: Comparing thermal efficiencies of the light water and the high temperature gas cooled reactor.

Fig. 1 demonstrates the superior thermal efficiency of the HTGR compared to the presently operating light water reactors. The superior safety characteristics of the PB-VHTR are assured by four major factors. Large thermal inertia - very slow transients, single phase coolant – no phase change during power excursions, large negative feedback-mitigating any accident and limiting the temperature increase, and a very low power density.

3 CONCEPTUAL DESIGN OF THE PEBBLE BED HIGH TEMPERATURE REACTOR

A conceptual design of the proposed Pebble-bed High-temperature Gas-cooled power plant is shown in Fig. 2. The PB core heats up the He gas to 1000°C or above. The He pressure is 60 bars. The gas flows inside a concentric hot duct (preheating the incoming cold He gas) through a series of heat exchangers, in each giving up part of the heat. Optionally, the hot He is transported directly to the hydrogen production plant or the turbine.

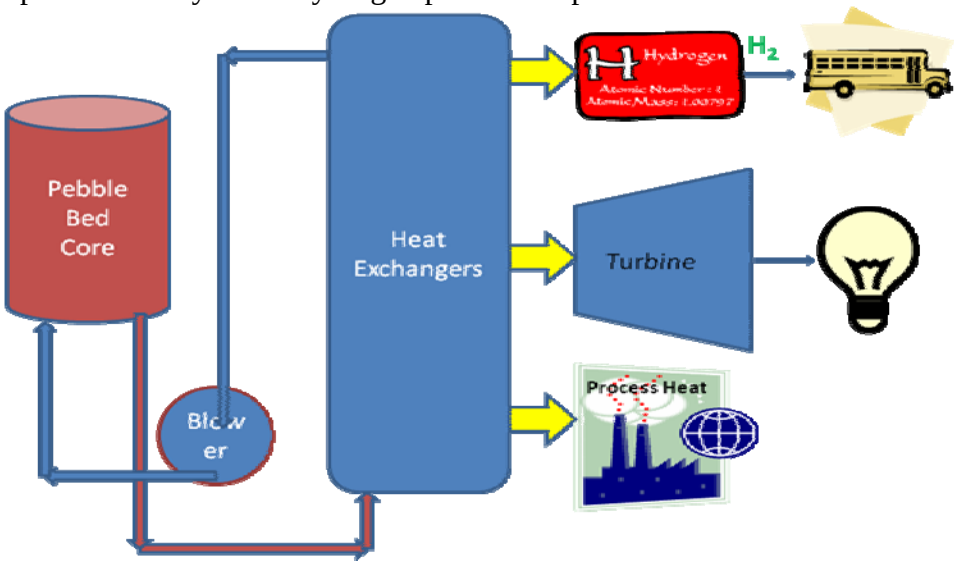

Figure 2: Schematic description of a high-temperature pebble-bed power plant.

The energy between 960°C and 540°C is used for hydrogen production in one of the chemical processes being developed for this purpose. The most probable candidate is the Sulphur-Iodine (S-I) process[10]. The energy between 540 and 350°C is used to drive the turbine-generator to produce electricity. This part of the energy can be driven either through a steam generator producing high pressure steam to drive a conventional steam turbine, or using the direct cycle to drive a gas turbine. Finally the energy between 350 to 250°C is used via appropriate heat exchangers as industrial process heat or to provide heat to a desalination plant.

The fuel used in the pebble bed core is made up of 6cm graphite spheres in which the TRISO fuel particles are

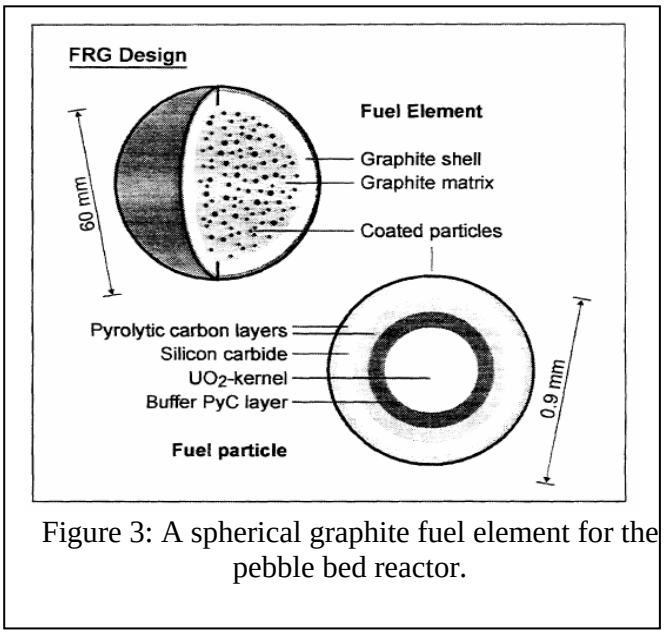

Figure 3: A spherical graphite fuel element for the pebble bed reactor.

embedded as shown in Fig. 3. The TRISO fuel particle includes a UO_2 fuel kernel surrounded by four layers of protective coatings, including two pyrolytic carbon layers, a silicon carbide layer, and an additional buffer zone of PyC to improve the fission product retention capability of the fuel even at very high temperatures. The fuel enrichment is about 10%, but depends on the particular fuel cycle chosen. The particles are dispersed in a graphite matrix sphere of 5cm, which is then surrounded by a denser graphite shell of 0.5cm. The TRISO particles can achieve very high burn-up, and experimental irradiations have shown that up to 747 Gwd/t, no detrimental effects were observed.

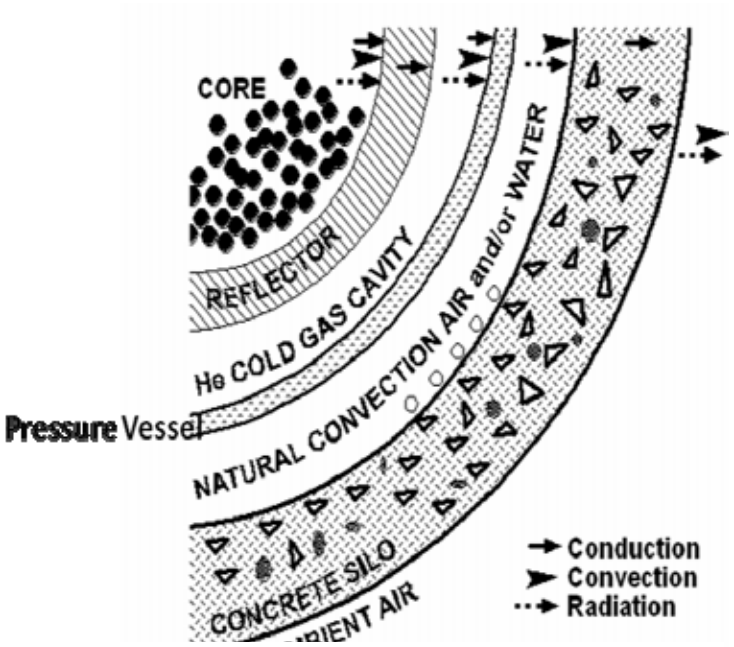

Figure 4: Radial cross section of a pebble bed core.

4 THE COMPUTATIONAL MODEL

The DSNP[11] simulation package was used to study the proposed PB VHTR response to various accident conditions. A schematic description of the core radial cross section and its various enclosures are shown in Fig. 4. Each of the shown elements is represented by a two dimensional cylindrical DSNP module surrounded by a one-dimensional cylindrical axial flow path. The axial flow schematics are presented in Fig.5.

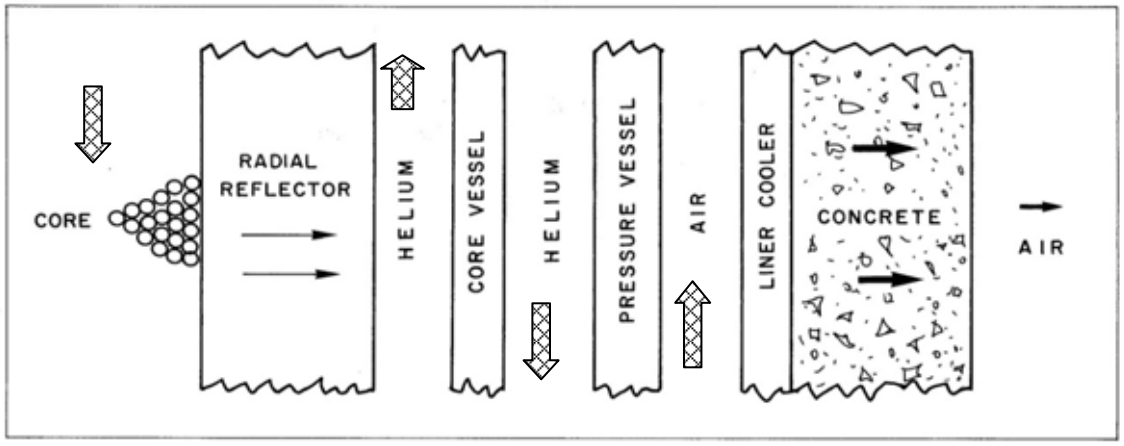

Figure 5: Schematic flow path representation of the High Temperature Pebble-bed Reactor.

The core is represented by a cylindrical element with 6 axial and 6 radial subdivisions. Each axial segment can be of arbitrary length, in the present case equal segments were assumed, and the radial sections have equal flow areas. Each cylindrical segment contains an

average spherical fuel element, the coolant flow is from top to bottom. The radial reflector which is cooled by incoming cold He also isolates the steel pressure vessel from the hot He. From the outside the pressure vessel is cooled by natural air flow. The reactor is enclosed in a concrete silo which is water cooled on its inner side by a special liner. The silo is cooled by the ambient air.

In addition to the reactor cylindrical elements and the flow hydraulics, the various heat exchangers, the pipes and valves, the steam generator, turbine and other component models were included in this simulation. The core neutronics was represented by the kinetic equations and the various control and safety features were also included. The thermal-hydraulic model is based on the three conservation equations, namely the conservation of mass, energy and momentum as shown below. In addition, the neutron kinetic equations resulting from spatial and energy integration of the neutron balance equations is used.

The conservation of mass equation,

$$\frac{D\rho}{Dt} = - \rho(\nabla \cdot \vec{v})$$

The conservation of energy equation,

$$\rho \frac{Dh}{Dt} = - \nabla \cdot q'' + q''' + \frac{Dp}{Dt} + \Phi$$

The conservation of momentum equation,

$$\rho \frac{D\vec{v}}{Dt} = - \nabla p + \mu \nabla^2 \vec{v} + \rho \vec{f}$$

The exact approximation used depends on the module level and application

5 RESULTS OF THE SIMULATIONS

The hypothetical accidents investigated in the present study include loss of flow as a result of a breach in the main coolant duct, which also includes depressurization of the core and a loss of heat sink by failure of one of the thermal loads, the turbine, the hydrogen production plant or the plant using the process heat. Three specific cases are presented below, namely, depressurized loss of flow with scram, depressurised loss of flow without scram, and a partial loss of load.

5.1 Depressurised Loss of Flow with Scram

A small part of the results are reproduced in the figures below. Figures 6 to 8 show the loss of coolant accident due to a break in the cold duct. As the safety system detects a change in the pressure the reactor is shut down. The He transient temperatures in the core hottest region - the 6th axial core region are shown in Fig. 6 for the 6 consecutive radial segments, with the highest temperature in the core central region. As can be seen there is an initial fast temperature drop, following the power reduction, to the level of the coolant cold gas temperature. This is then followed by a very slow temperature increase due to the presence of the decay heat and the absence of sufficient heat removal capability, reaching a maximum value after about 5 days and then a very slow temperature decrease following the decay heat reduction curve. The transient calculation is terminated after 1.5x10^{6}s (about 17days) at which

time some of the pebbles are still above 1000°C. Fig. 7 shows the 6 fuel spheres central temperatures for the same core regions. The maximum coolant temperature is 1360°C, while the fuel temperatures are a few degrees higher. It should be noted that the coolant temperatures are calculated for the section entrance and exit, while the fuel temperatures are computed for the centre of each axial and radial section under LOCA conditions. The heat is dissipated mainly by radiation and conduction.

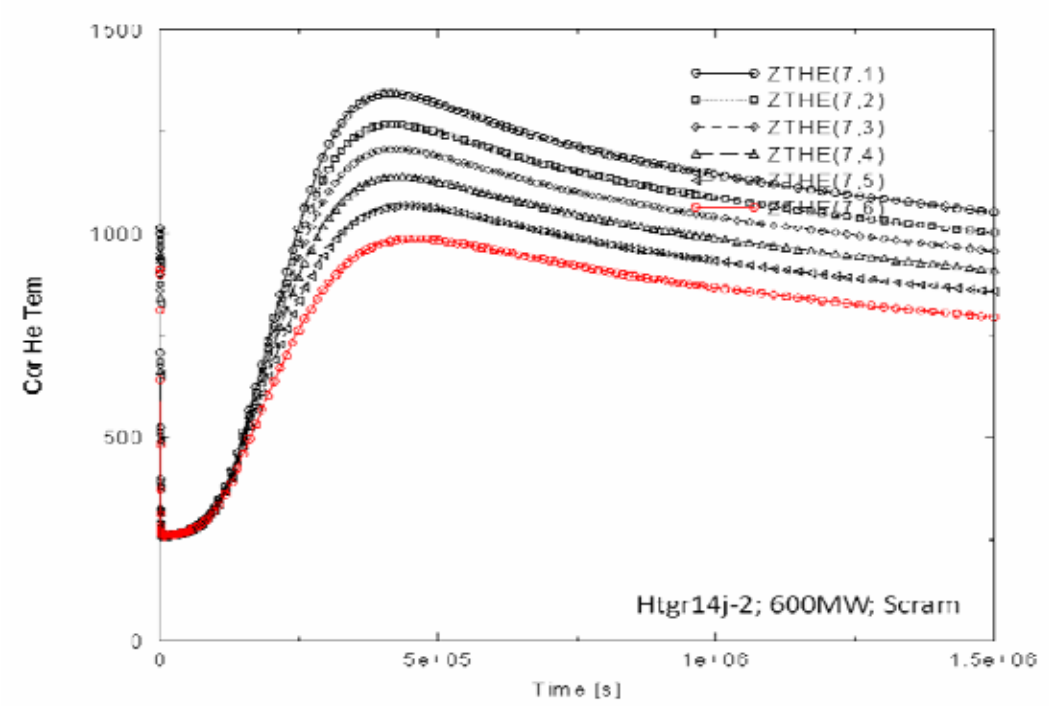

Figure 6: Coolant transient exit temperatures in the 6 radial regions following a depressurized LOCA accident in a 600MW PB-VHTR.

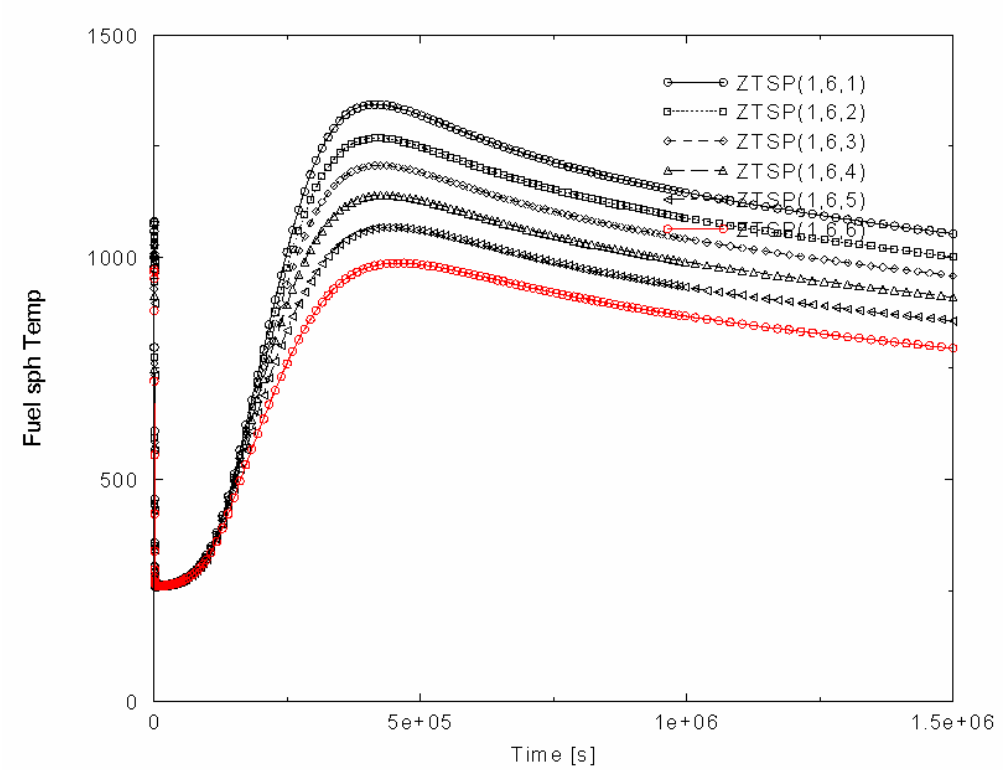

Figure 7: Fuel sphere centre temperatures in the 6th axial region, in 6 radial regions following a depressurized LOCA accident in a 600MW PB-VHTR.

The side reflector temperatures for this transient are shown in Fig.8 for the 6 axial segments of the innermost reflector region. In this study the reflector is modelled by 6 axial and 10 radial cylindrical shells using a two dimensional conduction model. As expected, the temperature decrease and the following increase are much slower and the peak temperature is reached after about 6 days.

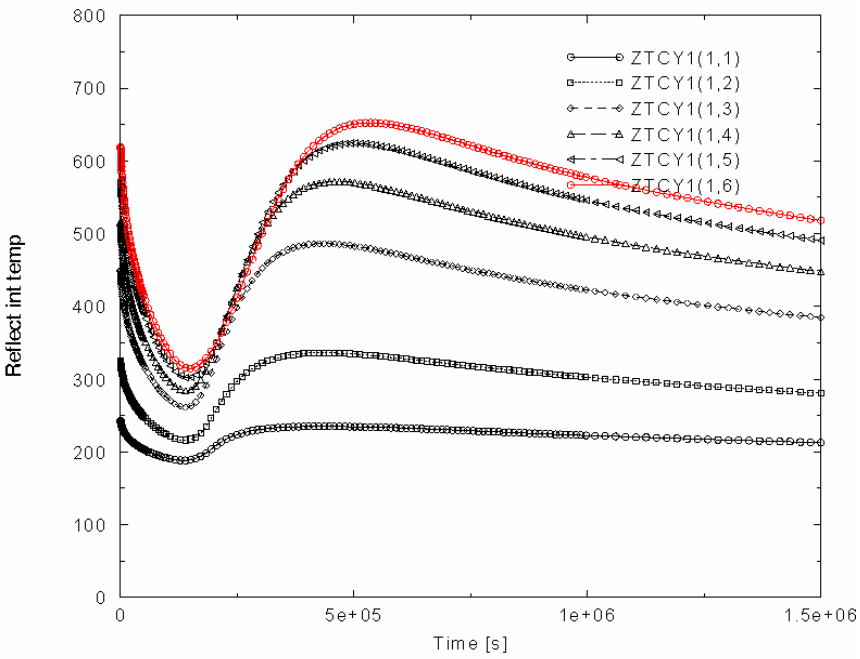

Figure 8: Temperature distribution in the radial reflector innermost region.

5.2 Depressurised Loss of Flow without Scram

Figures 9 to 12 show the same LOCA accident but a malfunction of the safety system, i.e. no scram is assumed. As in the previous case, Fig. 9 shows the coolant temperatures at the exit of the core last region along the 6 radial segments modelled. Comparing this figure to the previous case, fig 6, a very different transient behaviour can be observed. The temperatures start increasing following the flow reduction. The transient shape results from the changing nonlinear power - flow mismatch which is taking place during this event. The power is shutdown due to the negative reactivity coefficient of this core. The maximum temperature of the coolant is only about a 100^{o}C higher than in the scrammed case.

Fig. 10 presents the fuel temperatures in the centre of the fuel spheres in the core last axial region along the 6 radial segments. Somewhat higher temperatures (about 100^{o}C) than in the previous cases and a different transient behaviour can be observed. However, the maximum temperature is reached at about the same time as in the previous case.

Figure 11 shows the reactor power in MW on a logarithmic time scale. As can be observed, the power starts decreasing at about 100s, and decreases slowly to the decay heat levels. The power is reduced in this case due to the negative feedback reactivity inserted into the core by the increase in the fuel temperature. As can be observed, in all cases the power is reduced, either by the safety system or by the negative feedback, and no damage to the fuel will occur. Figure 12 shows again the reflector temperatures in the reflector innermost 6 axial segments. The reflector temperatures in this case are about a 100^{o}C higher than in the previous case, but no significant differences between the scrammed and un-scrammed case can be observed.

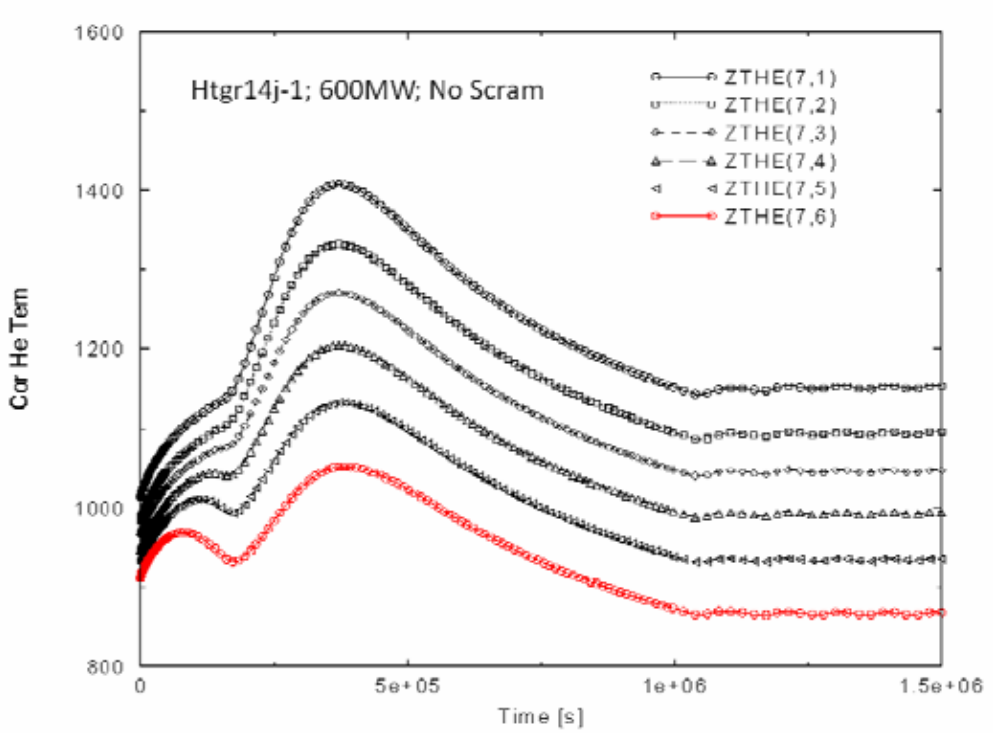

Figure 9: Coolant transient exit temperatures in the 6 radial regions following a depressurized LOCA accident in a 600MW PB-VHTR with malfunction of the safety system.

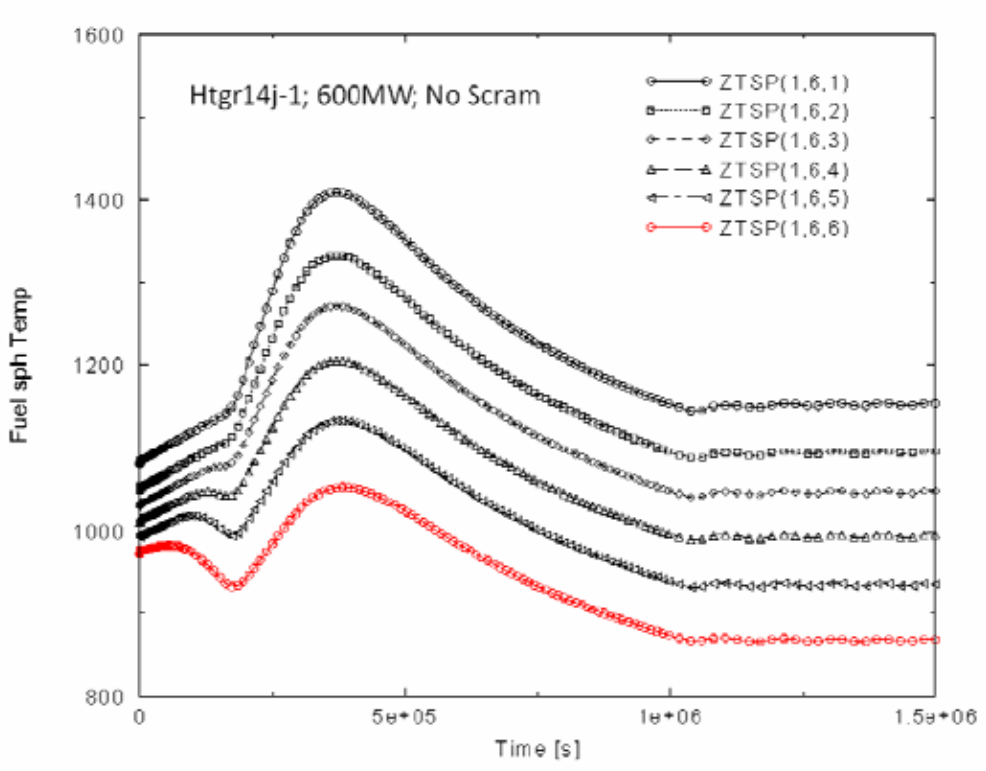

Figure 10: Fuel sphere centre temperatures in the 6th axial region, in the 6 radial regions following a depressurized LOCA accident in a 600MW PB-VHTR with malfunction of the safety system.

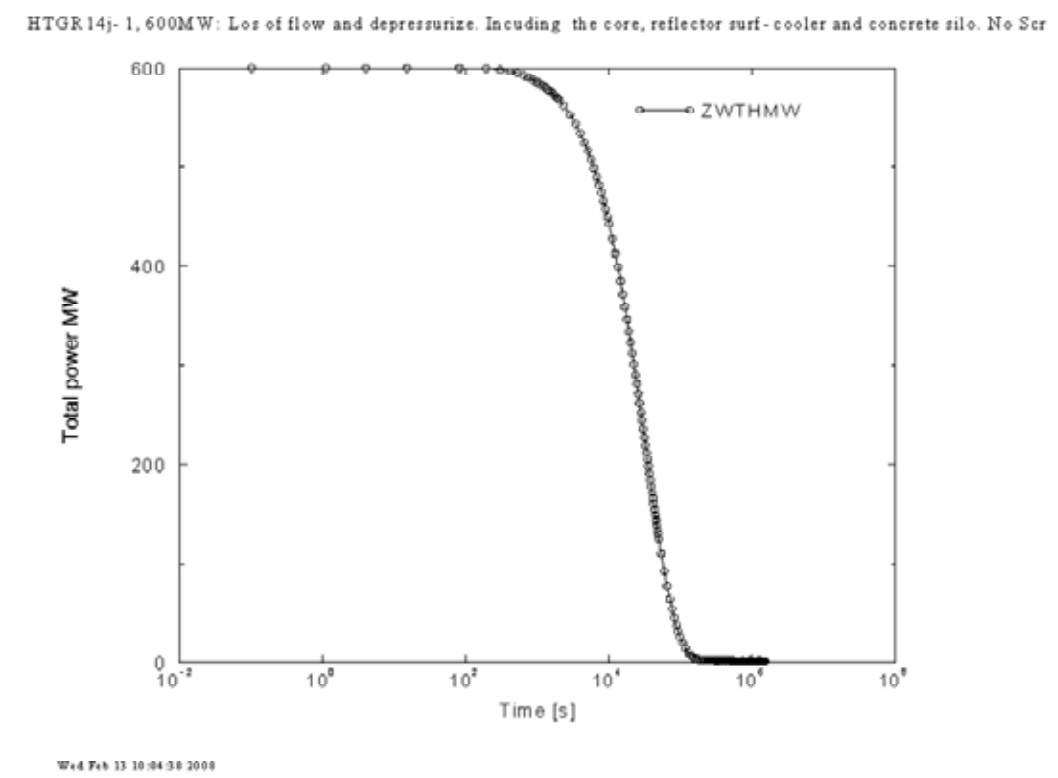

Figure 11: Reactor total power in MWt following a depressurized LOCA accident in a 600MW PB-VHTR with assumed malfunction of the safety system.

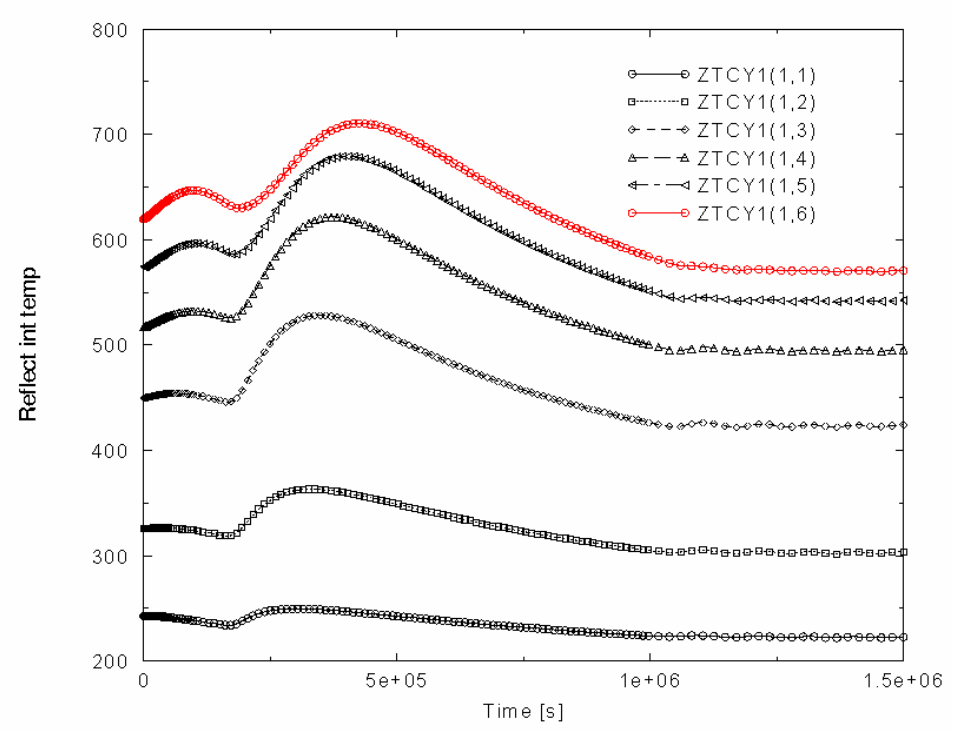

Figure 12: Temperature distribution in the radial reflector innermost region following a depressurized LOCA accident in a 600MW PB-VHTR with assumed malfunction of the safety system.

5.3 Partial Loss of Load.

In this accident a part of the load is lost. As a result, a core heat up is initially expected. Such an event can occur if ether the turbine, the hydrogen plant or the process heat utilization

malfunctions. The immediate consequence is an increase in the He temperature as seen in Fig. 13. As can be observed the coolant temperatures will undergo a transient during about 1000s, and afterward will stabilize on a new somewhat lower temperature level. The core negative feedback will adjust the new power level according to decreased demand as shown in Fig. 14.

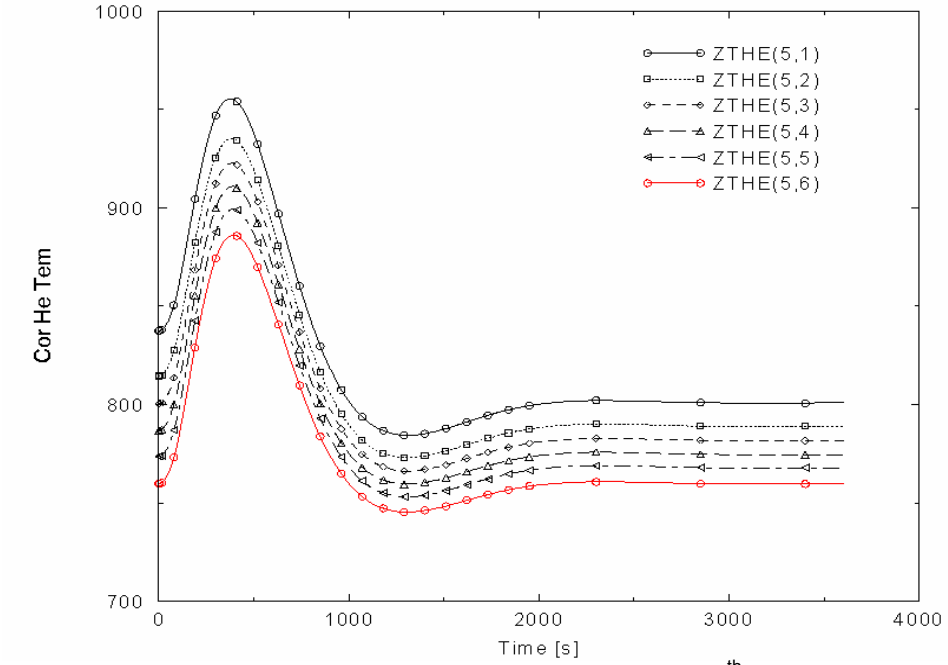

Figure 13: Temperature transient distribution in the coolant 5th axial region during a partial load rejection accident in a 600MW PB-VHTR.

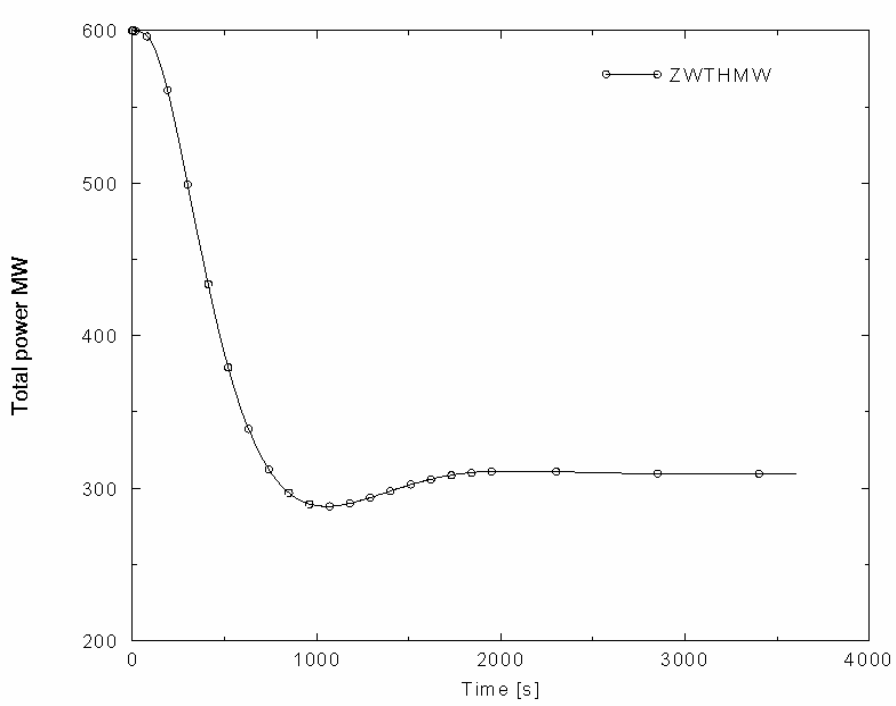

Figure 14: Power transient – readjustment during a partial load rejection accident in a 600MW PB-VHTR.

The resulting fuel temperatures in the centre of 6 spheres located along the axis in the second core radial region are shown in Fig. 15. A mild transient in the fuel temperatures is observed until the system is adjusted to the new power and temperatures.

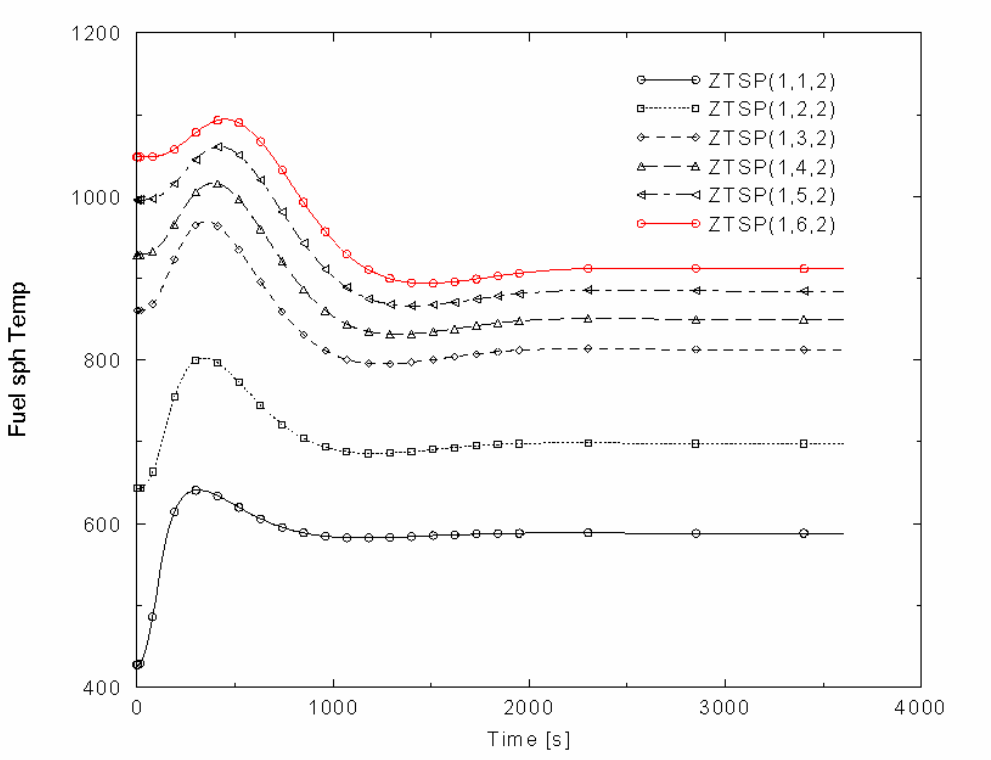

Figure 15: Fuel temperatures transient along the axis of the second core radial region during a partial load rejection accident in a 600MW PB-VHTR.

6 CONCLUSIONS

The major conclusions that can be deduced from the above accidents simulations is that the proposed VHTR is inherently safe and all major accidents will be mitigated by naturally occurring phenomena regardless of the availability of the safety system.

- None of the accidents resulted in core damage
- The reactor is shut down due to the existing negative feedback
- Decay heat can be easily removed by radiation and conduction to the ambient air
- No excessive temperatures are observed
- No fission products will be released in any of the modelled accidents

From the simulations of various hypothetical accidents of the PB-VHTR and on author experience in the safety analyses of different nuclear power plants, it is obvious that this reactor is safer than most presently operating reactor concepts. It can generate fuel, electricity and process heat to cover all energy needs by a single system. Further design studies are needed to resolve economic issues and technological concerns of the very high temperatures.

REFERENCES

[1] D. SAPHIER, *Parameterization of HTGR Safety Characteristics by Simulation of Severe accidents*, Proceedings of ICENES-05, August 21-26, Brussels, (2005)

[2] D.SAPHIER, P.T. León, J.Mª Martínez-Vall, *A Pebble-Bed HTGR Transmutation option*, Trans ANS, **85**, Winter (2001)

[3] M.A. FUTTERER et.al. *Irradiation Results of AVR Fuel Pebbles at Increased Temperature and Burn-up in the HFR Petten*, Proc. Of HTR2006, Johannesburg (2006)

[4] S. B. BENDOTTI, P. Guillermier, M. Phelip, *HTR and VHTR Fuel Irradiation Program in the OSIRIS MTR*, Second Int. Topical Meeting on High Temperature Reactor Technology, Beijing China (2004)

[5] D. SAPHIER, J. Rodnizky. *Dynamic Modelling and Simulation of a High Temperature Gas-Cooled Pebble-Bed Reactor.* ANS/CNS Topical Meeting on Numerical Methods in Nuclear Engineering, Montreal, Quebec, (1983)

[6] H. MATZKE, *Advanced LMFBR Reactor*, North Holland, Netherlands, *(1986*

[7] W.B. KEMMISH, M.V. Quick, I.L. Hurst, *Gas Cooled Fast Reactors*, Progress in nuclear energy, **10**, Num. 1, (1983) 1

[8] D. SAPHIER, E. Greenspan, D. C. Wade, M. Dzodzo, L. Conway, N.W. Brown, *An Inherently Safe Modular LMR Plant - the Encapsulated Nuclear Heat Source*, Trans. Am. Nucl. Soc. 85, (2001)

[9] R. SCHULTEN, et.al, *The Pebble Bed High Temperature Reactor as a Source of Nuclear Process Heat*, Kernforschunsanlage Jülich GmbH, Jül 1119 etc, Vols-1 to 10. (1974)

[10] A. TERADA et.al., *Development of Hydrogen Production Technology by Thermo chemical Water Splitting IS Process Pilot Test Plan*, Journal of Nuclear Science and Technology, **44**, No.3 (2007) 477-482

[11] D. SAPHIER, *The DSNP Users Manual – Dynamic Simulator For Nuclear Power Plants*, Vol. II, RASG-115-85, Rev 4.5, Soreq Nuclear Research Centre (1995)

[12] M.P. LaBar, *The Gas Turbine – Modular Helium Reactor: A promising Option for Near Term Deployment*, General Atomics, GA-A23952 (2002)

[13] T. FERREIRA, *PBMR: Clean, Safe and Affordable Energy*, Schiller Institute Conference, Kiedrich, Germany (2007)

[14] M. Freeman, *China's 21st –Century Nuclear Energy Plan*, EIR **32**, 8, (2005)

TOPSAFE
Dubrovnik, Croatia, 30.09 - 3.10.2008

A Coolant Void Reactivity Effect Evaluation of ELSY LFR: Optimization of a Mid-Plane Blanket for Void Effect Reduction.

Rasha Ghazy*, Enrico Padovani, Marco E. Ricotti
Politecnico di Milano – Department of Energy
Nuclear Division - CeSNEF
Via La Masa, 34 – 20156 Milano, ITALY
rasha.ghazy@mail.polimi.it, enrico.padovani@polimi.it, marco.ricotti@polimi.it

Carlo Artioli
FIS-NUC ENEA
National Agency for the New Technologies, Energy and Environment
Via Martiri di Monte Sole, 4 – 40129 Bologna, ITALY
carlo.artioli@bologna.enea.it

Giacomo Grasso
Nuclear Engineering Laboratory of Montecuccolino
University of Bologna
Via dei Colli, 16 – 40136 Bologna, ITALY
giacomo.grasso@mail.ing.unibo.it

ABSTRACT

Loss of coolant in a fast reactor is a crucial, safety-related issue that has two distinctive consequences on a reactor operation: first of all, heat removal ability is lost leading to overheating and possibly to loss of core integrity, standing for one of the main reasons for core melting accidents. Secondly, it can introduce reactivity into the system.
Void effect profile for ELSY fast reactor has been evaluated by means of MCNP code, simulating the gradual voiding of the active region, while keeping the lead reflector around. As expected for liquid metal reactors, a positive void reactivity effect (about 5200 pcm) has been calculated; the value corresponds nearly to the amount of reactivity coverable by the twelve B_4C control rods designed for the whole core. This fact leads to an important consequence: in case of such unbelievable complete voiding of the core, no more reactivity worth of the absorbers would be available.
In order to investigate a possible reduction of positive void feedback in case of hypothetical loss-of-flow (LOF) scenario, an internal blanket of some proper absorbing material has been inserted in the mid-plane of each fuel rod with consequent increase of core height. MCNP criticality calculations have been performed for different blanket thicknesses and for three kinds of materials: natural uranium in oxide form, and natural thorium in both metallic and oxide forms.
Results have shown that none of the three materials is able to decrease the void effect for small thickness: more than 300 mm of thorium (and even more than 400 for uranium) are necessary to start reducing the positive reactivity insertion.

* Corresponding author. E-mail address: rasha.ghazy@mail.polimi.it Tel: +39-02-23996327.

ACRONYMS

ELSY	European Lead System	**LMR**	Liquid Metal Reactor
IMPB	Internal Mid-Plane Blanket	**LWR**	Light Water Reactor
LFR	Lead Fast Reactor	**MCNP**	Monte Carlo N-Particle

1 INTRODUCTION

ELSY is a Generation IV power plant whose aim is the production of electricity in a competitive and safe design **[1]**.

Many factors can cause perturbations to the reactor operation, due to feedback effects. Temperature of materials, fuel properties change during operation, pressure and occurrence of void are all aspects related to neutrons balance in the reactor, and they must be carefully estimated to assure effective compensating action in case of reactivity swings.

In particular, accidental void occurrence in the system is a delicate issue concerning safety; the main cause for this accidental scenario is a rupture in the fissile rods which leads to fission gas release with consequent formation of void. Void reactivity effect - a measure of how the nuclear system reacts to accidental void occurring in the core - needs then to be core-widely evaluated for the promising ELSY fast reactor, and solutions for its mitigation pursued.

2 VOIDING IN LIQUID METAL FAST REACTORS

Several causes may give rise to extensive voiding in a liquid-metal reactor. Usually, LMR plant designs are arranged with backup protection to mitigate the impact of vessel leakage or rupture, to the degree that large-scale loss-of-coolant accidents (LOCA) are extremely unlikely. Pool systems typically have a second guard vessel, and loop systems are normally double pipe and tank designs. Since the liquid-metal coolant is not pressurized under normal operation, a leak in the primary system will not automatically result in coolant boiling due to the depressurization (as in LWRs). In a sodium-cooled reactor, voiding may arise due to boiling out of coolant. This is prevented in a lead system. In order for the lead to get hot enough to boil (Tb=2023 K), temperatures have to be above the melting point of steel (Tm=1700 K). In that case, much larger antireactivity becomes available due to fuel floating.

Another possible mechanism for coolant voiding, without the precondition of steel melting, is the possibility of entrance of air into the core from the cover gas region as well as steam during a failure in the steam generator, i.e., a so-called steam generator tube rupture (SGTR) event. In sodium plants, intermediate sodium-loops are introduced as a second physical barrier to minimize the consequences of SGTRs and to avoid violent chemical reactions between water and sodium in the primary system. Because lead is chemically inert with water/steam, two-circuit designs are suggested, with the steam generators located in the primary system. In such designs, there will only be one barrier to fail in order to get high-pressure steam into the primary system; the pressure on the steam side can be as high as 100-150 bars and low pressure on the metal side, about 1 bar.

Because of multiple coolant entries preventing blockage in fuel subassemblies (wrapperless assemblies) and avoidance of gas entrance in lead, voiding of the core in ELSY plant is rather unbelievable. The fatal context which is realistically taken into consideration is the gas release from failed pins.

Void fraction, i.e. the fraction of void in a certain "total volume" which is normally filled with coolant, can be written as:

$$\alpha = \frac{Void\ volume}{Total\ volume} = \frac{V_v}{V}.$$

Void reactivity effect estimates how much the reactivity changes as voids form in the coolant. It is defined as the relative change in reactivity per change in void fraction:

$$\alpha_v = \frac{1}{k_{eff}} \frac{\partial k_{eff}}{\partial \alpha}.$$

The total coolant void worth is just the difference in the k-eigenvalue between the flooded and voided state. The effect can be calculated by considering the effect of changes of void fraction on the different contributions to k_{eff}.

The magnitude and sign of the reactivity effect due to void is a complex function of core design, void location and void volume. Inherent stability of such a nuclear reactor, as any dynamic system, can be achieved only by *negative* feedbacks acting sufficiently fast so that the integrity of the reactor core is not compromised.

The coolant density change or **occurrence of the void** in the core can be a result of the following events:

- temperature increase of the coolant due to pump failure, inadequate instrumentation and prediction of hot-channel factors, crud deposition and plugging of the coolant channels; ultimately, this leads to a coolant phase change. Accident scenarios assuming coolant boiling are rather unbelievable for systems cooled with lead due to its high boiling temperature.
- blocking of the coolant circulation as a consequence of coolant freezing in the steam generator, i.e. overcooling.

Additionally, void cavities can appear in the core due to:

- **gas leakage from ruptured pins**,
- steam ingress from ruptured steam generator,
- blow-up of bubbles from gas injection system,
- coolant leakage caused by brittle failure of the reactor vessel.

The coolant acts in the reactor not only as a neutron absorber, but also as moderator, affecting the neutron spectra. The reactivity change when decreasing the density of the coolant in fast neutron cores is mainly due to three effects:

- reduction of neutron moderation (spectral hardening), increasing fission probabilities of even neutron number actinides, reduction of absorptions in fuel (and consequent increase of k_{eff});
- reduction of neutron parasitic absorption in coolant (consequent increase of k_{eff});
- increase of neutron leakage (consequent decrease of k_{eff}).

3 ELSY VOID REACTIVITY EFFECT EVALUATION

According to what has been recently done at ENEA national research laboratories **[2],** ELSY reactor has been modelled following the square wrapperless design option (Figure 1) in the preliminary configuration defined for a 1530 MW thermal power.

The core is made of three fuel zones of different enrichment (13.4, 15 and 18.5% v.f. of Pu enrichment). Externally, suitable elements and lead surround the core as reflector and shielding. Under active fuel a plenum zone is designed for fission gases, while structural parts surround on the top and at the basis. Absorbers are of two kinds: twelve control rods with a volumetric fraction of 70% in boron, and an upper cloak with v.f. of 15% in boron, which has the main purpose of regulation and compensation.

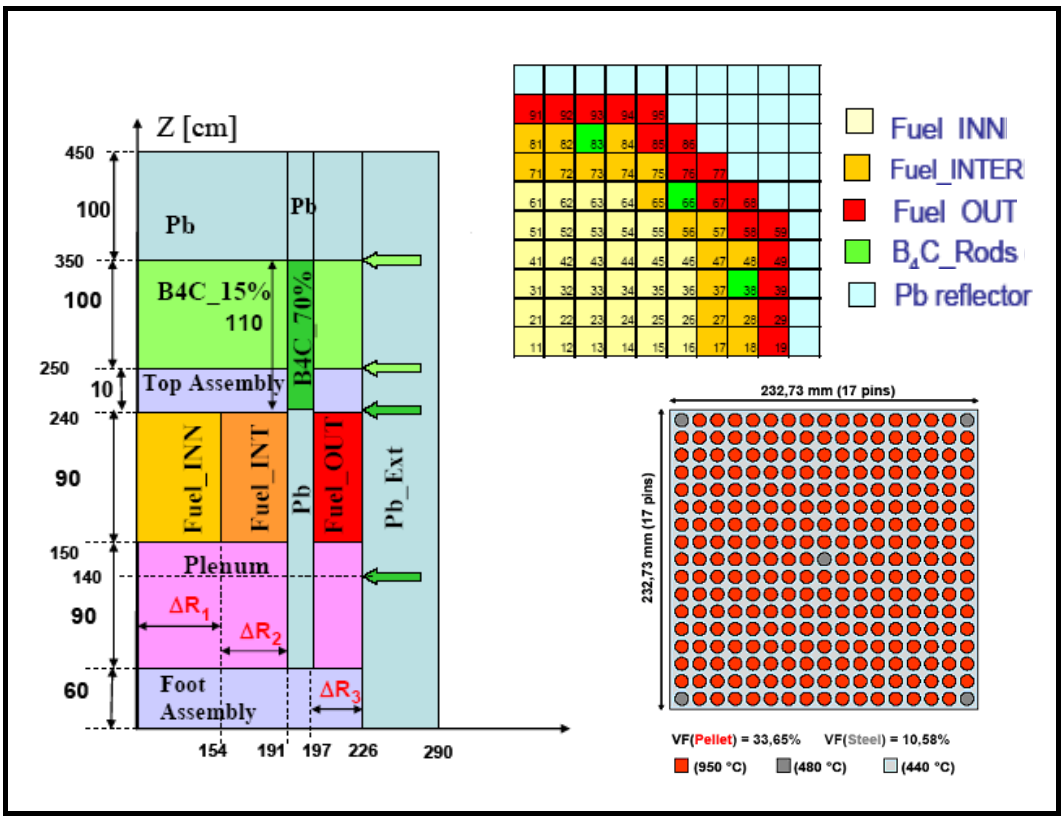

Figure 1: 1530 MWth ELSY Preliminary Configuration. Left side: R-z view of the core; right side: scheme of the core and square wrapperless fuel assembly.

Criticality calculations performed by MCNP with use of JEFF 3.1 nuclear data library have been run to obtain a first estimate of k_{eff} for ELSY reactor.

Results show that the present configuration has ρ = 193 pcm, and this is taken as reference value (std. dev. = 64 pcm).

A method for calculating the liquid metal loss effect is to use perturbation theory and determine the contributions separately **[3]**. This method provides useful insight into the physical processes, but the calculation is quite difficult. Therefore the method generally used to calculate liquid metal reactivity loss is to perform successive calculations (one with coolant present and the second one without coolant from the zone of interest) and to compare the criticalities.

Void reactivity effect has been studied applying the void into the core for successive steps. The Monte Carlo input file has been modified to simulate the situation in which void penetrates progressively into the core: a *void plenum* region, which gradually replaces the

coolant, has been added (Figure 2) as far as a complete void condition is reached. At each step the lead level in the core has been lowered of 10 cm each time to the end of the active region (90 cm).

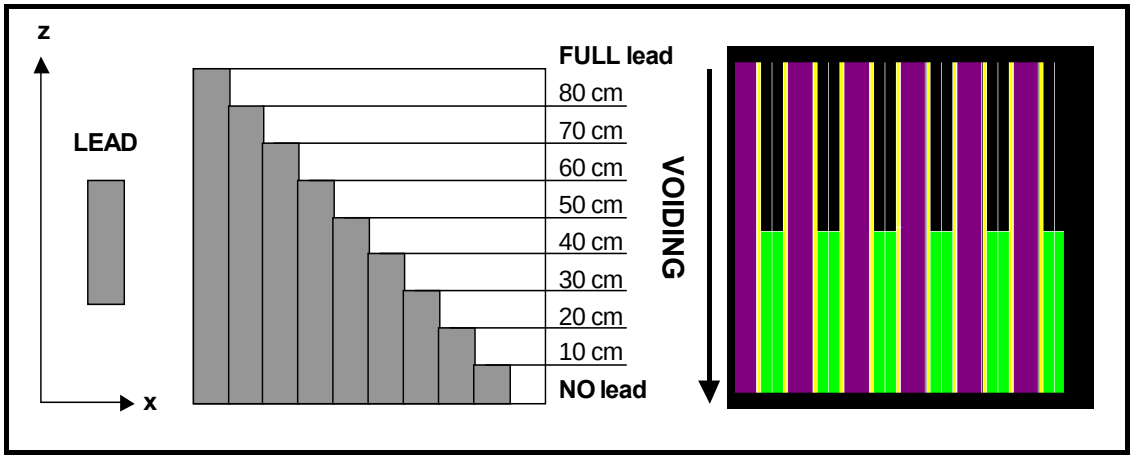

Figure 2: Scheme of the process of progressive voiding (left) and MCNP plot of the voided core (right).

k_{eff} and relative standard deviation have been reported at each step of voiding. As expected for liquid metal reactors, reactivity progressively increases to an amount of slightly more than 5000 pcm, which represents a large reactivity worth.

The profile of the resulted void reactivity effect has been plotted along with its differential with respect to the voided height (Figure 3).

Differential analysis gives information about *local void*: the maximum is located very close to the core mid-plane. Hence, **the reactivity insertion rate is highest at core midlevel**.

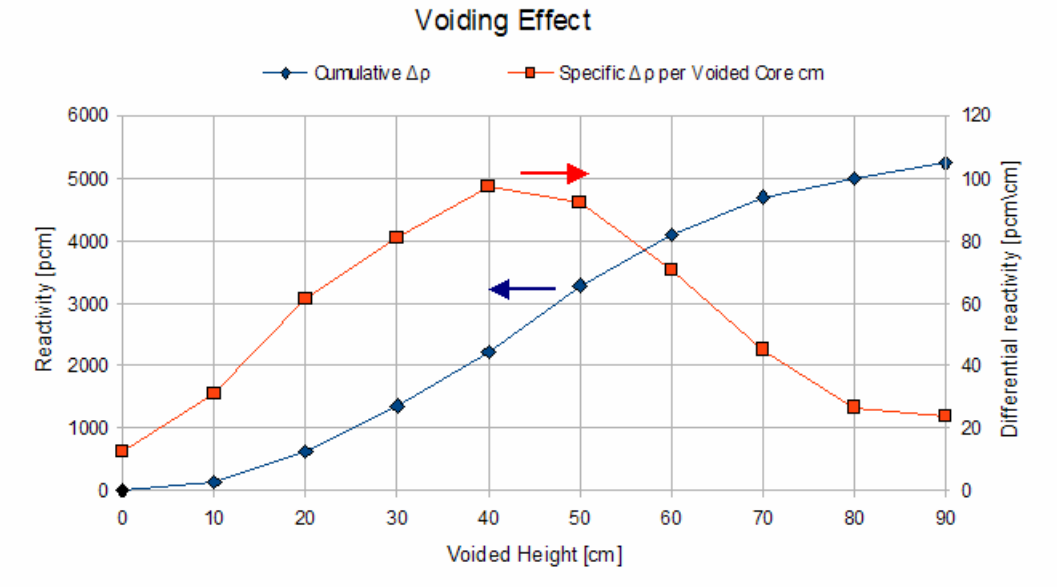

Figure 3: Void Effect and derivative function.

As shown in the graphs, reactivity worth due to void effect has resulted in a great swing which must be deeply analysed and controlled. Although this aspect is typical of liquid metal

fast reactors and cannot be avoided **[4]**, many measures have recently been investigated for reducing it.

4 OPTIMIZATION OF IMPB (INTERNAL MID-PLANE BLANKET) FOR VOID EFFECT REDUCTION

It was shown that in reactor systems cooled by liquid metals in a configuration consisting of steel pins acting as absorbers immersed in the coolant, void worth is significantly lowered. Several attempts have been already made to reduce void effect by design; most design modifications have focused on increasing the leakage component. The most promising appears to be the heterogeneous core concept, in which blanket assemblies (containing pure fertile material) are distributed through the core region to achieve a high neutron leakage rate from the active core to the blankets **[5]**. There are radial and axial heterogeneous cores, according to the option of arranging the blanket fuel assemblies among (*radial blanket)* or within (*internal blanket*) the seed fuel assemblies **[6]**. Another option concerns the combination of both types. In addition, other axial blankets can be added on and beneath the seed fuel. This design reduces void reactivity effect, while yields higher breeding ratios but consequently requires higher fissile inventories.

In the present work the concept of adding a blanket acting as absorbing material in the core has been considered; three different material solutions have been tested. A blanket of varying thickness for each material has been inserted in the mid-plane core, and void worth has been evaluated.

Analyses have been carried out for natural uranium in dioxide form and for thorium in both metallic and oxide forms.

4.1 Mid-Plane Blanket Design (Internal Mid-Plane Blanket configuration)

Since lower void reactivity can be attained through the leakage of neutrons from the active region, this effect may be enhanced by shortening the height of the core. This option is obviously limited by reactor design and constraints. However, a great challenge is represented by the possibility of reducing void effect inserting a blanket of some proper material as depleted UO_2 (for its absorbing power) inside the core.

The coolant loss (in the region around the inserted blanket) has two effects:

- an increase of the core transparency, so that a higher blanket absorption rate will occur; considering that the ratio $\sigma_{fission}/\sigma_{absorption}$ of the blanket is lower than the one of the fissile fuel, this will act in the sense of reducing the reactivity;
- because of the lack of the coolant moderating contribution, neutrons are kept to higher energies where the ratio $\sigma_{fission}/\sigma_{absorption}$ of both the blanket and the fissile fuel is higher; this will act in the sense of increasing the reactivity.

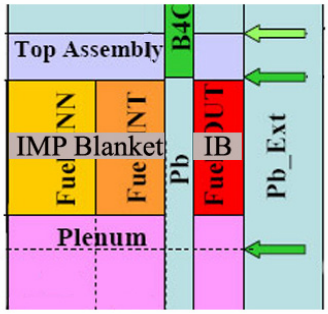

Figure 4: ELSY R-z view with IMPB.

Moreover, the spectral contribution to void reactivity effect (usually positive) is proportional to the flux intensity, and therefore is important near the centre of the core, while the leakage component (negative) becomes important near the edges where the flux gradient is stronger. As a result, expulsion of coolant from the central region results in a much more positive reactivity gain.

Due to the flux importance in the central axial position in the core, the internal blanket has been placed in the mid-plane of each fuel rod. If this solution succeeds, and void reactivity worth gets lower, the burden on control rods in any accidental case in which void fills the core causing a fatal increase of criticality will substantially decrease; **as a consequence, a great improvement in reactor safety would be gained.**

Criticality calculations have been performed for the three selected materials and then compared. For the case of natural uranium, MCNP tests have been carried out for layers of different increasing thickness starting from 4 to 400 mm of material, increasing therefore the total active height of the core. Figure 5 shows the results of criticality calculations. Reactivity, before and after any void occurrence, is plotted in the curve referenced to the left scale, showing clearly that reactivity drops after insertion of a blanket material in the core. This fact indicates that adding such an amount of absorbing material leads necessary to a higher enrichment of the fresh fuel as to assure criticality at starting. In the curve referenced to the right scale, the reactivity variation (the difference between reactivity after voiding and reactivity before voiding) is plotted for increasing blanket thickness.

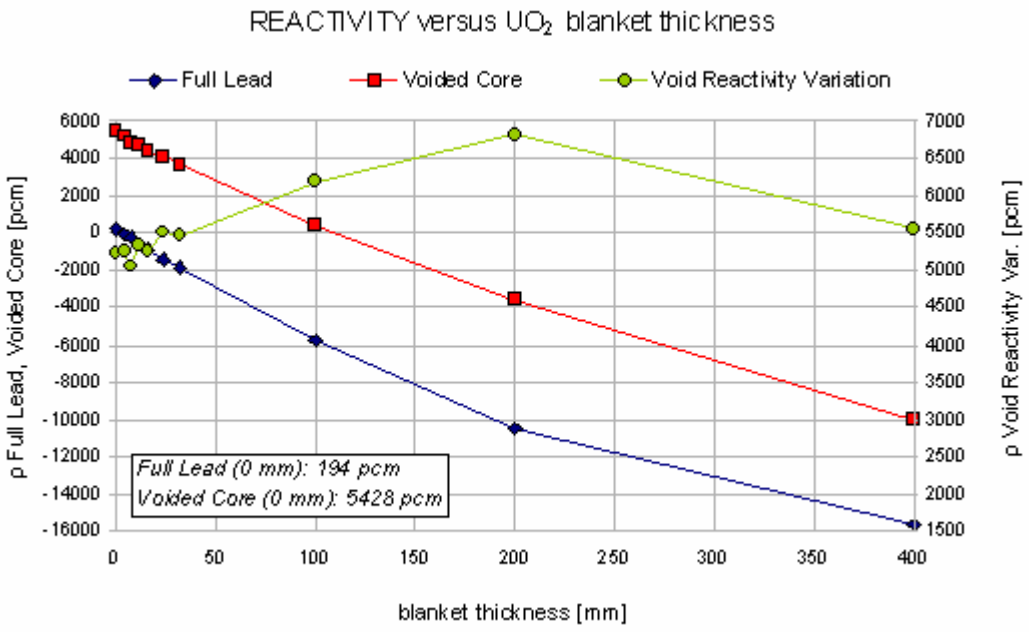

Figure 5: Reactivity and Void Effect in the UO2 IMPB insertion.

The same calculations have been made for thorium, and all the results, normalized to the configuration without blanket, have been plotted together (Figure 6), coherently with the expression:

$$\Delta\rho = \left(Void\ Worth\right)^{blanket} - \left(Void\ Worth\right)^{blanket\ free}$$

where:

$$Void\ Worth = \rho_{void} - \rho_{no\ void}\ .$$

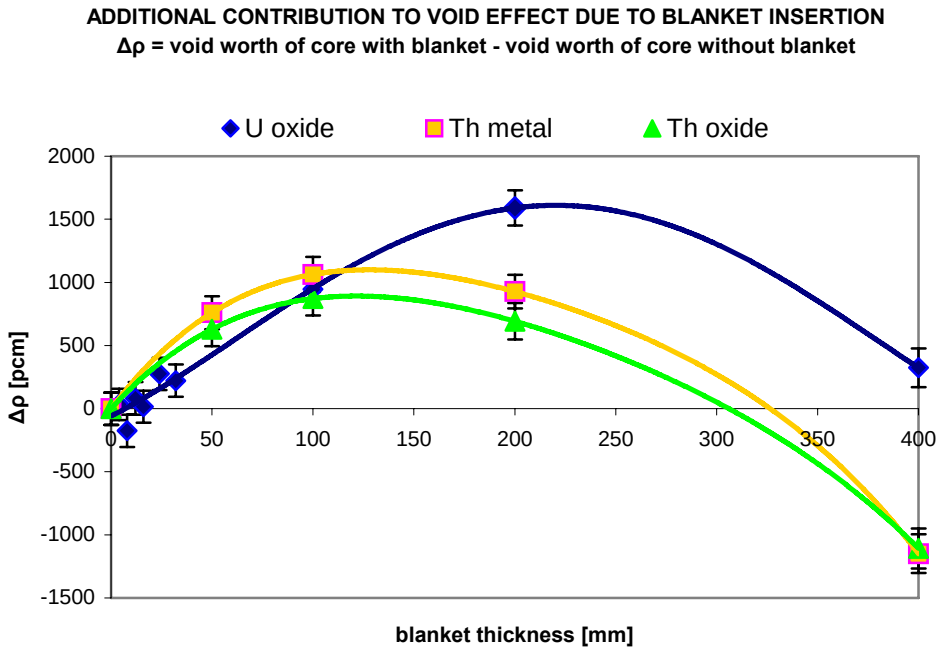

Figure 6: Additional contribution to void effect due to the IMPB configuration.

4.2 Results and flux analysis

As shown in Figure 5, the adding of an IMPB lowers consistently the criticality of the reactor. The contribution to void effect due to uranium insertion (blue curve in Figure 6) increases by about 1500 pcm with increasing thickness until 20 cm of material: this point represents the maximum positive variation to void effect for the present configuration. Then, void effect variation gets lower again, but actually uranium IMPB doesn't reduce void effect unless an amount of more than the upper tested limit (40 cm) is added.

Thorium metal and oxide appear as better solutions: both the curves show a maximum before the one related to uranium addition, between 10 and 15 cm of thickness, that means less amount is required to get similar values. Moreover, void effect gets finally lower then the reference value as at least 30 cm of thorium oxide are added.

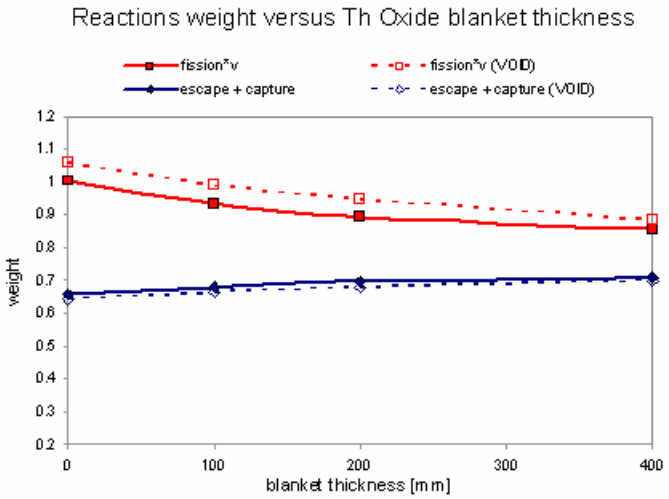

Figure 7: Reactions rates versus blanket thickness.

Creation and death of neutrons have been considered as discriminative aspects for explaining the reasons of the curves of Figure 6. In particular, MCNP output files have been analysed to get information about number of fissions, captures and escapes normalized with respect to one neutron history. Figure 7 show that production rate due to fission increases after voiding independently from the blanket thickness, whereas the sum of escape and capture rates related to the whole system

slightly decreases. Figure 8 compares singularly the various event types related to the active region for the three tested materials.

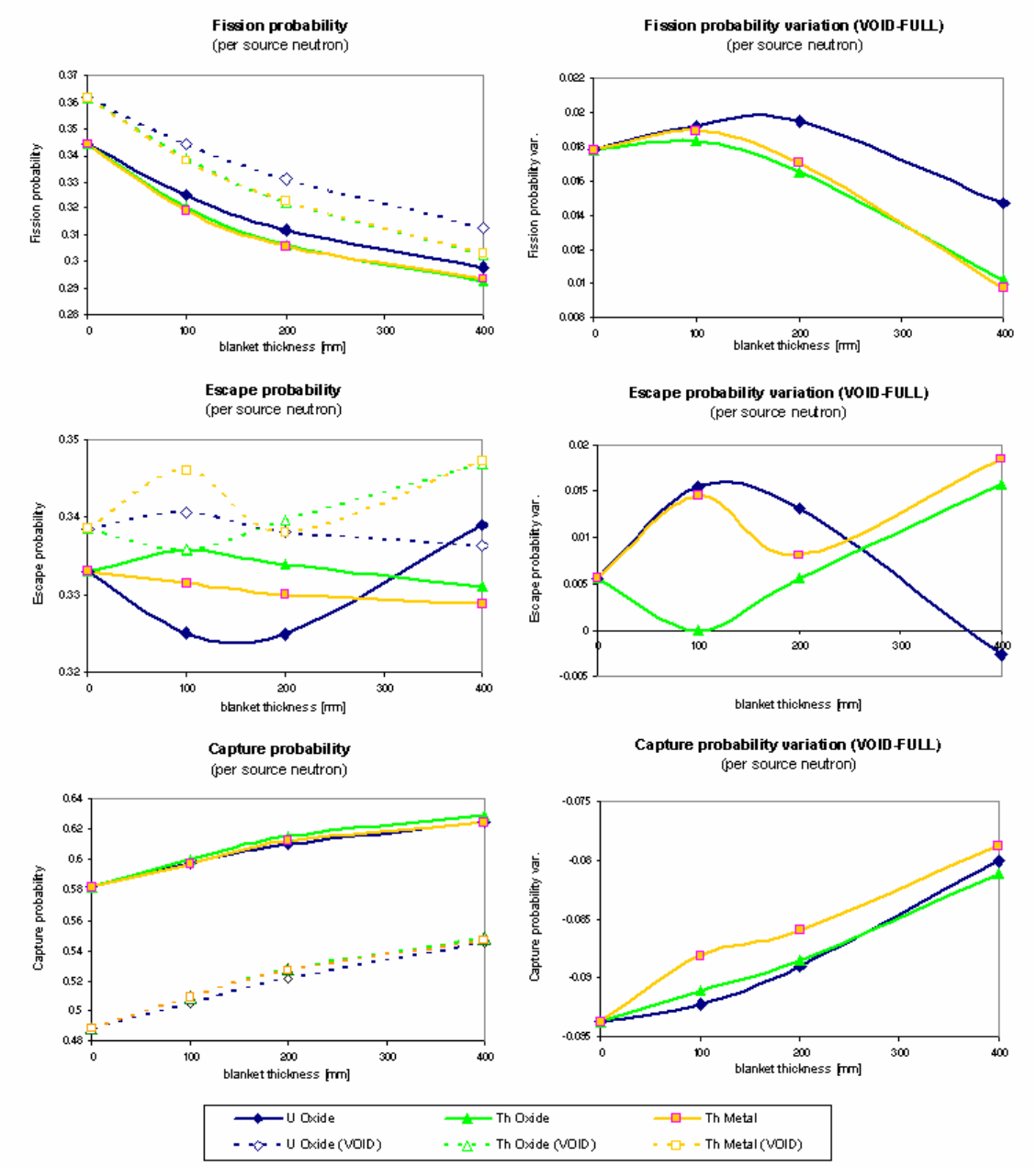

Figure 8: Contribution to rates probabilities referred to the active region due to the IMPB configuration.

Increase of fission rate and decrease of captures seem to be mainly responsible for reactivity gain after insertion of small uranium or thorium blankets; these variations in the rates become indeed less relevant with greater thicknesses.

The occurring of the maximum void reactivity worth at different blanket thicknesses (after 10 cm for thorium and after 20 for uranium) is probably due to a greater $\sigma_{fission}$ for uranium and a slightly greater $\sigma_{capture}$ at high energies for thorium (Figure 9).

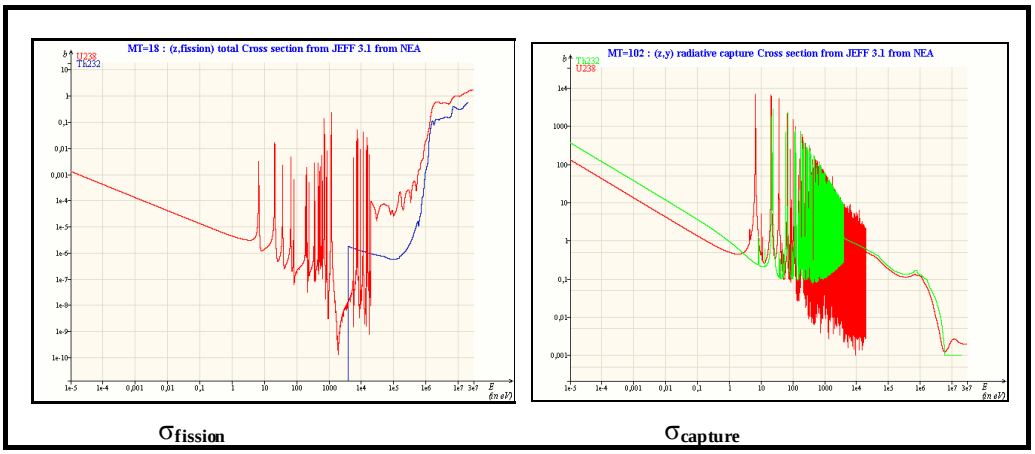

Figure 9: fission and capture cross-sections for U-238 and Th-232.

Last, MCNP neutron flux distributions have been analysed. With regard to neutron flux in the blanket-free configuration before void occurrence, the curve has the expected cosine trend (Figure 10); after voiding, it shows a flattening due to the increase of the neutron path.

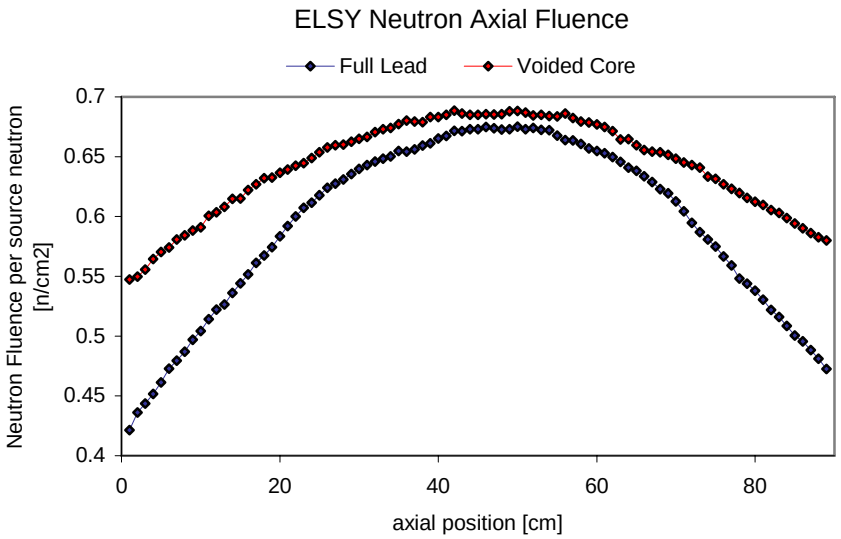

Figure 10: MCNP Neutron Axial Fluence of ELSY reactor.

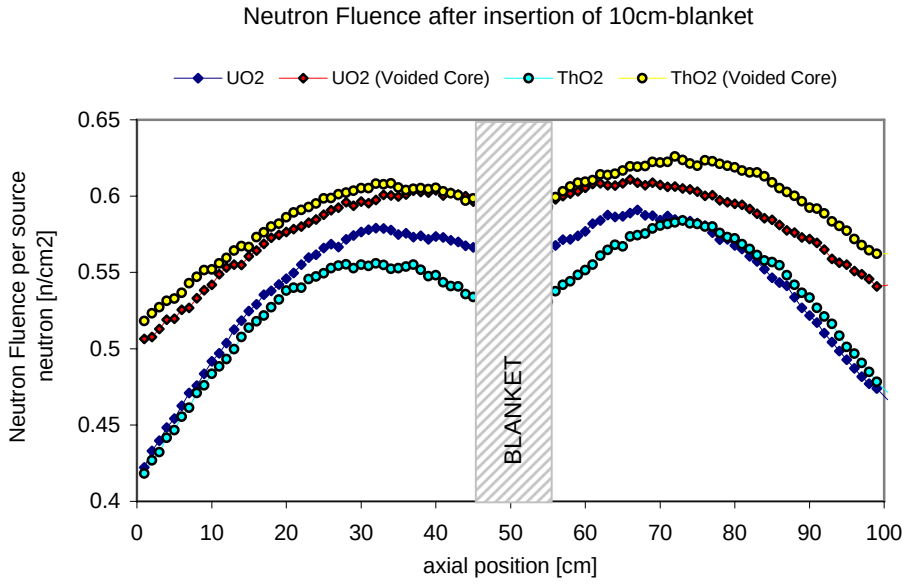

Figure 11: MCNP Neutron Axial Fluence after 10 cm blanket insertion.

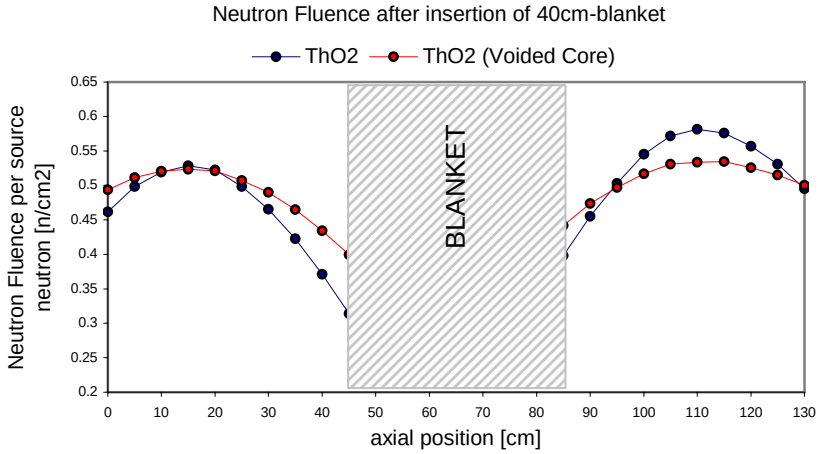

Figure 12: MCNP Neutron Axial Fluence after 40 cm thorium blanket insertion.

All the fluxes show a reasonable symmetry; greater values of the flux are in the upper part of the core: the reflector function of the upper lead zone influences strongly the neutron distribution, increasing probability of avoiding neutron escapes. Thorium curve shows a greater flux depression in the blanket zone in comparison to uranium curve, due to the worse neutron multiplication characteristics.

Internal mid-plane blanket tends to give axial decoupling, that is spatial separation of the neutron flux, as clearly shown in the middle of Figure 11. Flux distributions in a decoupled core are very sensitive to perturbations, and local reactivity insertion tends to cause very high local power peaking or unstable transients. Decoupling effects are thought to be undesirable, as the stability under transient conditions is affected: this is a strong drawback for the IMPB configuration.

The decoupling effect justifies the void effect reduction for great blanket thicknesses: 40 cm of IMPB lead to a two-separated-cores configuration (Figure 12), where each core is

characterized by half the initial H/D ratio. In this configuration the increased leakage component, as shown from the flux slope at the edges, is fundamental in reducing void effect.

5 SUMMARY AND CONCLUSIONS

With reference to the European design, a preliminary void effect study of ELSY reactor has been carried out. Reactivity worth due to void effect in the active region has resulted in a great swing, equal to about 5200 pcm. Although large void effect is a typical feature of liquid metal fast reactors and cannot be annulled, many measures have been studied in the past in order to mitigate it; in the present work the concept of adding some fertile through three different material solutions (natural uranium in oxide form, and thorium in metallic and oxide forms) has been considered. A blanket of varying thickness for each material has been inserted in the core mid-plane and void worth evaluated. Results have shown that uranium blanket doesn't reduce void reactivity effect unless great amounts are added, while thorium provides an actual improvement if at least 300 mm of blanket are inserted in the mid-plane of the core.

REFERENCES

[1] L. CINOTTI et al., "The Potential of the LFR and the ELSY Project", Proceeding of the International Congress on Advances in Nuclear Power Plants (ICAPP 2007), Nice Acropolis, France, May 13-18 (2007).

[2] C. ARTIOLI, M. Sarotto (ENEA), S. Massara (EDF), "Open Square Fuel Assembly design and drawings - Preliminary ELSY core design", Report Deliverable D6, FPN-P9IX-004 (2007).

[3] A. E. WALTAR, A. B. Reynolds, "Fast Breeder Reactors", Pergamon Press, New York (1981).

[4] K. TUČEK, J. Wallenius and W. Gudowski, "Coolant void worths in fast breeder reactors and accelerator driven transuranium and minor actinide burners", *Annals of Nuclear Energy,* 31 , 1783 (2004).

[5] K. HIBI, S. Shimada, T. Okubo, T. Iwamura and S. Wada, "Conceptual designing of reduced-moderation water reactor with heavy water coolant", *Nuclear Engineering and Design*, 210 (2001).

[6] A. SHELLEY, S. Shimada, T. Kugo, T. Okuboa and T. Iwamura, "Optimization of seed-blanket type fuel assembly for reduced-moderation water reactor", *Nuclear Engineering and Design*, 224 (2003).

European Nuclear Society

Rue Belliard 65
1040 Brussels
Belgium
Telephone +32 2 505 30 54
Fax + 32 2 502 39 02

topsafe2008@euronuclear.org

www.euronuclear.org